Trajectory prediction for drifting ship allision probability calculations

A trajectory prediction-based method for probability calculations to improve our understanding of drifting ship allision risks in the Dutch North Sea region

S. K. P. Eppenga

TU Delft

Trajectory prediction for drifting ship allision probability calculations

A trajectory prediction-based method for probability calculations to improve our understanding of drifting ship allision risks in the Dutch North Sea region

Thesis report

by

S. K. P. Eppenga

to obtain the degree of Master of Science
at the Delft University of Technology
to be defended publicly on June 20th, 2024 at 16:00

Thesis committee:

Chair:	Prof. Dr. Ir. M. van Koningsveld
Supervisors:	Ir. S. van der Werff, Ir. A. van der Hout & Ir. S. van Aartsen
External examiner:	Prof. Dr. Ir. P. H. A. J. M. van Gelder
Place:	Faculty of Mechanical, Maritime and Materials Engineering, Delft
Project Duration:	September, 2023 - June, 2024
Student number:	4743636

Faculty of Mechanical, Maritime and Materials Engineering Delft University of Technology

Abstract

The expansion of offshore wind farms in the North Sea is significantly impacting maritime safety. This expansion leads to more ships being present near infrastructure, thereby increasing the likelihood of collisions. In cases where ships become adrift and lose their ability to navigate, they are at an increased risk of colliding with nearby structures. The nautical term for this type of collision is *allision*. It refers to when a ship crashes or runs into a structure or another ship that is stationary. The consequences of such allisions can be severe, including loss of life, damage to property and cargo, and environmental pollution.

There are methods to prevent such accidents through monitoring and preventive measures. However, monitoring poses a significant challenge for the limited number of operators within the Dutch Coast Guard, and an Emergency Response Towing Vessel (ERTV) is the only external measure in place to prevent a drifting ship from alliding with a wind farm. Moreover, there is no established framework to optimise the deployment of ERTVs, which limits its effectiveness. To effectively manage the expansion of offshore wind farms in terms of maritime safety, Rijkswaterstaat, the executive agency of the Ministry of Infrastructure and Water Management, must minimise the risk of allisions. For risk-reducing purposes, this includes gaining a comprehensive understanding of the integral image of drifting ship allision risks across the Dutch North Sea region. This understanding must be valid, reliable, and provide the necessary insights, such as how dynamic factors like weather conditions and shipping activity affect these risks. However, the work of Ellis et al. (2008) highlights significant transparency issues and a heavy reliance on assumptions in state-of-the-art methods for estimating the probability of drifting ship allisions. These issues result in variations in the estimated return periods between different methods by up to a factor of seven. Exploring these state-of-the-art methods revealed that several assumptions made in these methods can not be validated. Moreover, each state-of-the-art method results in an allision occurrence rate estimate specific to each wind turbine and offers little insight for risk-reducing purposes on a North Sea scale. To achieve a valid, reliable, and insightful integral image of drifting ship allision risks across the Dutch North Sea region, risk assessment methods must be substantiated from the core of the incident: a ship's drift trajectory. This led to the exploration of a trajectory prediction-based approach for determining allision probabilities. This approach is summarised in the main research question: *How does a trajectory prediction-based estimation method improve our understanding of the integral image of drifting ship allision probabilities in the Dutch North Sea region to provide well-substantiated insights for risk-reducing measures?*

The ship drift trajectory prediction model OpenDrift has been chosen for this study due to its high accessibility and relatively simple approach to simulating trajectories. An analysis of how this model estimates a ship's drift trajectory yielded several insights, which concluded that accurately predicting a ship's trajectory requires knowledge of all three forces: wind, wave, and current. This conclusion is supported by the analysis of a real-world case, which could only be replicated with the exact combination of forces present at the time of the incident. Excluding any of these forces resulted in predictions that significantly deviated from the actual trajectory.

Following this, a method was developed to estimate the probability of allision, denoted as $P_{allision}$ in Figure 1. The primary component of this method is P_{drift}: the probability that an arbitrary drifting ship allides with a wind farm, considering all possible environmental conditions. In this study, P_{drift} is determined by conducting multiple OpenDrift simulations, and subsequently calculating P_{sim}—the probability of an allision in a single OpenDrift simulation—numerous times for all possible combinations of wind, wave, and current forces with occurrence rate (P_{env}) based on 10 years of historic data. Since each OpenDrift simulation is specific to a ship's geometry, the procedure must be repeated across different classifications of ships. The resulting allision

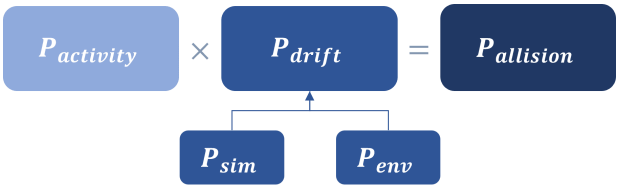

Figure 1: Methodology structure

probability for a specific starting location of a ship's drift is then calculated by multiplying P_{drift} by a shipping density value of the considered location, representing the probability of presence of an adrift ship. In this study, $P_{allision}$ does not reflect an actual allision occurrence rate but serves as a comparative value across different locations.

In simulating trajectories for the calculation of P_{drift}, it is assumed that the wind and waves remain constant throughout a ship's drift trajectory. Each combination of wind and wave conditions is simulated for multiple starting times along a current cycle. The consistency of P_{drift} results with those derived from simulations conducted using time-varying hindcast data validates the approach of keeping wind and wave conditions constant throughout a ship's drift trajectory for the P_{drift} definition in this study. Furthermore, it has been observed that including the current is essential, as excluding it leads to P_{drift} values that significantly deviate from the results of simulations conducted with time-varying hindcast data. Around the Hollandse Kust West wind farm, significant differences are consistently observed in the P_{drift} values. In the context of our definition of P_{drift}, it becomes apparent that two common assumptions in state-of-the-art methods are unjustified: (1) the assumption that the ship moves in a purely lateral direction, and (2) the estimation of the current as a uniform speed in the wind direction.

The probability of allision ($P_{allision}$) is estimated for this study for the wind farm areas Hollandse Kust West and Hollandse Kust Zuid. The results indicate that Hollandse Kust West has the highest allision probability, both overall and for specific wind direction ranges. Furthermore, the greatest contribution to the overall probability for all wind farms comes from the southwest, as winds from this direction occur more frequently and are on average stronger than those from other directions. A more detailed analysis of the influence of current for a specific wind direction range revealed that the highest probabilities are not necessarily found in the area corresponding to the range from which the wind originates. Different current segments lead to varied distributions of the allision probability level around a wind farm, and the time required to reach a particular probability level also varies across these segments.

The analysis of $P_{allision}$ across multiple wind farms showed significant advantages of the established method. This method provides detailed insights into the origins of potential threats and the time available to respond at a given probability of allision, and can be easily extended to multiple wind farms. Furthermore, the method offers detailed insights for specific environmental conditions, such as wind directions and current segments. This information is invaluable for optimising risk-reducing measures, such as monitoring and the strategic deployment of ERTVs. Moreover, this information can serve as a basis for dynamic strategies, including repositioning of ERTVs and the implementation of rerouting strategies.

Overall, the assumptions in state-of-the-art methods might not sufficiently capture the risks associated with drifting ships. The established method broadens the ability to improve monitoring accuracy and optimise the positioning of ERTVs, even for specific environmental conditions. As a next step, this method should be extended to estimate actual risk levels by considering the potential consequences of an allision. With this approach, decision-making regarding allision threats can be contextualised alongside other maritime safety risks, facilitating the development of a robust risk mitigation strategy that enables Rijkswaterstaat to responsibly exploit the abundant potential the North Sea has to offer.

Preface

Before you is the thesis 'Trajectory prediction for drifting ship allision probability calculations: a trajectory prediction-based method for probability calculations to improve our understanding of drifting ship allision risks in the Dutch North Sea region'. This thesis has been conducted to fulfil the requirements for a Master's degree in Offshore & Dredging Engineering at the Faculty of Mechanical Engineering, TU Delft. The work was carried out at Rijkswaterstaat, the executive agency of the Ministry of Water Management and Infrastructure, and Deltares, an independent knowledge institute dedicated to developing innovative solutions in the fields of water and subsoil.

I would like to express my gratitude to my group of supervisors for their support, input and the many critical discussions that shaped the final result. In particular, thank you Solange van der Werff—my daily supervisor at TU Delft—for your unconditional weekly guidance and for steering me towards scientifically relevant research. Despite my firm opinion about my deliverables, you always managed to put me on the right track. Secondly, I would like to thank Arne van der Hout—my supervisor at Deltares—for his subject-specific insights and the warm welcome at Deltares. Thirdly, my thanks go to Mark van Koningsveld, the chair of my committee. Fellow students who have been mentored by you have shared stories about the enthusiasm with which you give your mentorship and the critical thinking required to produce scientifically significant work, and I have found this to be extremely true! Next, I would like to thank Simon van Aartsen—my supervisor at Rijkswaterstaat—for his drive to improve my work and for connecting me with the right people within Rijkswaterstaat. Lastly, I would like to thank Pieter van Gelder—the independent examiner of my committee—for his feedback and willingness to engage during the final stages. Without all of you, this thesis would not be what it is today.

Finally, I would like to thank my friends for listening, helping out where needed, and supporting me throughout this process.

S. K. P. Eppenga
Delft, June 2024

Contents

1 Introduction **1**
1.1 Impact of growing offshore activity on maritime safety in the North Sea . . . 1
1.2 Research objectives and questions . . . 3
1.3 Report structure . . . 5

2 Literature study **6**
2.1 Methodology of literature review . . . 6
2.2 Purpose of ship collision risk assessments for maritime safety . . . 7
2.3 Ship collision types and their assessment methods . . . 10
2.4 Probability of a drifting ship causing an allision . . . 13
2.5 Knowledge gaps . . . 17

3 Trajectory prediction-based method **18**
3.1 Rationale and model selection for trajectory prediction . . . 20
3.2 Sensitivity of a ship's drift trajectory to environmental conditions and ship geometry . . . 24
3.3 OpenDrift's predictive performance . . . 31
3.4 Trajectory prediction-based method for drift probability calculation . . . 36
3.5 Determining the level of detail of scenarios through drift probability analysis . . . 47
3.6 Summary of outcomes and decisions . . . 56

4 Implementation of method **58**
4.1 Scaling drift probability calculations to multiple wind farms . . . 58
4.2 Probability of presence of a drifting ship . . . 61
4.3 Summary of outcomes and decisions . . . 63

5 Allision probability results **64**
5.1 Allision probability results . . . 64
5.2 Allision probability results for specific environmental conditions . . . 71

6 Interpretation & discussion **74**
6.1 Interpretation of results . . . 74
6.2 Implications for risk-reducing strategies . . . 75
6.3 Research validity and limitations . . . 77

7 Conclusion & recommendations **78**
7.1 Conclusions to the research questions . . . 78
7.2 Further research recommendations . . . 82

References **85**

A SAMSON **86**

B OpenDrift **87**
B.1 Wind Forcing . . . 87
B.2 Wave Forcing . . . 87
B.3 Diffusion of simulations . . . 88

C Additional results **89**
C.1 Overall allision probability results Hollandse Kust Zuid . . . 89
C.2 Hourly allision probability results Hollandse Kust Zuid . . . 91
C.3 Influence of different current segments for a specific wind direction range . . . 93

D Python modules **95**
D.1 Environment . . . 95

D.2 Geography . . . 95
D.3 Methodology . . . 95
D.4 Visualisation . . . 95

E Data sources **96**
E.1 ERA5 . . . 96
E.2 DCSM . . . 96
E.3 DCSM-FM . . . 96
E.4 Wind-wave scenarios used in OpenDrift . . . 97
E.5 Current field used in OpenDrift . . . 98

1

Introduction

1.1. Impact of growing offshore activity on maritime safety in the North Sea

The North Sea offers numerous opportunities for offshore activities, and in the coming years, the North Sea will undergo significant transformations with the development of additional marine infrastructure, such as offshore wind farms. By the end of 2032, the Dutch government aims to achieve 21 gigawatts (GW) of offshore wind energy capacity, which is projected to supply 16% of the Netherlands's energy needs. This initiative involves expanding to eight designated areas. Looking ahead, the government's strategy includes reaching approximately 50 GW of offshore wind energy by 2040 and about 70 GW by 2050 (Government of the Netherlands, 2024). At the same time, the North Sea remains one of the busiest maritime regions in the world, with around 260,000 ships navigating its waters annually (Bahlke, 2017). Given these factors, the question arises of how shipping accidents will evolve with this transformation.

1.1.1. Safety concerns in the North Sea

A conservative assumption is that as the North Sea becomes busier, the risk of shipping accidents may increase, if there are no risk-reducing developments. This hypothesis is supported by research conducted by the Maritime Research Institute Netherlands (MARIN), which showed a significant increase in the probability of ship collisions with wind turbines (Duursma et al., 2019). Rijkswaterstaat, the executive agency of the Ministry of Infrastructure and Water Management, has therefore been given the task of maintaining and, where possible, improving current safety standards. This raises an important question: what measures should be taken and how can they be applied most effectively? To address this, Rijkswaterstaat created the Wind at Sea Monitoring and Research Programme. This initiative includes an assessment of the risk of collisions between ships and marine infrastructure and an evaluation of the feasibility of measures to prevent such accidents (Noordzeeloket, 2023).

1.1.2. Risk of collision across the North Sea

Collisions between ships and marine infrastructure can have serious consequences, including loss of life, damage to property and cargo, and environmental pollution. These collisions can occur in two ways: by ramming or by drifting. Ramming collisions result from navigational errors, such as insufficient information, poor visibility, an unmanned bridge or similar factors. Drifting collisions occur when a ship near marine infrastructure experiences problems with its propulsion or steering gear (i.e. a blackout). As the ship gradually loses control and speed, it becomes subjected to wind, wave and current forces. This forcing environment may push it towards marine infrastructure. The nautical term for this type of collision is *allision*. It refers to when a ship crashes or runs into a structure or another ship that is stationary. Every year, tens of ships experience a blackout in the North Sea, fortunately most of them with a harmless outcome (Hermans et al., 2020). However, there are exceptions. On 31 January 2022, the ship Julietta D allided with the oil tanker Pechora Star due to its dragging anchor, which failed to keep it in place.

Following this allision, the Julietta D lost its anchor and, while adrift, allided with a wind turbine foundation and a transformer platform. This incident highlights the potential risk of ships drifting uncontrollably in the North Sea (Kustwacht, 2022).

The increasing activity in the North Sea results in more ships being present near marine infrastructure. This contributes to the risk of allisions involving drifting ships as it increases the likelihood of an adrift ship being pushed towards a structure. The responsibility for monitoring and preventing these accidents lies with the Dutch Coast Guard. Their approach is to continuously monitor traffic in the North Sea. When a ship becomes adrift, they deploy their resources where necessary. An important challenge in this context is the expansion of marine infrastructure combined with the high level of activity in the North Sea, putting pressure on the capacities of the limited number of operators of the Dutch Coast Guard. In terms of resource deployment, the Emergency Response Towing Vessel (ERTV) is currently the only external measure to prevent a ship adrift from an allision. However, its deployment lacks of an established framework such as adjusting its position to changing factors such as weather conditions and shipping patterns (Duursma et al., 2019). To maintain current safety standards, especially in anticipation of future developments, Rijkswaterstaat should evaluate and, where necessary, improve monitoring capabilities and available assets to minimise the risk of allisions.

1.1.3. Problem statement

To effectively manage the expansion of offshore wind farms, it is crucial to gain a thorough understanding of the allision risks associated with drifting ships across the North Sea. This understanding depends on accurately estimating the probability of ships becoming adrift, their potential locations, and the likelihood a ship's drift motion results in an allision. However, the work of Ellis et al. (2008) highlights significant transparency issues and a heavy reliance on assumptions in state-of-the-art methods for estimating this probability. These issues result in variations in the estimated return periods between different methods by up to a factor of seven. For risk-reducing purposes, it is essential to establish an integral image of drifting ship allision risks across the Dutch North Sea region that is valid, reliable, and provides the necessary insights, such as how dynamic factors like weather conditions and shipping activity affect these risks. This comprehensive insight will enable Rijkswaterstaat to optimise monitoring procedures and the implementation of preventive measures. To achieve this, risk assessment methods must be substantiated from the core of the incident: a ship's drift trajectory. By applying a valid and reliable method, Rijkswaterstaat can ensure responsible exploitation of the abundant potential the North Sea has to offer.

1.2. Research objectives and questions

The main research question defines the scope of this study, which aims to improve our understanding of the probability of drifting ship allisions across the Dutch North Sea region to provide well-substantiated insights for preventive measures. This research seeks to develop an approach to a valid and reliable method for estimating the probability of an allision from the core of the incident: a ship's drift trajectory. A method that offers a more detailed understanding of high-probability areas, supported by insights into available response times and the influence of dynamic factors such as weather conditions and shipping activity, can be used to optimise risk-reducing measures. The central research question is as follows:

How does a trajectory prediction-based estimation method improve our understanding of the integral image of drifting ship allision probabilities in the Dutch North Sea region to provide well-substantiated insights for risk-reducing measures?

1.2.1. Research objectives

To be able to answer this question, three objectives are defined:

- **Explore state-of-the-art methods for estimating the probability of drifting ship allisions and identify potential areas for improvement in these techniques:** The first objective includes examining the different types of collisions and the methods used to estimate their probabilities, thereby establishing a theoretical foundation of risk assessments in the field of maritime safety. By discussing probability estimations specifically related to drifting ships, the aim is to identify areas for improvement and highlight the potential benefits of such improvements.
- **Explore the advancements and substantiation offered by a trajectory prediction-based approach to estimating the probability of drifting ship allisions:** The second research goal is to develop and outline a new method that integrates trajectory predictions to calculate allision probabilities. In this phase, we will formulate and substantiate necessary assumptions and simplifications, which are essential for developing a robust method to estimate the probability of allisions across multiple wind farms. The focus here is not on creating a finalised operational model but rather on demonstrating how this method offers improvements in estimating the probability of drifting ship allisions.
- **Evaluate the practical implications of a trajectory prediction-based approach to estimating the probability of drifting ship allisions for optimising risk-reducing strategies:** The final objective is to assess the practical implications of the new method by interpreting the calculated allision probability distributions across multiple wind farms. This involves analysing the overall distributions, as well as variations in these distributions under the influence of specific environmental conditions. These interpretations will serve as the foundation for outlining the potential value of these insights in improving the effectiveness of risk-reducing measures.

1.2.2. Research questions

Each of the defined research objectives is translated into a sub-question.

Sub-question 1

The first sub-question forms the basis of this study and lays a theoretical foundation by exploring how the probability of a drifting ship allision is currently determined:

1. How do state-of-the-art methods determine the probability of drifting ship allisions, and what potential areas for improvement can be identified in these techniques?

This question will allow us to contextualise a method based on trajectory prediction within the research landscape.

Sub-question 2

Next, a method will be developed based on a trajectory prediction model to examine potential improvements in estimating allision probabilities:

2. How does a trajectory prediction-based method advance and substantiate drifting ship allision probability estimations in the North Sea?

To develop this method, a supplementary literature review is conducted to examine existing drift motion models. This review aims to justify the selection of a specific drift motion model. It will provide an overview of the available types of drift motion models, focusing on one model in particular that will be used to calculate the probability of drifting ship allisions across multiple wind farms.

Using this model, we will explore the trajectory of a drifting ship through two key questions; (i) how do environmental and geometrical parameters affect a ship's trajectory, and (ii) can these effects, as analysed using the model, be validated against real-world cases to assess the model's performance?

Identifying and quantifying the parameters that influence a ship's drift trajectory is important for integrating them into our probability calculation method. By comparing the model results with real-world cases, we aim to analyse the same influences that are embedded in the drift motion model. By evaluating its performance and subsequently confirming its validity, we can strengthen the integration of this model into an allision probability estimation method. Using our understanding of ship drift trajectories, we will develop a theoretical framework for integrating trajectory prediction into an allision probability estimation method for a single starting location of a ship's drift.

Sub-question 3

The established method will be implemented across multiple wind farms to create and assess the implications of its insights:

3. What are the practical implications of a trajectory prediction-based method for estimating the probability of drifting ship allisions to improve risk-reducing strategies for maritime safety in the North Sea?

Here, we face the challenge of extending the method to multiple wind farms. By analysing each assumption and simplification through results from the established method, we aim to achieve a computationally efficient implementation while maintaining reliability and validity. The implementation will result in probability distributions around multiple wind farms, and these results will be central to identifying the improvements brought by this new method. The insights will involve interpreting the results, identifying areas of high probability, and demonstrating how these areas vary with drift duration. Additionally, these findings will be compared with probability distributions under the influence of specific environmental conditions. Subsequently, the focus will shift to how these insights are relevant for the implementation of risk-reducing measures.

1.3. Report structure

To summarise, the present research aims to offer an improved understanding of the probability of drifting ship allisions across the North Sea through three main objectives: First, it explores state-of-the-art methods for determining the probability of drifting ship allisions and tries to identify potential areas for improvements in these techniques. Subsequently, the present study introduces a trajectory prediction-integrated method for estimating allision probabilities, demonstrating its improvements over state-of-the-art methods. Finally, by applying the established method to multiple wind farms and interpreting the results, the present study seeks to provide new insights valuable for optimising risk-reducing measures. Figure 1.1 provides an overview of how these objectives are structured throughout this study.

Figure 1.1: Report structure

2

Literature study

Chapter 2 presents a literature review on the available methods for determining the probability of drifting ship allisions. This review explores the state-of-the-art methods for determining the probability of drifting ship allisions and tries to identify potential areas for improvements in these techniques. The chapter begins with an overview of ship collision risk assessments for maritime safety, specifically highlighting the use of probabilistic methods to determine these risks. It then addresses research specifically focused on allision risks and introduces the methods currently used to estimate the probability of allision. Finally, the chapter examines how drift motion is incorporated within some of these methods.

2.1. Methodology of literature review

To carry out the present literature review, extensive literature was gathered from the databases Google Scholar and Science Direct. A keyword search was performed using the following terms: *(”drifting ship” OR ”drifting vessel”) AND (”collision risk” OR ”collision probability” OR ”allision probability” OR ”allision risk”)* to collect all literature related to the risk assessment of drifting ship allisions. All titles and abstracts of articles obtained through this keyword search were examined to exclude references that were not closely related to the topic. This literature search revealed that methods related to the risk of drifting ship allisions are not extensively studied in the available literature but are mainly developed commercially. To understand how these commercial methods work, snowballing was used to investigate the references cited in the initial literature, complemented by specific Google searches focusing on the commercial methods that were mentioned. This search was completed on January 22, 2024. Further research was conducted to gain a comprehensive understanding of these conventional methods and to reveal possible limitations. These studies examined the objectives of ship collision risk assessments for maritime safety, particularly those conducted for the North Sea.

2.2. Purpose of ship collision risk assessments for maritime safety

Protecting marine infrastructure, especially offshore wind farms, is important to prevent undesirable events such as ship collisions and ensure their operational reliability. This is especially important given the increasing reliance on energy generated from offshore wind farms in the future. The European Union SAFESHIP project, titled 'Reduction of ship collision risks for offshore wind farms', highlights that the nature of consequences of ship collisions can vary considerably. According to Friis-Hansen et al. (2004), the potential consequences of incidents can be categorised into five groups: health and life impacts on human beings, environmental impacts, economic impacts, social impacts, and ethical, political, and legal impacts.

A risk perspective in the maritime industry, with special attention to maritime transportation systems, is considered to include:

- a set of plausible scenarios leading to an accident,
- the probabilities of unwanted events within these scenarios,
- the consequences of the events and a description of uncertainty,

according to Montewka, Goerlandt, and Kujala (2014).

The International Maritime Organisation (IMO) has developed a rational and systematic process for assessing the risks associated with shipping activities and, by extension, for evaluating the cost-benefits of risk reduction. An example flowchart of this method is shown in Figure 2.1.

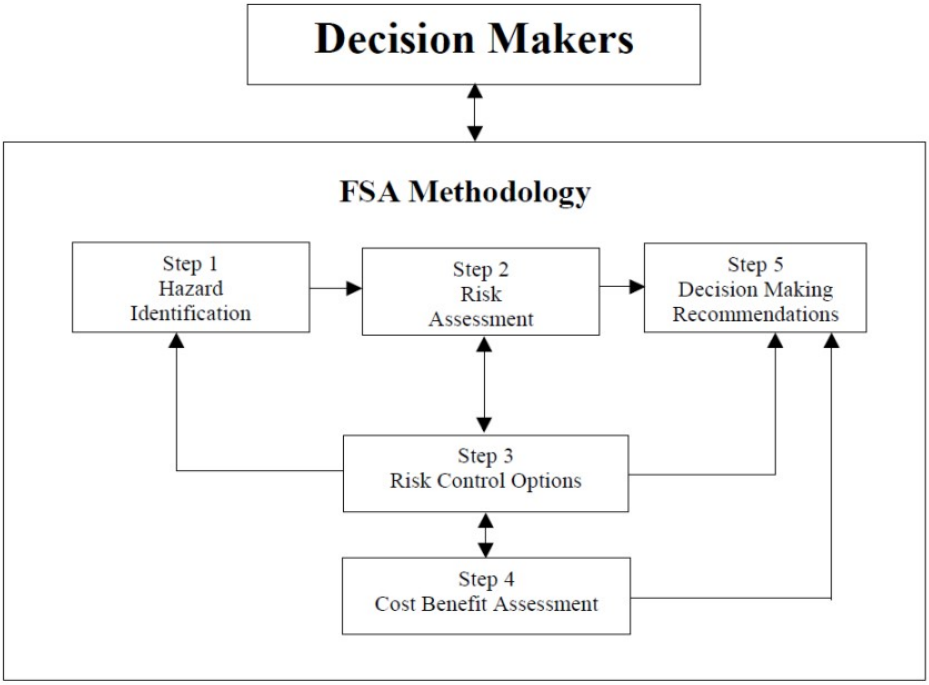

Figure 2.1: Formal Safety Assessment flowchart (IMO, 2018)

In the Netherlands for example, during the approval process of offshore wind farms in the Netherlands, a Navigational Risk Assessment (NRA) is carried out by Rijkswaterstaat. The purpose of this NRA is to assess the risk of shipping accidents near offshore wind farms. The Dutch authorities prefer to conduct this NRA according to the FSA methodology and often choose to use MARIN's 'Safety Assessment Models for Shipping and Offshore in the North Sea' (SAMSON) for quantitative probability and consequence calculations. However, this preference for methodology and models varies by country (Mehdi et al., 2018).

The techniques used for assessing risks, including models like SAMSON, vary from qualitative to traditional quantitative methods. Many factors can influence the choice between a qualitative and a quantitative risk assessment. Obviously, if data needed for analysis are not available, it becomes impossible to carry out a quantitative risk assessment because of concerns about unreliability and invalidity. Reliability refers to the consistency of results when repeated and validity to whether the analysis addresses the intended concepts. In a case study examining ship-ship collision risks, Goerlandt and Kujala (2014) suggest that relying on probability-based risk perspectives may not consistently produce a reliable risk picture. Therefore, it is reasonable to moderate claims regarding the numerical accuracy of probability-based risk calculations.

The significant consequences of ship collisions and the accuracy of ship-ship collision probability estimations provide a good basis for focusing on the methods used to understand the threat addressed in the present study: drifting ship allisions. A risk of collisions is, as described by Goerlandt and Montewka (2015), often considered a product of probability and potential consequences of a certain threat. The present literature review adopts this definition, but focuses on the methodologies for determining the probability of drifting ship allisions.

On behalf of Rijkswaterstaat, MARIN carried out a study of the impact of additional wind farms in the North Sea, as outlined in the Dutch government's Roadmap 2030, on maritime safety. This study included both a quantitative analysis, calculating the probability of collisions, and a qualitative analysis, looking at the effectiveness of various preventive and mitigating measures. The research results indicated that none of the measures evaluated, individually or in combination, can reduce the risk sufficiently to uphold current safety standards (Duursma et al., 2019). ERTVs are the only implemented measure that effectively reduces the risk of drifting ship allisions, as they can prevent such allisions while drifting. Additional wind farms in the North Sea result in a shorter reaction time to intervene when ships become adrift. Therefore, a larger number of ERTVs is needed to adequately address this problem. This is supported by the research conducted for the SAFESHIP project, which showed that the collision frequency depends considerably on the location and number of ERTVs (Friis-Hansen et al., 2004).

In response, MARIN conducted a study to identify wind farm areas where the risk of ship collisions is higher. The aim of MARIN's research is to enable a more targeted deployment of risk mitigation measures, such as ERTVs and Vessel Traffic Management (VTM) (Nap, 2022). This research involved mapping key risk indicators, determining whether they represent a permanent or dynamic risk and investigating how these indicators vary between different wind farms. Each indicator was assigned a weighted score on a scale from -2 (indicating a significant contribution to collision risk) to +2 (indicating a significant reduction in risk) for each wind farm area. The weight of each indicator is aggregated for each wind farm area. These research results indicate that Borssele, Hollandse Kust West and Hollandse Kust Zuid have the highest permanent risk profiles of all wind farm areas. This is also supported by the results of the SAMSON model calculations, as described in Duursma et al. (2019). Figure 2.2 indicates the locations of these wind farms.

Regarding the environmental conditions considered in the second study by MARIN, it is important to note that the influence of waves was excluded due to insufficient data. Furthermore, similar to other indicators, wind and current conditions are represented as weighted values. This representation may not adequately reflect the actual conditions, especially considering that the study is intended to inform the deployment of ERTVs. A more thorough analysis of the influence of environmental conditions on the probability of drifting ship allisions could offer a new perspective, suggesting that certain wind farms may have a higher risk profile than others. Consequently, a more accurate risk profile could improve the effectiveness of risk-reducing measures, such as the deployment of ERTVs. This approach could also improve quantitative models like SAMSON by providing more accurate probability estimations. However, a deeper understanding of such quantitative risk assessment models is required.

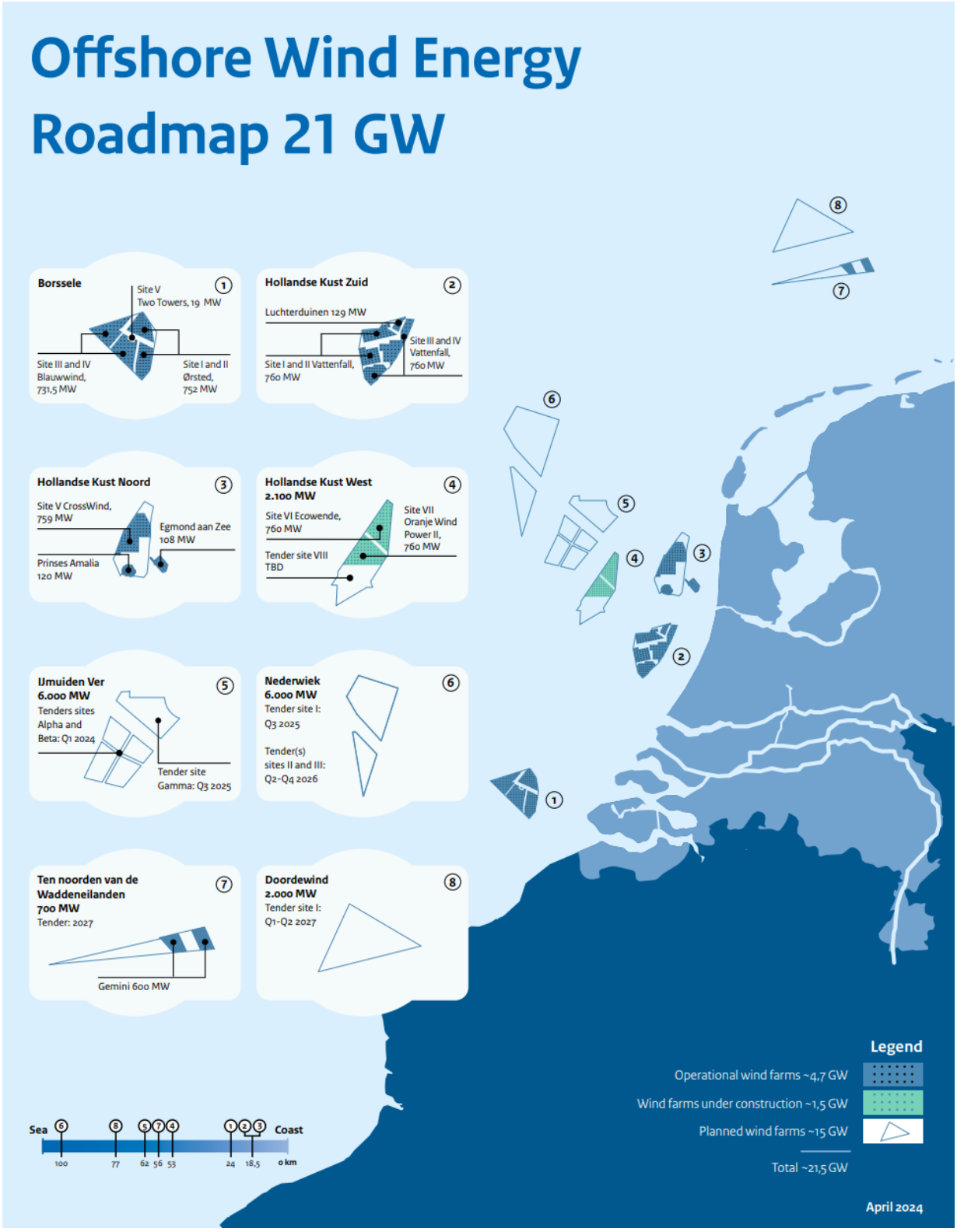

Figure 2.2: North Sea wind farms (Government of the Netherlands, 2024)

2.3. Ship collision types and their assessment methods

When assessing ship collision risks, we are essentially trying to understand potential threats to ships and marine infrastructure. These assessments can be specific, focusing either on methods to prevent collisions between individual ships or on the overall risk of collisions. Research on ship collisions shows a wide range of approaches, from small-scale studies focused on individual ships to large-scale studies assessing occurrence rates in a given geographical area. Collision risk assessments of individual ships are crucial for collision avoidance and primarily focus on ship dynamics. Therefore, these assessments are mainly embedded in collision avoidance systems. On the other hand, risk assessments conducted on a much larger scale are designed to assess safety within a specific area and tend to rely more on statistical data. The latter, a macroscopic approach, corresponds to the type of assessment studied in this research. In the upcoming sections, macroscopic probabilistic methods for determining two types of collision risks are discussed: ship-ship collisions and collisions with marine infrastructure.

2.3.1. Probability of ship-ship collisions

When examining collision risks from a broader perspective, the risk of ship-ship collisions stands out as a separate topic of study. According to P. Chen et al. (2019) there are two ways to estimate the probability of a collision between ships: a statistical estimation method and a synthetic estimation method.

The statistical approach estimates the probability using techniques such as statistical analysis and regression on historical accident data and traffic information (e.g. Kujala et al., 2009). The synthetic approach estimates the probability of ship collision using a framework proposed by Fujii and Shiobara (1971):

$$P_{Collision} = N_{Candidate} \times P_{Causation} \tag{2.1}$$

This formula determines the probability of a collision between ships by two components: the number of collision candidates, also known as geometric probability, and the causal probability. Collision candidates are ships positioned in scenarios where there is a potential for collision. The number describes either the probability of a collision candidate or a collision candidate frequency. Assuming the presence of a collision candidate, the causation probability indicates the probability of an actual collision occurring due to factors like human reliability, organisational issues, or mechanical defects.

Geometric collision probability analysis requires mathematical modelling to identify potential collisions based on traffic statistics (Lušić & Čorić, 2015) or, more specifically, analysing overlaps of predefined ship-domains, indicating that a ship is involved in an encounter with a potential for collision (Chai et al., 2017). In causation probability analysis, probabilities are determined by analytical methods such as Fault Tree analyses (Martins & Maturana, 2010) or Bayesian networks (Montewka, Ehlers, et al., 2014). A Fault Tree analysis is a method to analyse system failures. It uses a tree-like diagram to illustrate the logical relationships between events and faults that lead to a failure. A Bayesian network is a graphical model representing probabilistic relationships between variables. Both methods are well suited to integrate multiple sources of information, such as historical data and expert interviews.

P. Chen et al. (2019) conclude that the geometric probability analysis methods carry the risk of over/underestimating the results. This is because the probability estimates are derived by analysing specific data intervals. Regarding the methods within causal probability analysis, P. Chen et al. (2019) conclude that the lack of data and uncertainty is still a problem to obtain accurate and reliable estimates. These findings reveal that simplifying a complex environment for macroscopic probability calculations and the lack of relevant data present significant challenges. Such challenges will allegedly impact the probability calculations of drifting ship collisions. Therefore, it is important to balance the level of detail in these calculations.

2.3.2. Probability of collisions with marine infrastructure

The EU supported SAFESHIP project was launched to explore technologies that could mitigate collision risks and develop assessment methodologies specifically for offshore wind farms. This project gives an overview of the methodologies used to evaluate the risk of ship-marine infrastructure collisions. This project identifies two distinct scenarios regarding ship collisions with fixed offshore installations, like offshore wind farms.

1. Collision of powered ships
2. Collision of drifting ships (referred to as 'allision' in this study)

In addressing the collision probability of powered ships, the SAFESHIP project adopts the same approach as ship-ship collisions. The number of collision candidates is determined by the area under the relevant distribution function of ship traffic. This area is constrained by the projection of the respective wind turbine and half of a ships' width on both sides of the projection, as indicated by the collision diameter in Figure 2.3 (Friis-Hansen et al., 2004). The probability of a ship not recovering from a collision course is established by considering the likelihood of no corrective action being taken. This probability is also determined by analysing historical accident data or by means of analytical methods such as Fault Tree analyses or Bayesian networks, although based on other causation variables.

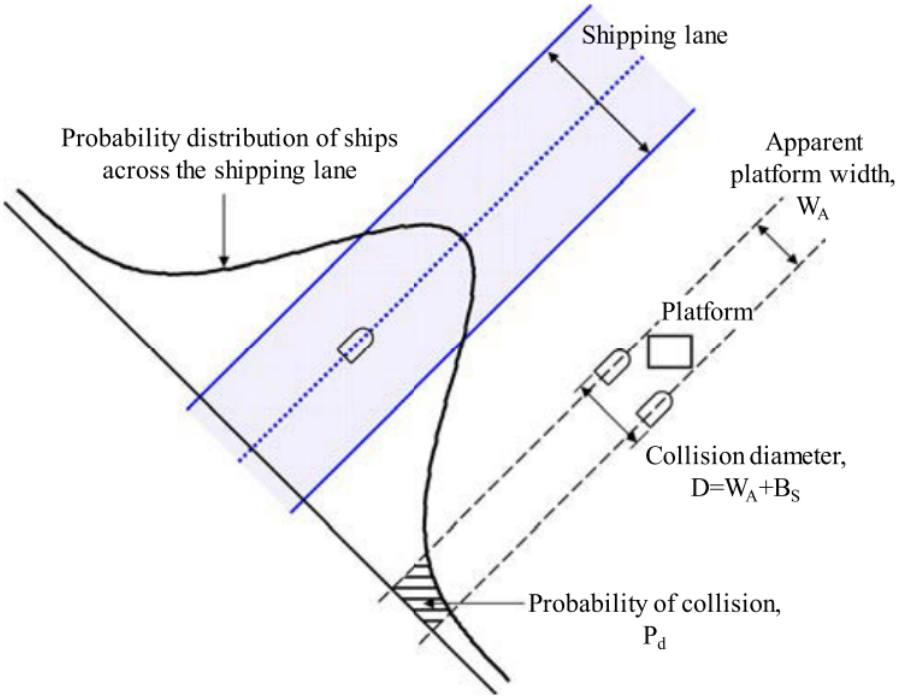

Figure 2.3: Visualisation of the area indicating a collision under the relevant distribution function of ship traffic (Kim et al., 2021)

For drifting ships, the allision probability is influenced by five factors:

1. failure rate of propulsion system,
2. time to repair before allision,
3. emergency anchoring,
4. recovery by salvage tugs, and
5. the drift motion of the ship, depending on the existing wave, current, and wave conditions and ship size and type.

There are several collision risk models developed that consider both powered and drifting ship allisions. The available collision models and the companies responsible for development are given in Table 2.1.

Model	Company
COLLIDE	Safetec Nordic AS
COLLRISK	Anatec UK Ltd
COLWT	Germanischer Lloyd (GL)
CRASH	Det Norske Veritas (DNV) (Spouge, 1991)
DYMITRI	British Maritime Technology (BMT) Limited
SAMSON	MARIN (Koldenhof, 2021)

Table 2.1: Collision risk calculation models

The SAFESHIP project concluded, upon reviewing the models COLLRISK, COLWT, and SAMSON, that all models cover the most important influencing factors of drifting ship allisions. However, these factors are treated with different levels of sophistication.

The SAMSON model determines the probability of drifting ship allisions by:

- a danger part, indicating whether a ship's drift motion causes an allision,
- an engine failure probability per sailed mile, and
- a repair and anchor function, corresponding to self-initiated allision avoidance measures.

A similar method is used in the CRASH model:

$$P_{CD} = N \cdot F_{\text{drift}} \cdot T \cdot P_{D1} \cdot P_{D2} \cdot P_{D3} \tag{2.2}$$

Where:

N is the number of ships per year within the considered area,
F_{drift} is the frequency of drifting/machinery breakdown per hour while in the considered area,
T is the number of hours a ship is in the considered area,
P_{D1} is the probability of unfavourable drift direction,
P_{D2} is the probability of no effective external assistance,
P_{D3} is the probability of no allision avoidance by own measures.

Both models have a similar approach to calculating the probability of drifting ship allisions. The SAMSON model uses a so-called 'danger area' for specific sets of wind conditions and ship types to indicate when the drift motion of an adrift ship will result in an allision. In the CRASH model, this is embedded as a probability of an unfavourable drift direction. By identifying which ships and under the influence of what conditions will result in an allision, and combining this with the probability of engine failure and the probability of ship presence—represented as N, the number of ships per year, and T, the average time spent in an area—we can calculate the probability of drifting ship allisions, excluding any risk-reducing factors

Both models incorporate risk-reducing factors. Allision avoidance through self-initiated measures includes repairing the engine within a specified period and performing emergency anchoring procedures. The approach to engine repair is primarily based on available historical statistics of engine failures. Performing an emergency anchoring procedure depends on factors such as drifting speed, ship size, weather conditions and the composition of the seabed. The models also consider collision avoidance through external assistance, such as an ERTV. This probability is directly influenced by the drift motion of the ship. The closer an ERTV is to a certain area, the greater the probability of effective external assistance in that area. Therefore, we will explore in greater detail how these methods incorporate the drift motion of a ship and how they define the probability that its drift causes an allision.

2.4. Probability of a drifting ship causing an allision

The drift direction, or more specifically, the trajectory of a disabled ship, determines whether it will collide with a structure. To effectively reflect the probability of an allision, this measure of unfavourable direction must accurately represent the ship's trajectory. Therefore, we will first review the methods for determining how a ship's drift causes an allision as embedded in the risk assessment models. This review will cover multiple models, highlighting the lack of detailed explanations available for each model (Mehdi et al., 2018). Subsequently, we will explore how the drift motion of a ship is theoretically determined according to the available literature on drift motion.

2.4.1. Methods for determining the probability a ship's drift causes an allision

As mentioned in the previous section, the SAMSON model uses a 'danger area' for specific sets of wind conditions and ship types to indicate when the drift motion of an adrift ship will result in an allision. Given a certain wind direction and ship type, the danger part can be illustrated as shown in Figure 2.4.

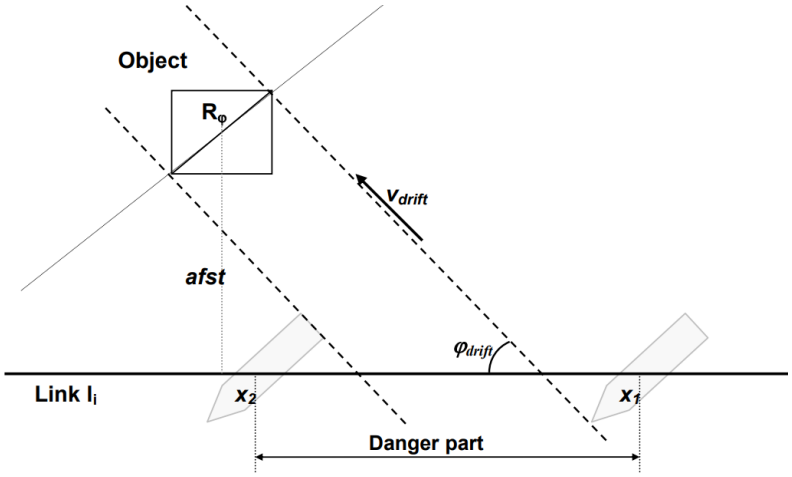

Figure 2.4: Illustration of defining the danger part around an object for a specific link, wind direction and ship type.

Another model from Safetec Nordic AS, the COLLIDE model, uses a similar approach by defining 'box' lengths for specific wind directions.

$$P_{CD} = N_b \cdot P_b \cdot P_w \cdot D/BL \tag{2.3}$$

Where:

- N_b is the annual number of ships in the box affected by the specific wind direction towards the platform,
- P_b is the breakdown probability, which is the recovery failure rate along the drifting lane,
- P_w is the probability of a particular wind direction,
- D is the allision diameter,
- BL is the box-length perpendicular to the wind direction (see Figure 2.5).

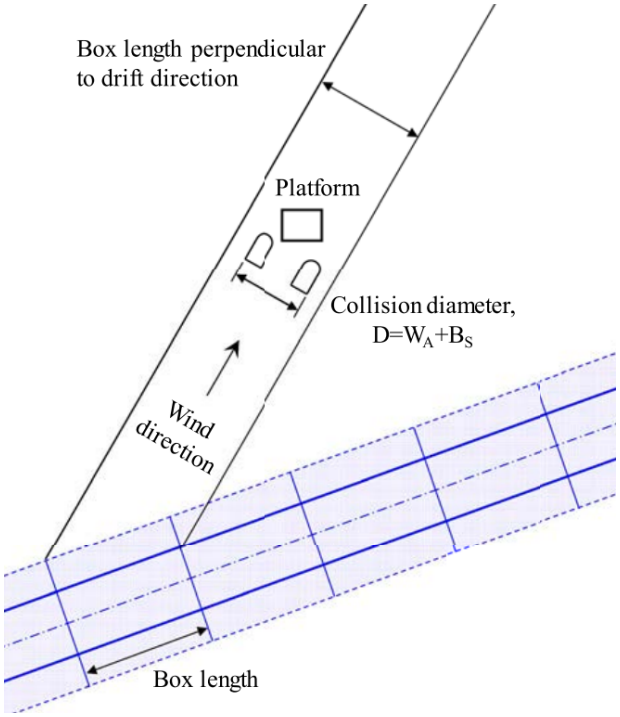

Figure 2.5: Illustration of defining the box length around an object (Kim et al., 2021)

These approaches result in wind direction-specific areas within which an adrift ship will cause an allision over time. The probability of this specific situation, therefore, depends on the wind direction and is suggested by Ellis et al. (2008), a report from SSPA Sweden AB, to be calculated using wind direction statistics with the following formula:

$$P_{D1} = \sum_{w=1}^{N_{wd}} \left(\frac{R_w \times \alpha_w}{360/N_{wd}} \right) \tag{2.4}$$

where:

N_{wd} is the number of divisions in different wind directions.
α_w is the angle covered by the wind farm in the wind direction w.
R_w is the frequency for wind from direction w.

Alternatively, the model developed by GL and COLWT determines the probability of this unfavourable direction by applying a Monte Carlo technique on available wind data (Povel, 2006).

The next step is determining whether the drift motion of a ship, its trajectory, will result in an allision over time. Ellis et al. (2008) evaluates the models SAMSON, COLWT, and CRASH, concluding that the assumptions made about the influence of the forcing environment on the ship's drift motion are consistent:

- the wind and waves act in the same direction
- the wind direction and velocity are kept constant during the drifting
- mass effects are not included in the model
- the forces consist of the wind force, the averaged second order wave force and the resistance of the ship through the water
- the effective allision width is the ship length plus the dimension of the object perpendicular to the drifting path

What remains is the time until allision, which can be determined by the drift velocity. In the SAMSON model, this drift velocity is determined for a specific ship type, in a certain loading condition, by wind and wave belonging to a certain Beaufort class. Details on how the SAMSON model calculates wind and wave forces, as well as wave resistance, are provided in Appendix A. Both wind and resistance forces are derived using the drag formula, which relates the force experienced by an object moving through a fluid to the fluid's density, the object's velocity, and its exposed surface area. In contrast, the calculation of wave force is based on an empirically derived coefficient that accounts for wave-induced drift, reflecting the complex interaction between ships and waves.

As stated in an international comparison of navigational risk assessment processes by Mehdi et al. (2018), these models are commercial and lack comprehensive documentation. Therefore, it is challenging to ascertain the data on which these calculations are based and to what degree they are reliable. To the best of our knowledge, the model suggested by SSPA Sweden AB calculates the probability of an unfavourable drift direction, followed by a drift speed calculation considering potential wind, wave, and current forces. Moreover, the SAMSON model accounts for the current as an estimated speed in the direction of the drift velocity but does not account for its direction, as noted by Ellis et al. (2008). To substantiate such assumptions requires extensive knowledge of the drift motion of a ship.

2.4.2. The representation of drift motion

To most effectively represent the probability of an unfavourable drift direction (P_{D1} in formula 2.2), it is important to understand the drift motion of a ship. This understanding involves introducing the physics of drift motion.

The motion of a drifting object is the cumulative outcome of various forces exerted upon this object. According to Hackett et al. (2006), the position of a floating object is determined by numerically integrating its total drift velocity (V_{drift}), where (V_{drift}) equals the sum of ($V_{current}$), which represents the ocean current velocity relative to Earth and (V_{rel}), which represents the object's drift velocity relative to the surrounding water:

$$V_{drift} = V_{current} + V_{rel} \tag{2.5}$$

The ocean current velocity includes the surface current and the Stokes drift induced by the waves. Surface currents can be further divided into tidal currents and inertial currents, among others. This ocean current velocity is commonly equated with the (near-) surface current derived from a numerical model. Such models utilise a parameterisation based on wind velocity, and/or local observations. The underlying assumption for using such models is that the ocean current velocity uniformly impacts all floating objects. The object's drift velocity relative to the surrounding water is the sum of the wind and wave forces exerted upon its surface, and is strongly dependent on the characteristics, like geometry, of the object. According to MacDonald et al. (1999), the equilibrium of forces acting on the ship can be visually represented, as depicted in Figure 2.6, and can be expressed as:

Where:

F_{wind} is the wind drift force acting on the ship,
F_{wave} is the wave drift force acting on the hull,
f_{form} is the form drag or damping forces exerted by the water on the hull due to the relative motion,
f_{wave} is the wave damping (a counter force that occurs as the moving hull generates its own wave field.

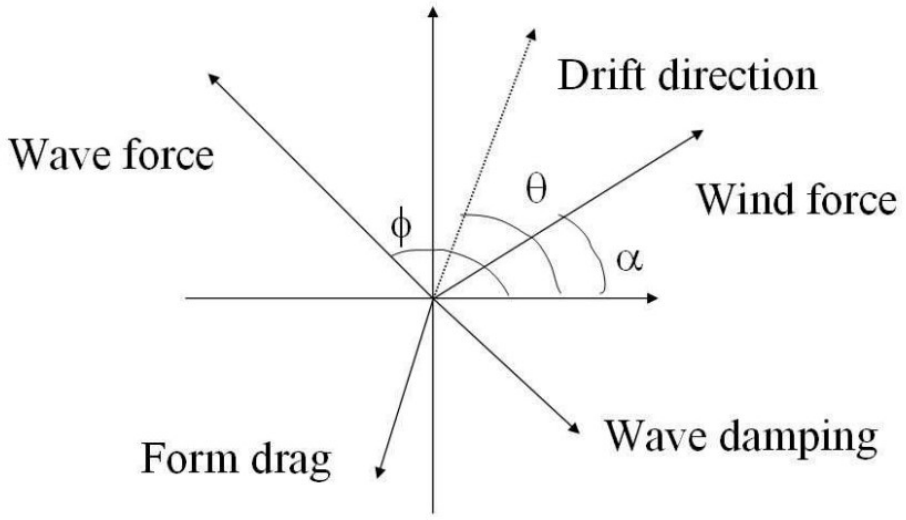

Figure 2.6: Forces acting on a drifting ship (Hackett et al., 2006)

Predicting the drift of objects, such as ships in the present literature review, is challenging because of its reliance on empirical formulas. This challenge is compounded by the fact that crucial information, such as ocean current velocity, often comes from numerical models. Consequently, we face unavoidable uncertainties in the wind, wave and current data that drive the drift models. To address these uncertainties, a probabilistic framework is a practical solution. This involves assigning probabilities to key parameters, allowing a series of numerical integrations to be performed for improved prediction accuracy.

On the other hand, according to Hackett et al. (2006), the drift motion of ships is approached with a more analytical methodology, using insights from ship architecture and hydrodynamics. For example, the ship drift model developed at the Meteorological Institute of Norway is based on estimates of wind and wave-induced forces to calculate a ship's drift velocity (Hackett et al., 2006). The key advantage of this approach lies in its ability to reduce the knowledge required of the object to a few essential parameters. Another significant finding relevant for the drift analysis of ships, reveals that the relative drift speed of a ship undergoes a rapid increase, typically within 2-10 minutes, toward a stationary solution. Therefore, for simulations of several hours or longer, it is not necessary to integrate the acceleration in time. Instead, a good approximation can be achieved by applying the stationary solution.

The calculation of drift motion and the formation of a drift trajectory are, in theory, more complex than the assumptions made in current models suggest. Whether these assumptions remain valid requires analysis of real-world cases.

2.5. Knowledge gaps

Following an extensive exploration of the probability of drifting ship allisions, we have identified knowledge gaps regarding the validity of these probability estimations and its use for risk-reducing purposes.

2.5.1. The validity of state-of-the-art probability estimations

The methods used to assess allision risks involving drifting ships rely on several assumptions. Furthermore, these methods are not documented in detail, making it difficult to verify their validity. The extensive coverage in literature of detailed methods and studies focused on ship-ship collisions, along with concerns about the reliability and validity of these macroscopic approaches, indicates a need for further research into drifting ship allisions. It is important to determine the most reliable and valid approach for representing the risk of drifting ship allisions. This could challenge the assumptions made in current models, which include a predefined drift direction based on wind direction (assuming alignment with wave direction), a purely lateral drift motion (one degree of freedom), and the way the influence of the current is accounted for. Variations in these assumptions lead to considerable differences in estimated allision frequencies (Ellis et al., 2008). Therefore, it is important to understand the parameters that influence a ship's trajectory and the extent to which they do so. Analysing actual trajectories of drifting ships can provide a strong foundation for making assumptions and, ultimately, defining how to accurately represent a ship's drift motion.

2.5.2. Limited insights of probability estimations for risk-reducing purposes

Regarding the assessment of allision risks over larger geographical areas, current models are primarily used for assessments of individual wind farms. Existing research on allision risks within the Dutch North Sea region is limited to:

- A quantitative assessment by the model SAMSON, focusing on the increase in overall ship allision risks with the expansion of offshore wind farms, and
- A qualitative assessment aimed at identifying wind farm areas at a higher risk of ship collisions.

The quantitative assessment results in a probability value, which can be translated into an occurrence rate per wind turbine. Furthermore, in addition to the probability of unfavourable drift direction, this value also accounts for the influence of allision avoidance through own measures and external assistance such as ERTVs. Despite this, a qualitative assessment is conducted for the use of ERTV positioning.

Both assessments fall short in offering strategic insights necessary for the effective implementation of risk-reducing measures. Insights into available response times, and the origins of potential threats are not thoroughly discussed in these assessments. Such insights, and additionally, a better understanding of the impact of dynamic factors such as weather conditions and shipping activity, can be valuable for risk-reducing strategies.

3

Trajectory prediction-based method

For the sake of structure and clarity, the various components of the probability of allision will be explained in advance. For a certain area, the probability of allision is determined by:

1. **the probability of presence of an adrift ship**
2. **the probability of a drifting ship causing an allision**
3. **the probability of allision avoidance**

The probability of presence of an adrift ship is determined by the probability of engine failure, the number of ships in an area, and the average time a ship spends in that area. The probability of engine failure may vary depending on location, which can be determined using historical data. However, for the purposes of this study, it is assumed to be constant across the North Sea. Given this assumption, the presence of more ships at a location over a certain period increases the probability that a ship will become adrift there. For instance, the presence of ships can be determined by multiplying the number of ships per year passing certain areas by the number of hours a ship is present in those specific areas. These values are then multiplied by the probability of engine failure per ship per hour. This multiplication yields a probability distribution across the specific areas, indicating where the probability of the presence of an adrift ship is highest. For simplicity, besides assuming it constant, the probability of engine failure is neglected in this study. The probability of the presence of an adrift ship is further simplified to represent shipping density, denoted by $P_{activity}$ in Figure 3.1. The higher this density, the greater the likelihood that a ship will become adrift at that location compared to other areas. Consequently, the allision probability in this study does not represent actual allision occurrence rates but rather comparative values or probability levels.

The focus of this study is on the likelihood of a drifting ship causing an allision. In the present study, the probability of a drifting ship causing an allision, represented by P_{drift} in Figure 3.1, will be assessed using trajectory predictions. The method for calculating P_{drift} will be introduced in Section 3.4. This method consists of the following components:

- P_{sim} is the probability that a specific ship allides with a wind farm under the influence of specific environmental conditions based on an analysis of its trajectories.
- P_{env} is the probability that certain environmental conditions are present.
- Both combined result in P_{drift}: the probability that a drifting ship allides with a wind farm from a certain starting location, considering all possible environmental conditions.

The third and last component of the probability of allision, the probability of allision avoidance by either self-initiated measures or external interventions, is neglected in this study. Therefore, the probability of allision is in this study estimated by the components $P_{activity}$ and P_{drift}, as illustrated in Figure 3.1.

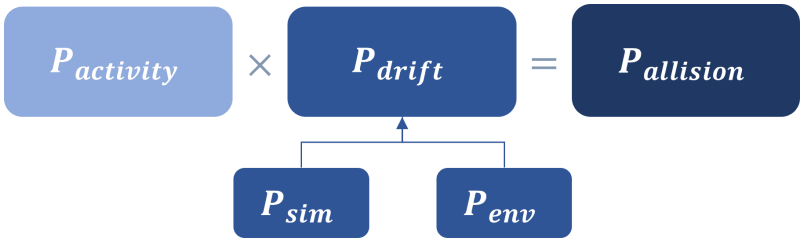

Figure 3.1: Components of method for calculating $P_{allision}$ in this study

The established method for P_{drift}, as will be introduced in Section 3.4, is applied to calculate this value across multiple areas, each corresponding to the start of a ship's drift. As previously mentioned, for each starting location, the P_{drift} value will then be multiplied by the area's corresponding shipping density value, representing the probability of presence of an adrift ship. Thus, the resulting allision probability, denoted by $P_{allision}$, is defined as the probability that an allision occurs given the ship's starting location. It is important to reiterate that these $P_{allision}$ values represent relative probability levels rather than actual occurrence rates. They do not take into account the probability of engine failure or the probability-reducing effects of either self-initiated measures or external assistance. These calculated probabilities provide a distribution of the probability of an allision around a wind farm and indicate areas for which starting locations the probability of an allision is highest compared to other locations.

Referring back to the identified knowledge gaps in Section 2.5, starting from the a ship's drift trajectory enables us to make substantiated assumptions for calculating the drift probability. Following this objective, we aim to improve our understanding of the integral image of drifting ship probabilities in the Dutch North Sea and offer a way of generating insights valuable for optimising risk-reduction strategies. In Section 3.1, we discuss existing ship drift trajectory prediction models and select a model for this study. In Section 3.2, we examine a ship's trajectory's sensitivity to environmental conditions and ship geometry to identify challenges in accurately calculating a ship's drift trajectory. In Section 3.3, it will be investigated whether these effects can be validated using a real-world case to assess the performance of the model and to strengthen the concept of using it to calculate the drift probability. The model selection and trajectory and performance analysis aim to establish a valid an reliable approach to calculating a ship's trajectory and to determine what parameters are necessary to calculate P_{sim}, the probability of allision corresponding to a single trajectory prediction.

Section 3.4 introduces a scenario-based method for calculating the drift probability P_{drift} using OpenDrift simulations. First the probability that an adrift ship will allide with a wind farm under the influence of specific environmental forces (P_{sim}) based on an analysis of its simulated trajectories is defined for this study. Next, it is discussed how to account for the variety of environmental conditions to which an adrift ship can be subjected and their probability of occurrence (P_{env}). Both aspects come together in Section 3.4.2, where it is explained how P_{drift} is determined for a single location using OpenDrift simulations. Finally, several decisions regarding the calculation of P_{drift} for this study will be discussed. It is crucial to ensure that the environmental conditions used to simulate drift trajectories are a valid representation of the variety of environmental conditions for calculating P_{drift}. However, this should be done in a way that does not lead to excessive computation time, ensuring the method to calculate P_{drift} remains feasible for expansion to multiple wind farms.

3.1. Rationale and model selection for trajectory prediction

To substantiate the proposition of integrating trajectory prediction into probability analysis, two other research projects that incorporate trajectory-based probability models are discussed. Subsequently, we explore the available drift trajectory models for large ships. Next, a model is selected which will be used to calculate P_{sim} in this study. This model is explored in detail.

3.1.1. Cross-industry reference of trajectory-based probability models

The probability of a drifting ship allision can be estimated quite accurately when its trajectory is known. Given the uncertainty in parameters such as environmental conditions, the ship's geometry, and its orientation relative to the environmental forces, calculating its exact trajectory is difficult. By computing across a range of these uncertain parameters, using a technique similar to a Monte Carlo method, we can gain insights into the possible final positions of a ship after a certain duration.

The relevance of this method for calculating collision probabilities is supported by benchmarking in various industries, with two notable examples: its use in trajectory prediction for ship collisions in inland waterways (Hörteborn & Ringsberg, 2021) and air traffic control (Crisostomi et al., 2008)

The first study develops a methodology for using AIS data and a ship manoeuvring simulator to simulate and analyse collision risks. The study covers three events that could lead to a ship-bridge collision: a drifting ship, a sharp turning ship and missing the turning point. The ship manoeuvring simulator was used to perform Monte Carlo simulations for these three events around the Great Belt bridge.

In the second study, the aim is to calculate and update potential aircraft trajectories using the estimated position and status of the aircraft, intention information, weather data and a performance model. These potential trajectories create an empirical distribution useful for estimating various factors, including the probability of conflict and expected arrival time.

As noted by 'An introduction to Monte Carlo simulations' by Harrison (2009), while there is a wide variety of Monte Carlo methods, many simulations tend to follow a similar pattern:

1. Generate initial states or inputs (the unknowns) randomly or by sampling from a system of probability density functions.
2. Perform computations based on these initial states or inputs.
3. Collect and analyse the results from each computation to derive the statistics of interest.

The research on ship collisions with the Great Belt Bridge suggests that employing a Monte Carlo approach is a viable method for calculating the probability of drifting ship allisions. However, as will be explained further on, such a simulator may be too ship-specific to compute probabilities across the Dutch North Sea region. This is because, as the area considered increases, more variables, such as environmental forces, shipping activity, and offshore infrastructure, need to be taken into account. To identify a model suitable for calculating trajectories, and consequently, allision probabilities across the entire Dutch North Sea region, we will explore the models available for describing drift motion.

3.1.2. Existing drift trajectory models

Research on object drift plays an important role in improving maritime safety, environmental conservation and the effectiveness of rescue missions. In the field of maritime safety, understanding the drift of large objects, such as lost containers, ensures safer navigation. For environmental protection, understanding the movement of oil spills helps to respond efficiently. In addition, predicting trajectories in search and rescue operations helps determine an accurate search area for individuals or life rafts. In the context of predicting the trajectory of objects, there are two primary approaches: a physics-based and a data-driven approach.

Regarding the physics-based approach, there are two methods to simulate drift in the ocean: Lagrangian and Eulerian. Lagrangian simulation uses the floating objects as reference, while Eulerian simulation uses the volume through which the drift passes as reference. The Lagrangian method requires a sufficiently large number of particles to result in a meaningful simulation result. It relies on a Monte Carlo approach, which integrates the stochastic nature of drift. This Lagrangian representation of the motion of a drifting object is integrated into several traditional numerical methods for predicting drift trajectories. Zhang et al. (2020) used Lagrangian models to study the prediction accuracy of forcing datasets for trajectory prediction

in the South China Sea and Y. Chen et al. (2022) used a Lagrangian backtracking model for source analysis of floating objects at sea.

The data-driven approach presents a promising alternative to traditional physics-based models, particularly through the development of innovative neural network models. As discussed by Yan et al. (2023), neural network models are distinguished by their potential for greater adaptability and generalisation, higher prediction accuracy, improved computational efficiency, and a more efficient use of data. Achieving these benefits necessitates training the models on sufficiently large and representative datasets, which could include data from buoys or other objects tracked in the ocean. The potential benefits of neural network models make them very interesting for research into the prediction of object drift (Yan et al., 2023).

For this study, we only consider relatively large ships, which are typically prohibited from navigating through wind farms and are assumed to result in more significant damage in the case of an allision. This makes them particularly relevant for studying allision probabilities with wind farms. As mentioned in Section 2.4.2, the drift of large ships is approached with a more analytical methodology, focusing on the calculation of wind- and wave-induced forces. This methodology, which directly calculates the forces acting on a ship, is simpler than the one used for modelling object drift. Models for object drift are based on empirical formulas to account for leeway. A Lagrangian modelling technique based on this analytical methodology is considered a feasible option for modelling the drift of large ships. In contrast, it is suggested that neural network models are as yet less suitable for modelling the drift of large ships. This is attributed to the lack of a large amount of data on real ship drift cases, which is essential for the development of such models. This limitation is also evidenced by the lack of mention in the literature of neural networks used for modelling the drift of large ships.

In addition to an analytical Lagrangian approach, simulators represent another method for determining the drift motion and possible trajectories of large ships. These maritime simulators replicate the manoeuvring behaviour of ships within harbours and fairways, allowing for typical port manoeuvres like turning and berthing under autopilot guidance. By setting the ship's status to 'disabled', the simulator then models the behaviour of a drifting ship. However, this method requires detailed input specific to each ship, making it less practical for calculating numerous trajectories.

3.1.3. Drift trajectory model selection

The previous section introduced two types of models suitable for predicting the drift of large ships: analytical Lagrangian models and simulators. This study evaluates the benefits of a trajectory prediction-based method for calculating the probability of drifting ship allisions. The aim is to both explore the method's improvements for probability analysis and assess its applicability in enhancing risk-reduction measures. Therefore, the goal is not to achieve absolute precision but to provide a method that enables more detailed probability analysis than traditional methods allow, as discussed in Section 2.4. Given that simulators are often too specific to individual ships, this study will utilise a less complex analytical Lagrangian model.

A model that stands out, particularly due to a course at TU Delft, is the open-source Python package OpenDrift (Dagestad et al., 2018). This package includes a specific model, ShipDrift, designed for simulating the drift trajectory of large ships. Given its simplicity and the high accessibility of being open-source, this package has been chosen as the foundation for developing a methodology to calculate allision probabilities.

However, if the findings prove valuable in shaping the overall risk landscape or facilitating the deployment of risk mitigation measures, it may be reasonable to consider the use of simulators, or to develop neural network models specifically for simulating the drift of large ships.

Insights into OpenDrift

OpenDrift, developed by the Meteorological Institute of Norway is an open-source, Python-based framework for Lagrangian particle modelling with multiple applications, including:

- oil spills (OpenOil),
- oceanic circulations (OceanDrift),
- drift for search and rescue operations (Leeway),
- drift of large ships (ShipDrift),

among others. ShipDrift is designed to estimate the drift trajectory of ships larger than 30 metres. The model requires as input spatial and temporal datasets of the variables:

- wind speed along the horizontal and vertical axes, reflecting the wind's speed and direction,
- sea water velocity along the horizontal and vertical axes, indicating the speed and direction of the current,
- stokes drift velocity along the horizontal and vertical axes, reflecting the direction of the waves,
- significant wave height, and
- mean period from variance spectral density's second frequency moment, which is a measure of the average time between waves in a wave spectrum.

Furthermore, it requires parameters describing the geometry and orientation of the ship.

Parameter	Units	Range	Description
Orientation	-	N/A	Oriented left or right of the downwind direction
Length	m	1-500	Length of the ship
Height	m	1-100	Total height of the ship
Draught	m	1-30	Depth below water
Beam	m	1-70	Width of the ship
Jibe Probability	1/h	N/A	Probability of jibing (changing of orientation)

Table 3.1: Input parameters for the ShipDrift model

Using this information, the model can calculate the forces acting on a drifting ship, as illustrated in Figure 2.6, along with geometry-specific wind and water drag coefficients. These coefficients are based on formulas calibrated through empirical methods in DNV reports (Sørgård and Vada, 1998 and 2011), which are not publicly available.

The environmental forces that cause a ship's drift depend on both temporal and spatial datasets. Thus, they are influenced by the start time and location of the simulations. As mentioned earlier, the ShipDrift model uses an analytical methodology that deterministically predicts outcomes based on ship size. It includes a built-in horizontal diffusion component to address uncertainties and simulate the effects of random movements not captured by the model by calculating random travelled distances based on a diffusion coefficient. These travelled distances are then added to the deterministic motion derived from the analytical method. This feature, along with the jibing probability which alters the ship's orientation relative to the wind, contributes to the variability in final locations. Ensuring reliable outcomes necessitates the simulation of a sufficient number of trajectories. For further insights, an analysis of the observed diffusivity in the simulation across different environmental conditions and ship types can be found in appendix B.

To accommodate the model's dependency on these factors, the following settings must be specified:

- Longitude
- Latitude
- Starting time
- Time step
- Duration
- Number of trajectories

With all this information, the model is capable of calculating the ship's trajectory based on velocity, similar to the method described by Hackett et al. (2006):

$$V_{drift} = V_{current} + V_{rel} \tag{3.1}$$

The model assumes the ship moves with the current, displacing the ship at each defined time step for the defined current in time and space. Additionally, it calculates V_{rel} as the sum of the forces, encompassing wind and wave forces. The calculation of the wind and wave forces are further explained in Appendix B

3.1.4. OpenDrift trajectory predictions for probability calculations

Now that we have an understanding of how OpenDrift works, we can compare its potential use for allision probability calculation with the methods employed in current models. By basing P_{sim}, and ultimately P_{drift}, on trajectories calculated using OpenDrift, we have the opportunity to move beyond the need for the following assumptions that state-of-the-art methods rely on:

- the ship moves in a purely lateral direction (one degree of freedom),
- the wind and waves act in the same direction,
- the wind direction and wind speed are kept constant, and
- the current is accounted for as an estimated speed in the already established drift direction (wind direction).

OpenDrift calculates a ship's trajectory by computing the resultant of the forces acting on it at each time step, as illustrated in Figure 2.6. There is no need to keep any force constant; the wind and wave forces can be decoupled, and the current can be accounted for through Equation 3.1. Consequently, the ship does not move in a purely lateral direction.

It is important to note that the ShipDrift model is calibrated using empirical methods described in DNV reports, which are not publicly available. The calibration specifically ensures that the influences of the forces correspond to the ship's size. Therefore, optimising the analytical ShipDrift model presents challenges. As the focus of this study is to evaluate the contribution of integrating such a model into probability analysis to current research on the risk of drifting ship collisions in the Dutch North Sea region, we keep the model unmodified. As we leave the model unmodified, and more importantly, as we intend to use this model for allision probability calculations, we need to understand two key aspects: What parameters influence a ship's trajectory and to what extent, and how well does OpenDrift predict?

3.2. Sensitivity of a ship's drift trajectory to environmental conditions and ship geometry

Now that OpenDrift has been chosen for allision probability calculations, understanding the formation of a ship's drift trajectory is crucial. Therefore, the challenges involved in accurately calculating a ship's drift trajectory are explored. The influence of environmental forces and geometrical parameters on a ship's trajectory, which in turn affects P_{sim}, is addressed. This analysis will demonstrate the complexity of accounting for all possible outcomes of P_{sim}, considering the variety of possible environmental conditions and ship types. Multiple simulations have been conducted for three ship types under the same settings, each influenced by different environmental conditions—combinations of wind, wave, and current forces—to analyse their individual and combined impacts on a drifting ship's trajectory.

3.2.1. Selecting OpenDrift settings for comparative trajectory analysis

As, OpenDrift models a ship's wind-exposed surface as a square determined by the ship's height from the waterline, length, and orientation, the simulations have been conducted for three different container ship types: the first corresponds to the size of early container ships, while the second and third are comparable to the size of a Post-Panamax I (Rodrigue, 2024). The second and third types differ in overall height to analyse the influence of the exposed area to the wind for a similar ship type. The geometries are detailed in Table 3.2. All simulations are conducted for the same settings, as detailed in Table 3.3.

	Ship size		
Geometry	**Medium**	**Large (1)**	**Large (2)**
Length [m]	140	300	300
Beam [m]	20	40	40
Draught [m]	10	15	15
Height [m]	25	30	40

Table 3.2: Geometry of analysed ships

Setting	**Value**
Starting location (lon, lat)	3.6°, 52.4°
Starting Time	-
Time Step	1 hour
Duration	8 hours
Number of Trajectories	1000

Table 3.3: ShipDrift settings

For all three ship types, simulations are performed for environmental conditions that are constant in direction and intensity for a drift duration of eight hours:

- An eastward wind force, for three different wind speeds,
- An eastward wave force, for three different wave conditions,
- A combination of eastward wind and wave forces, for three different sets of conditions,
- A combination of misaligned wind and wave forces, for three different sets of conditions,
- A combination of a wind, wave, and a typical cyclical current force

3.2.2. Results of sensitivity analysis

The simulations for each set of environmental conditions will be analysed using a figure for the medium-sized ship, which will display its average travelled distance as a thick coloured line. Additionally, a table will detail the travelled distance (x) and orientation (Δ), measured anticlockwise from east, for each ship type for each specified environment. Additionally, to analyse the influence of the current, a comparison is made between the ship's actual travelled distance and its straight-line travelled distance (x_{SL}).

Constant wind forcing

For solely wind forcing, simulations have been performed for wind speeds of 3.5, 9.5 and 16 m/s, for the three ship types. Figure 3.3 shows the average travelled distance values and the direction, and Figure 3.4 shows the trajectories of the medium ship for increasing wind speeds.

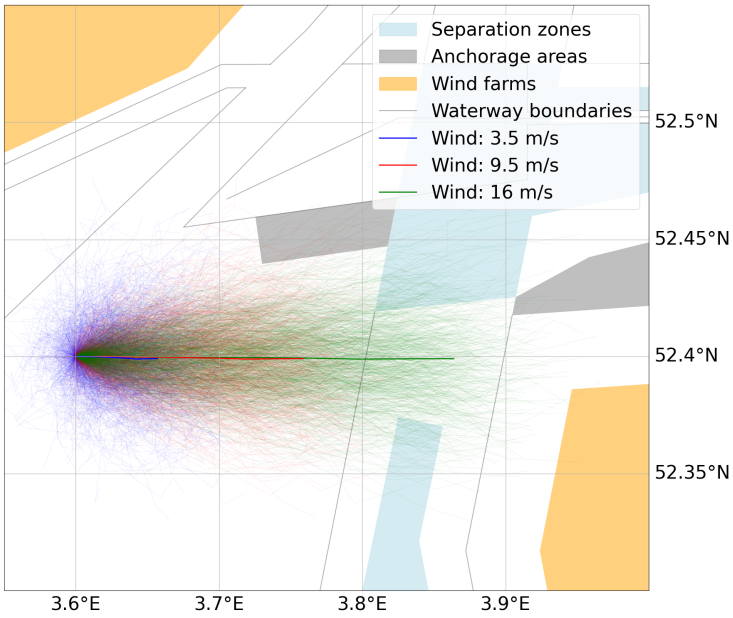

Figure 3.2: Trajectories of medium ship for constant wind forcing

Ship type	U_{10} (m/s)	x (km)	Δ
Medium	3.5	3.88	1.36°
Large (1)	3.5	3.10	1.71°
Large (2)	3.5	4.31	1.22°
Medium	9.5	10.81	0.44°
Large (1)	9.5	9.33	0.52°
Large (2)	9.5	12.36	0.37°
Medium	16.0	17.96	0.21°
Large (1)	16.0	15.61	0.26°
Large (2)	16.0	20.64	0.15°

Figure 3.3: Results for constant wind forcing

The results show that a ship displaces further in a non-linear manner for increasing wind speeds. This is logical, as according to Equation B.1, the wind force depends on the square of the wind speed. The results further indicate that the medium-sized ship displaces more than large ship 1. Despite having the same height above the waterline, the medium-sized ship is smaller overall, resulting in a smaller area exposed to the wind. Nevertheless, it exhibits a longer trajectory. This longer trajectory can be explained by the larger ratio of the area exposed to the wind to the wetted area of the medium-sized ship. Although the total area exposed to the wind is smaller, this favourable ratio likely results in relatively lower water drag, enabling the ship to travel further.

The direction is on average purely eastward, as indicated by the thick coloured lines. The observed spread is due to the diffusion coefficient and the jibing probability, as discussed in Section 3.1.3.

Constant wave forcing

To analyse the influence of wave forcing, simulations have been performed for significant wave heights of 0.5, 2, and 4 metres, all directed eastward, with corresponding mean periods based on the empirical relationship:

$$T_{m02} \approx 4\sqrt{H_s} \tag{3.2}$$

These three wave conditions commonly occur during wind speeds of 3.5, 9.5, and 16 m/s, according to the Pierson-Moskowitz spectrum. For fully developed seas, the empirical relation is:

$$U_{10} \approx 0.71 \cdot T^{1.5} \tag{3.3}$$

As wind and wave conditions are aligned in terms of magnitude, this correspondence enables a clearer understanding of their relative influences. Furthermore, OpenDrift assumes the ship to be oriented to the left or the right relative to the wave direction, resulting in a wave-induced direction that differs by either plus or minus 20 degrees from either the wave direction or, if unspecified, the wind direction. Therefore, it was decided to simulate only one orientation, in which the waves push the ship to the left (or north in this example). Table 3.4 shows the average travelled distance values and direction values, and Figure 3.4 illustrates the trajectories of the medium ship for the three different wave conditions.

Ship type	Hs (m)	Tm_{02} (s)	x (km)	Δ
Medium	0.5	3.0	0.25	-2.11°
Large (1)	0.5	3.0	0.19	3.63°
Large (2)	0.5	3.0	0.19	3.63°
Medium	2.0	5.5	5.4	-19.27°
Large (1)	2.0	5.5	4.86	-19.18°
Large (2)	2.0	5.5	4.86	-19.18°
Medium	4.0	8.0	8.23	-19.56°
Large (1)	4.0	8.0	13.11	-19.78°
Large (2)	4.0	8.0	13.11	-19.78°

Table 3.4: Results for constant wave forcing

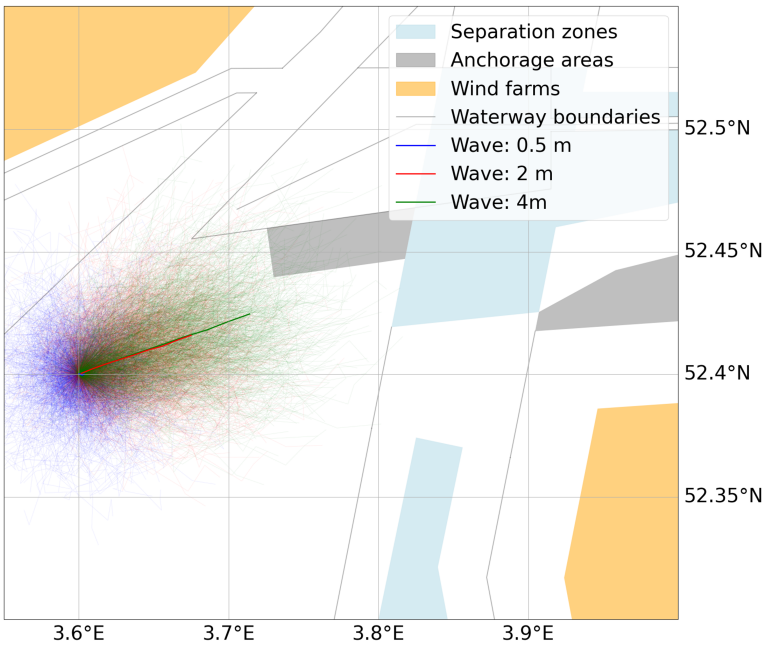

Figure 3.4: Trajectories of medium ship for constant wave forcing

The results indicate that the influence of waves is less significant compared to wind forcing. For small waves (wave condition 1), the effect is almost negligible for both ship types. In the case of medium waves (wave condition 2), the impact remains similar for both ship types. For more extreme waves, however, the influence is larger for larger ships. Additionally, under the influence of medium and extreme wave conditions, the ship is pushed 20 degrees anticlockwise from east, which aligns with expectations due to the ship's orientation and the way OpenDrift calculates the wave-induced force. Furthermore, the results are identical for both large ship types, as only their height above water differs.

Figure 3.4 shows the angle the ship makes with respect to the wave direction. The observed spread for wave condition 1 is due to OpenDrift still using a diffusion coefficient, even though there is almost no travelled distance. If a ship's orientation is unspecified, it will be simulated considering both orientations with equal probability. This approach ensures that the average result of the ship's travelled distance due to wave forcing is purely eastward.

Constant wind and wave forcing

The combined influence of wind and wave forces is analysed by combining the previously used wind and wave conditions into three sets. Table 3.5 displays the average travelled distance and direction values, and Figure 3.5 illustrates the trajectories of the medium ship under the influence of these three different sets of conditions.

The results reveal similar observations to those seen in the analyses for solely wind and solely wave forcing. In terms of travelled distance, wind forcing is dominant, and wave forcing becomes noticeable from the second wave condition. In case of more extreme waves, the influence is greater for larger ships. This is particularly evident from the fact that for wave conditions 3, the results for the medium ship and large ship 1 are now almost identical. For only wind forcing, the medium ship travelled further due to its larger ratio of its area exposed to the wind to its wetted area.

Ship type	U_{10} (m/s)	Hs (m)	Tm_{02} (s)	x (km)	Δ
Medium	3.5	0.5	3.0	3.89	1.25°
Large (1)	3.5	0.5	3.0	3.11	1.60°
Large (2)	3.5	0.5	3.0	4.31	1.16°
Medium	9.5	2.0	5.5	11.68	-3.34°
Large (1)	9.5	2.0	5.5	9.65	-4.25°
Large (2)	9.5	2.0	5.5	12.59	-2.31°
Medium	16.0	4.0	8.0	18.90	-2.06°
Large (1)	16.0	4.0	8.0	18.77	-8.42°
Large (2)	16.0	4.0	8.0	22.94	-5.11°

Table 3.5: Results for constant wind & wave forcing

In terms of deviation, due to the assumed orientation of the ships, wave forcing causes them to deviate anticlockwise. In more extreme wave conditions (combination 3), this effect is more pronounced for larger ships. Regarding the different ship types, the deviation is always greatest for large ship 1, as it is proportionally less influenced by the wind compared to large ship 2 and has a larger wet area compared to the medium ship.

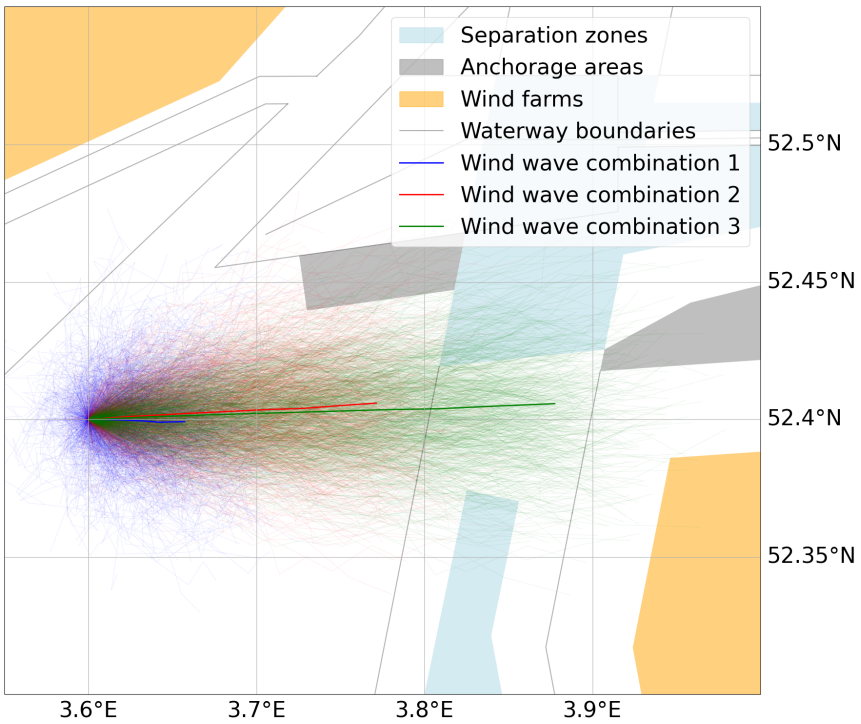

Figure 3.5: Trajectories of medium ship for wind and wave forcing

Constant, misaligned wind and wave forcing

The same simulations are performed for identical wind and wave magnitudes, differing only in direction. The wind direction is eastward, while the wave direction is northeastward (directed 45 degrees anticlockwise from east). Table 3.6 shows the average travelled distance and direction values and Figure 3.6 shows the trajectories of the medium ship for the three different sets of conditions.

The results are consistent with previous observations. With more extreme wave heights, the influence of waves is more pronounced for large ships in terms of travelled distance and deviation. Furthermore, large ship 1 consistently deviates the most and travels the shortest distance. This is due to its ratio of the area exposed to the wind relative to its wetted area, which results in it being less influenced by the wind compared to large ship 2 and more influenced by water drag compared to the medium-sized ship.

Ship type	U_{10} (m/s)	Hs (m)	$Tm02$ (s)	x (km)	Δ
Medium	3.5	0.5	3.0	3.88	1.08°
Large (1)	3.5	0.5	3.0	3.10	1.42°
Large (2)	3.5	0.5	3.0	4.31	1.08°
Medium	9.5	2.0	5.5	11.18	-10.55°
Large (1)	9.5	2.0	5.5	9.14	-13.72°
Large (2)	9.5	2.0	5.5	12.18	-7.24°
Medium	16.0	4.0	8.0	18.45	-6.29°
Large (1)	16.0	4.0	8.0	17.52	-27.76°
Large (2)	16.0	4.0	8.0	21.76	-15.94°

Table 3.6: Results for constant, misaligned wind & wave forcing

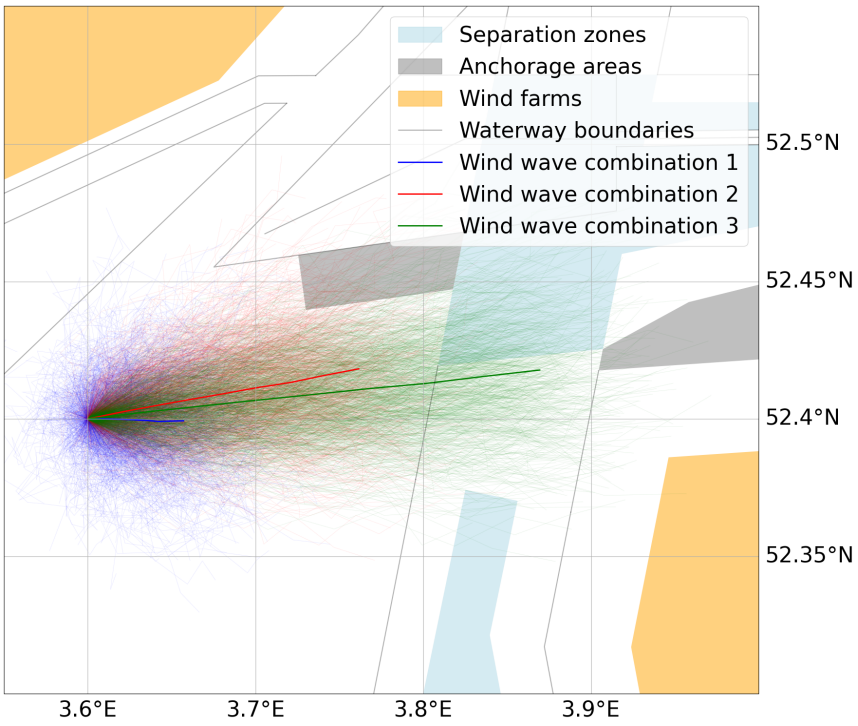

Figure 3.6: Trajectories of medium ship for misaligned wind and wave forcing

Wind, wave and current forcing

Next, a typical current cycle is added on top of the third wind and wave combination. This current cycle is an above-average forcing, characteristic of the location of these simulations, which is near the Hollandse Kust wind farms. Given that the magnitude and direction of the current continuously vary, and considering that we are simulating trajectories for an 8-hour drift duration, simulations are performed for various starting times along the current cycle. This is illustrated by the coloured vertical lines in Figure 3.7. Correspondingly, Figure 3.8 displays the results for each starting time, using the same colour as those in Figure 3.7.

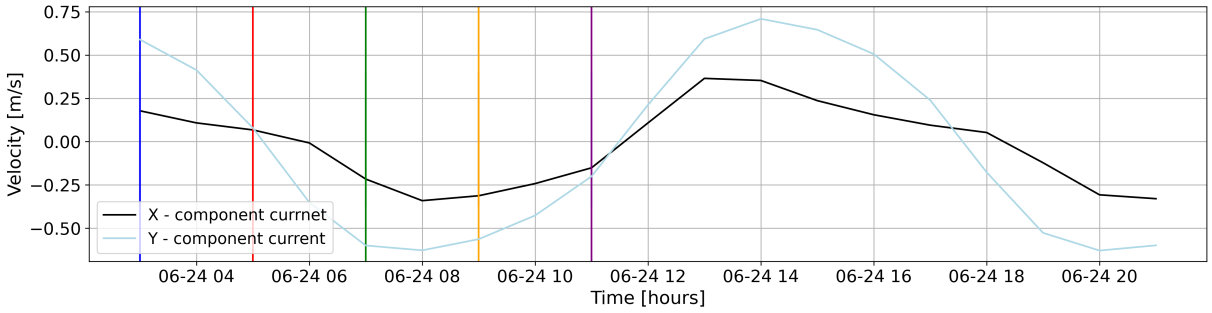

Figure 3.7: X-, Y-components of the current

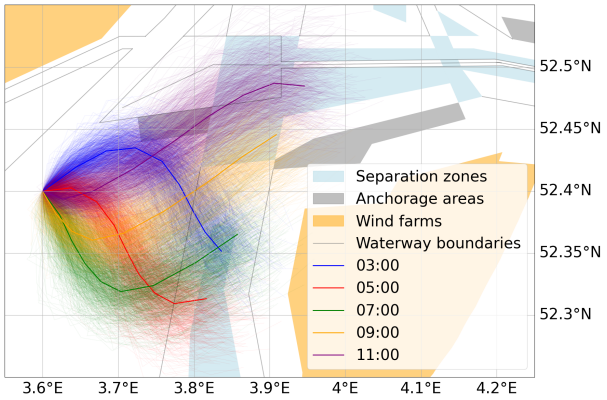

Figure 3.8: Trajectories of medium ship for wind, wave and current forcing

Starting time	x (km)	x_{SL} (km)	Δ
03:00	21.82	16.97	18.46°
05:00	19.88	17.61	33.23°
07:00	23.57	17.95	12.38°
09:00	25.72	21.61	-13.73°
11:00	26.48	25.33	-22.04°

Table 3.7: Results for wind, wave, and current forcing

From the figure, it can be concluded that the current significantly impacts a ship's trajectory. Furthermore, this influence depends on the specific current forcing, or segment the ship encounters. For example, over a period of 8 hours, the trajectory marked in blue first encounters a more northward directed current, followed by a more southward directed current. Conversely, the trajectory marked in green experiences the opposite. The results in Table 3.7 demonstrate that the specific current segment affects all three parameters. Depending on the current segment, its travelled distance is either substantially larger or smaller, and its deviation is either to the left or right from the wind direction.

In this example, the deviation or curve generated by the current forcing is quite pronounced because the current is almost perpendicular to the wind direction. A wind direction more towards the south or north would have resulted in a less pronounced curve. If the wind and current directions were aligned, they would either amplify or diminish each other, resulting in either a larger or smaller travelled distance, respectively.

3.3. OpenDrift's predictive performance

The simulations performed using OpenDrift for the medium and both large ships demonstrated how wind, wave, and current forcing influence a ship's trajectory. Given that these simulations rely on OpenDrift, examining its predictive performance is crucial. Therefore, it will be investigated whether these effects can be validated using a real-world case to assess the performance of the model. By doing so, we can strengthen the concept of including a trajectory prediction model in the method for calculating P_{drift}. Although many ships experience blackouts annually, these incidents are often brief and/or occur during low environmental forcing, offering limited insight into OpenDrift's predictive capabilities. The impact of initial speed, anchor use, and other factors complicates comparisons of short drift trajectories with OpenDrift simulations, which assume a 'clean drift'. This assumption disregards a ship's inertia by assuming it has reached equilibrium. However, the 2021 Julietta D incident does provide a unique case of a 'clean drift'. By reconstructing this incident, we aim to observe the same effects of environmental forcing in the trajectory of the Julietta D.

3.3.1. Reconstruction of the Julietta D incident

On the morning of January 31st, an incident involving the Julietta D, a handymax-sized bulk carrier, took place. The Julietta D was adrift for a certain period during storm Corrie. AIS data received from Rijkswaterstaat (Dutch Government, 2024), combined with specific information from the Safety Investigation Report by Transport Malta (Transport Malta, 2023), are used to illustrate the event in Figure 3.9.

According to the Safety Investigation Report, the Julietta D began to drag anchor in an anchorage area near wind farm Hollandse Kust Zuid. At 09:44, the Julietta D allided with the bow of the Pechora Star, resulting in two hull breaches near Julietta D's engine room. Following this allision, the main engine of the Julietta D was shut down, and the crew was ordered to abandon ship. While drifting southward, the Julietta D struck a wind turbine transition section at Hollandse Kust Zuid, which was under construction at the time. After this second allision, the crew of the Julietta D was airlifted from the ship. Subsequently, the Julietta D also allided with a transformer platform also under construction.

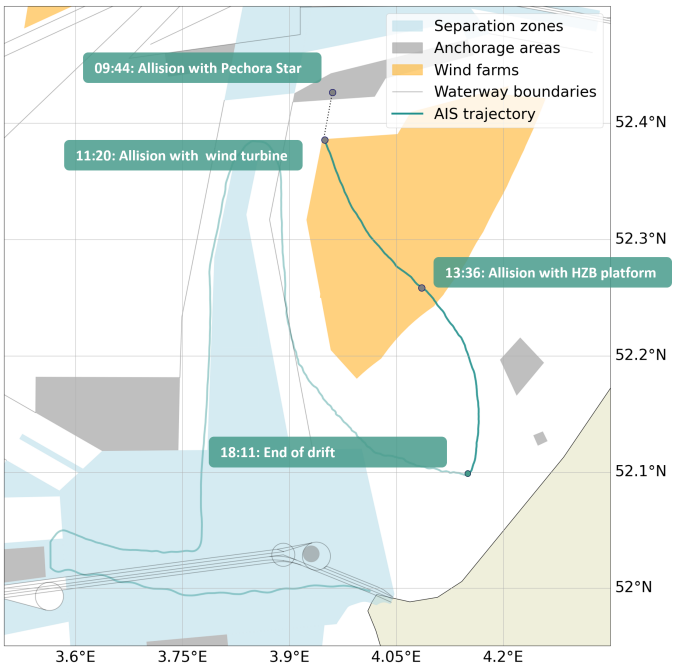

Figure 3.9: Reconstruction of Julietta D's trajectory using AIS data

An ERTV was dispatched to assist the Julietta D, reaching it approximately 5 hours after the incident. Nearly three hours later, the ERTV successfully connected with the Julietta D. Once secured, the Julietta D was towed to the port of Rotterdam. According to AIS data, the Julietta D was adrift for a period of approximately eight and a half hours, from the moment it collided with the Pechora Star at 09:44 until around 18:11.

Figure 3.9 illustrates the trajectory of the Julietta D, with the segment in which the ship was adrift highlighted in thick green. To better understand the Julietta D's trajectory, it is tried to reconstruct it using hindcast data of the environmental conditions at that time. This reconstruction excludes the ship's dragging anchor and specific incidents like the allisions with the wind turbine transition section and the transformer platform. This approach assumes a clean drift, influenced solely by the environmental conditions present.

Environmental conditions during the incident

Figure 3.10 presents the environmental conditions at the location where the drift started, from January 31st, 2022, to February 1st. These environmental conditions are obtained from the databases detailed in Appendix E. The time span highlighted in red corresponds to the environmental conditions during the period of Julietta D's drift, starting at 09:44, the moment the ship collided with the Pechora Star. During the drift, the wind was directed towards the southeast, with an approximately constant wind speed of around 20 metres per second.The waves, originating from the north, reached heights of 6 metres with a corresponding mean period of approximately 8 seconds. At the start of the drift, the current was directed southward and varied throughout the duration of the drift according to a typical tidal cycle.

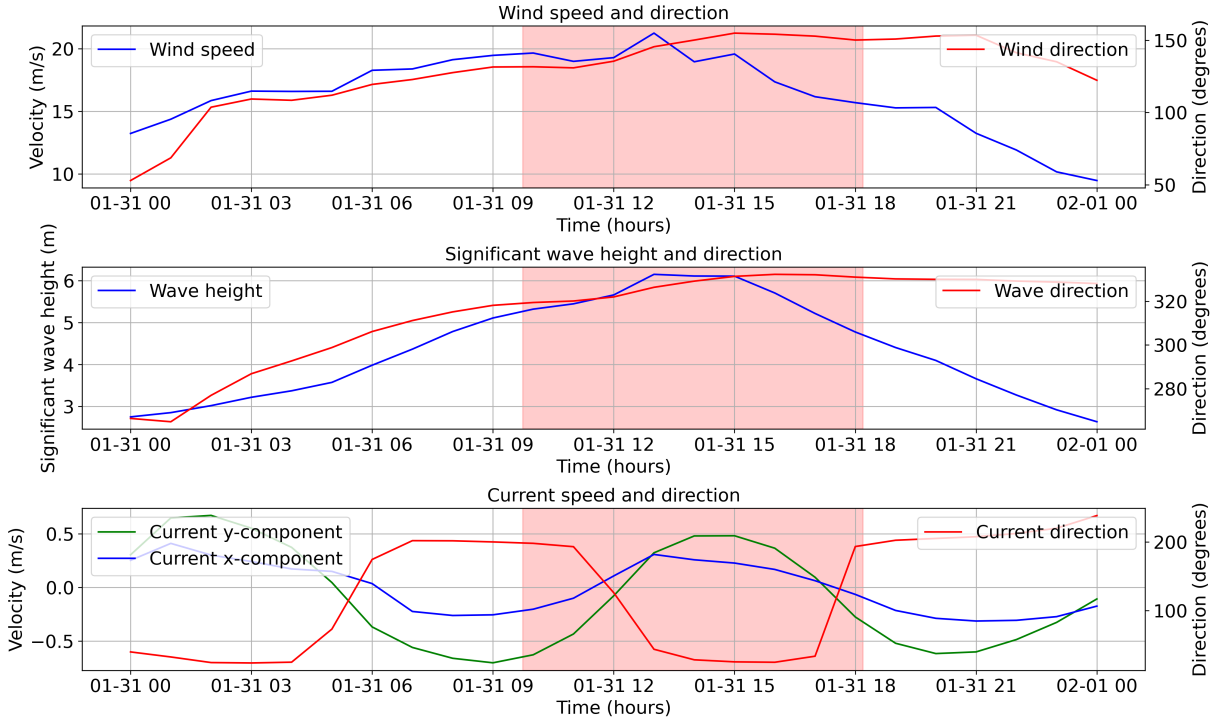

Figure 3.10: Environmental conditions at Julietta D's starting location

OpenDrift setup

The simulation is started at 10:11, in position 52°23'38" N 3°56'52" E. It was decided to start the simulation at this time because it is believed to be the time when the Julietta D lost its anchor. To reiterate, it is important to note that simulation, assuming a 'clean drift,' neglects the two allisions with the wind turbine transition section and the transformer platform.

Besides the environmental conditions in time and space along a drifting ship's trajectory, OpenDrift also requires the ship's geometry and allows for the definition of its initial orientation relative to the environmental forces. The Julietta D is a handymax-sized bulk carrier, with its geometry detailed in Table 3.8. The height of a ship above the waterline, which determines the degree of wind force it is subjected to, varies depending on the ship's loading conditions and is not uniform along the length of the ship. Specifically for the Julietta D, accounting for the effect of the cranes on this measurement presents a challenge. The draught is known to be 10 metres, and the overall height is assumed to be 15 metres greater than its draught. In addition, except for the starting location, the OpenDrift settings are defined as specified in Table 3.3.

Length overall	190 m
Beam	28 m
Draught	10 m
Height overall	25 m

Table 3.8: Geometry of Julietta D

OpenDrift simulation results

OpenDrift simulations were performed both without and with knowledge of the ship's initial orientation, as illustrated in Figures 3.11 and 3.12, respectively. The green lines represent the simulated trajectories, of which the average is presented by the thick green line. These trajectories correspond to a drift period of 8 hours, which is equal to the drift period of Julietta D's AIS track, represented by the black line.

The figures indicate that OpenDrift is somewhat capable of replicating the shape of the trajectory. However, the simulated trajectory is significantly shorter for the same period compared to the actual track. According to AIS data, the Julietta D already had considerable speed at 10:11. This initial speed might have caused discrepancies in the timing and location within the simulations, leading to mismatches between the modelled and actual environmental forcing conditions. Other potential causes could include the ship catching more wind due to features such as cranes, or the two collisions that may have influenced its drift trajectory. Additionally, the simulation is based on modelled environment data, which may not perfectly reflect the actual conditions at each specific time and location during the incident.

Knowing the initial orientation significantly improves the accuracy of predictions, as seen in Figure 3.12. However, foreseeing how a ship will be oriented relative to the forcing environment beforehand presents a challenge.

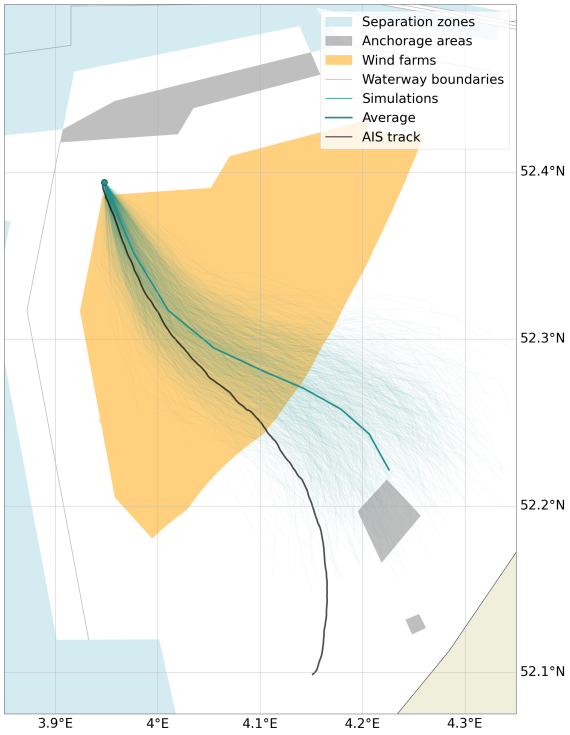

Figure 3.11: OpenDrift simulations without knowledge of Julietta D's orientation

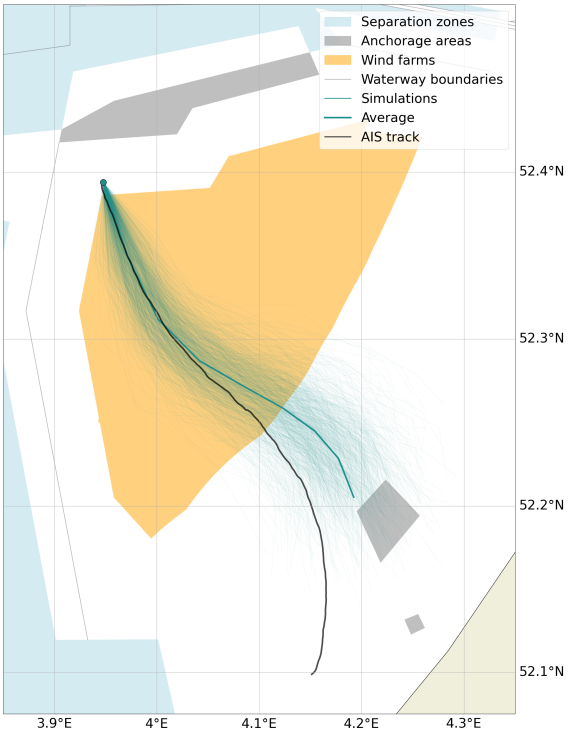

Figure 3.12: OpenDrift simulations with knowledge of Julietta D's orientation

3.3.2. Analysing Julietta D's trajectory

The trajectory of the Julietta D displays a pronounced curve, initially directed south, then shifting north in the middle section, and finally turning south again. To demonstrate that this effect is caused by the current at that time, simulations were run exclusively with wind forcing, and with both wind and wave forcing. These figures are presented in Figure 3.13 and Figure 3.14, respectively.

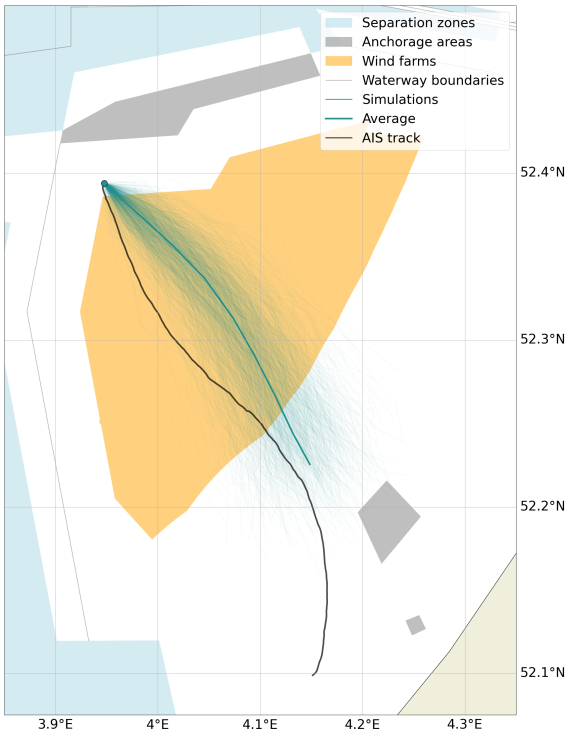

Figure 3.13: OpenDrift simulations for only wind forcing

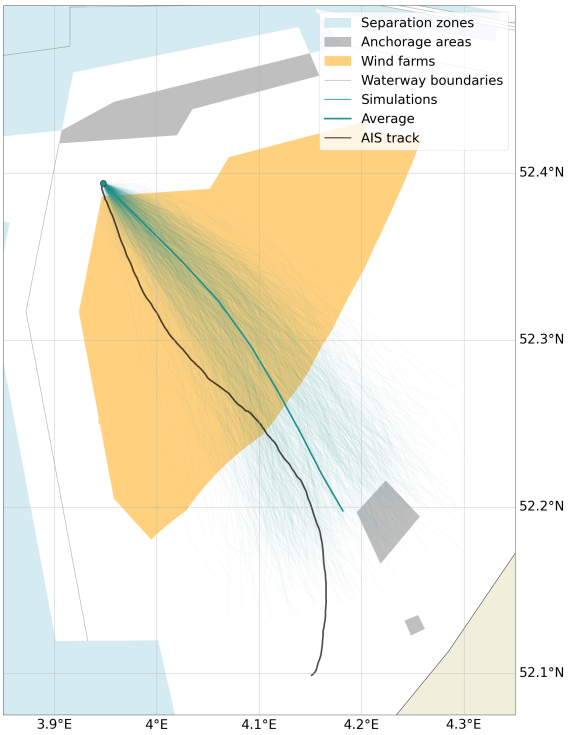

Figure 3.14: OpenDrift simulations for only wind and wave forcing

These figures demonstrate that the simulated trajectories do not match the actual track of the Julietta D compared to the simulation for all three forces, as shown in Figure 3.11. Particularly in the first part of the drift, the simulated trajectories significantly diverge from Julietta D's actual track. In Figure 3.13, a minor change is observable due to the change in wind direction over time. Figure 3.14 reveals that wave forcing not only results in a greater travelled distance but also in a broader spread of trajectories. This variability is due to the wave-induced force being directed either plus or minus 20 degrees from the wave direction, as discussed in Section 3.2.2. The wave direction, approximately from the north, is indicated in the red part of Figure 3.10.

These results suggest that wind forcing alone is insufficient to predict the direction and travelled distance, or speed, of a drifting ship. The waves are necessary to account for any additionally travelled distance and deviation from the wind direction. Finally, especially the current is crucial to fully explain Julietta D's entire trajectory.

To better illustrate the effect of the current, OpenDrift simulations were initiated both 5 hours earlier and 5 hours later than the original event. Within this 5-hour window, while the magnitude and direction of the wind and wave forces remain relatively unchanged from the conditions during the drift period, the specific current segment affecting the ship varies significantly. The effects of these different force combinations are detailed in Figure 3.15 and Figure 3.16, respectively.

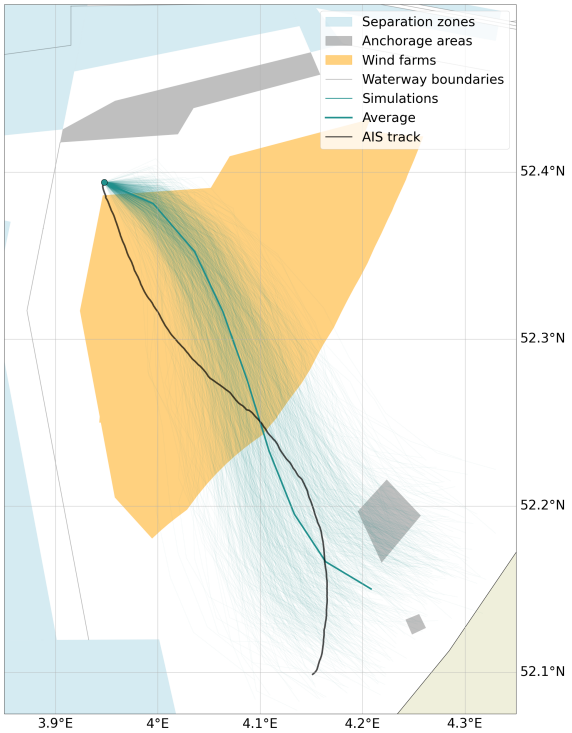

Figure 3.15: OpenDrift simulations starting at 05:11

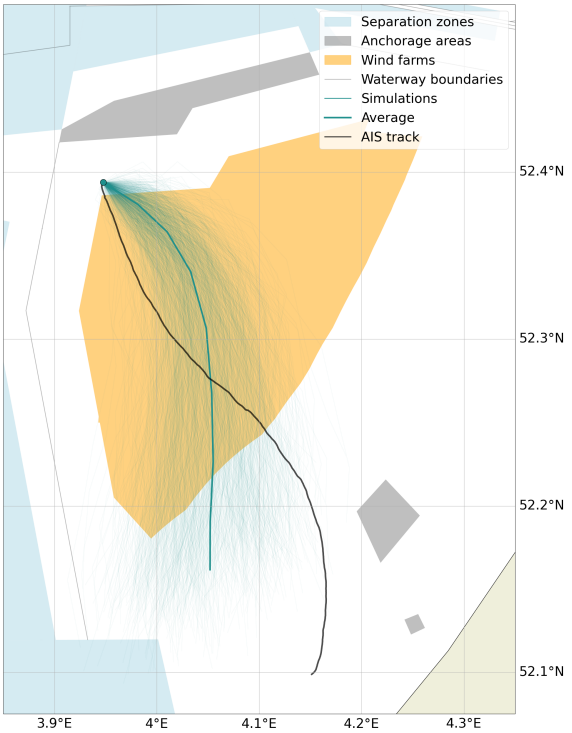

Figure 3.16: OpenDrift simulations starting at 15:11

Both figures show completely different outcomes, and neither aligns with the original AIS track. The observed differences are attributed to the specific timing when the current is at one of its maxima. For the original AIS track, at the start of the drift, the current was directed southward. In contrast, the simulations initiated 5 hours earlier and later subjected the ships to currents directed more to the north.

In conclusion, to most accurately predict a ship's trajectory, all three forces-current, wind, and wave forces-must be known. Excluding any of these forces will result in significant differences in both a ship's direction and travelled distance.

3.4. Trajectory prediction-based method for drift probability calculation

The objective of this study is not to determine a specific allision occurrence rate for any particular wind turbine. Instead, this study simplifies the approach by focusing on the probability of a drifting ship entering, or more specifically, crossing the boundary of a wind farm area. From a risk-reducing perspective, the event of an adrift ship entering a wind farm area is in any case undesired and makes ship recovery difficult. To determine whether the allision risk for a single wind turbine specifically is unacceptably high, a more comprehensive risk analysis is required. This analysis should include the consequences of such an accident and the effectiveness of risk-reducing measures. By focusing our allision probability calculations exclusively on the probability of crossing a wind farm boundary, we ensure that our results are comparable for different orientations and distances relative to a single wind farm, as well as for multiple wind farm areas.

Referring back to Section 3.1.3, a drift trajectory can be determined by OpenDrift's ShipDrift model when specifying:

1. The location of the start of the drift
2. The environment (wind, wave and current forcing)
3. The ship's geometry and initial orientation
4. The OpenDrift settings (drift duration, time step and number of trajectories)

Having specified these parameters and simulated a sufficient number of trajectories, the allision probability of this simulation can then be determined by the proportion of trajectories that indicate an allision, which involves crossing any wind farm boundary throughout its drift. Referring back to the beginning of this chapter, the probability is based on a trajectory prediction of a 'clean drift', meaning it is not influenced by either self-initiated measures or external interventions.

For a specific ship known to be adrift for a certain duration, the formula for calculating the allision probability is defined as follows:

$$P_{sim} = \frac{N_{cross}}{N_{sim}} \tag{3.4}$$

Where:

P_{sim}	is the probability of allision in a single OpenDrift simulation
N_{cross}	is the number of trajectories that crossed any wind farm boundary
N_{sim}	is the total number of simulated trajectories

To provide an overview of drifting ship allision probabilities across multiple wind farms, OpenDrift simulations can be conducted for classifications of ships that were present in the area of interest over the past few years at specific starting locations and time intervals. At each time interval, the simulations are then conducted using hindcast data to account for the environmental conditions during a ship's potential drift period, taking into account variations in wind, wave, and current forces acting on a ship's surface over time and across space. Subsequently, an allision probability value can be estimated by calculating P_{sim}—as previously defined—for each simulation, and multiplying each P_{sim} by a value representing the probability that a ship becomes adrift. To conduct these hindcast data-based simulations for several locations and over a sufficiently representative number of years leads to extensive computation time. This is because such a hindcast data-based approach accounts for the variability in forcing factors in both time and across space throughout a ship's trajectory, with each simulation taking approximately one minute. For example, simulating a ship's trajectory using five years of hindcast data, starting at each consecutive 3-hour interval, results in a total computation time of about ten days for just a single starting location.

Instead of conducting simulations for various classifications of ships across multiple positions in the North Sea at specific time intervals using this hindcast data-based approach, we must make assumptions that reduce computation time while striving to maintain the validity of our analysis.

In the following sections, we will explain:

1. how this study accounts for the variability in wind, wave, and current forces (P_{env}),
2. how we subsequently use OpenDrift simulations to define the drift probability (P_{drift}), which considers all possible environmental conditions and ship types,

and thus transition from a hindcast data-based approach to what will be termed a scenario-based approach for a single starting location.

3.4.1. A scenario-based approach to environmental forcing

The wind, wave and current forces acting upon a ship's surface vary over time and across space. These variation present two main challenges:

1. **Environmental conditions at the moment a ship becomes adrift**: The complex interplay of simultaneous wind, wave, and current conditions makes predicting the exact force combinations the ship will be subjected to challenging. The drift motion of a ship depends on all three forces, and simply analysing a wind rose is insufficient for representing the occurrence rate of a specific combination of wind, wave and current forces.
2. **Force variations throughout a ship's drift trajectory**: It is uncertain how these conditions will vary over time, which could significantly affect the ship's trajectory. This uncertainty makes it difficult to predict the range of possible environmental scenarios a ship may be subjected to throughout its drift.

For a specific location, one method to account for the variety in possible environmental conditions at the moment a ship becomes adrift is by defining a limited set representing all possible combinations, or scenarios, of these forces, each with a corresponding probability of occurrence.

As environmental conditions may also vary throughout a ship's drift trajectory, we assume:

1. the wind and wave forces to remain constant throughout a ship's drift trajectory.

And to simplify creating such scenarios, we also assume:

2. the current forces to be independent of the wind and wave forces.

Assuming that wind and wave forces are spatially constant limits the possible combinations to those observed in hindcast data from a single location. While the assumption that wind and wave forces remain constant may seem simplistic, it significantly restricts the variety of possible environmental conditions that need to be considered. This is crucial because, as concluded in Section 3.2 and Section 3.3, predicting a ship's trajectory requires accounting for all three forces.

To support this decision, 10 years of wind observation data were analysed to examine variations over 8-hour periods, helping to understand how much conditions can change throughout a ship's trajectory. The focus is solely on wind conditions, since wind forcing is significantly more dominant than wave forcing, as observed in Section 3.2, and its variation over time is greater compared to wave conditions. The wind observations are analysed for periods of 8 hours as this duration is considered significant for drift analysis. For both wind speed and wind direction, for each 8-hour segment consisting of 8 observations, the mean is calculated, and for each observation within these segments, the deviation from its mean is determined.

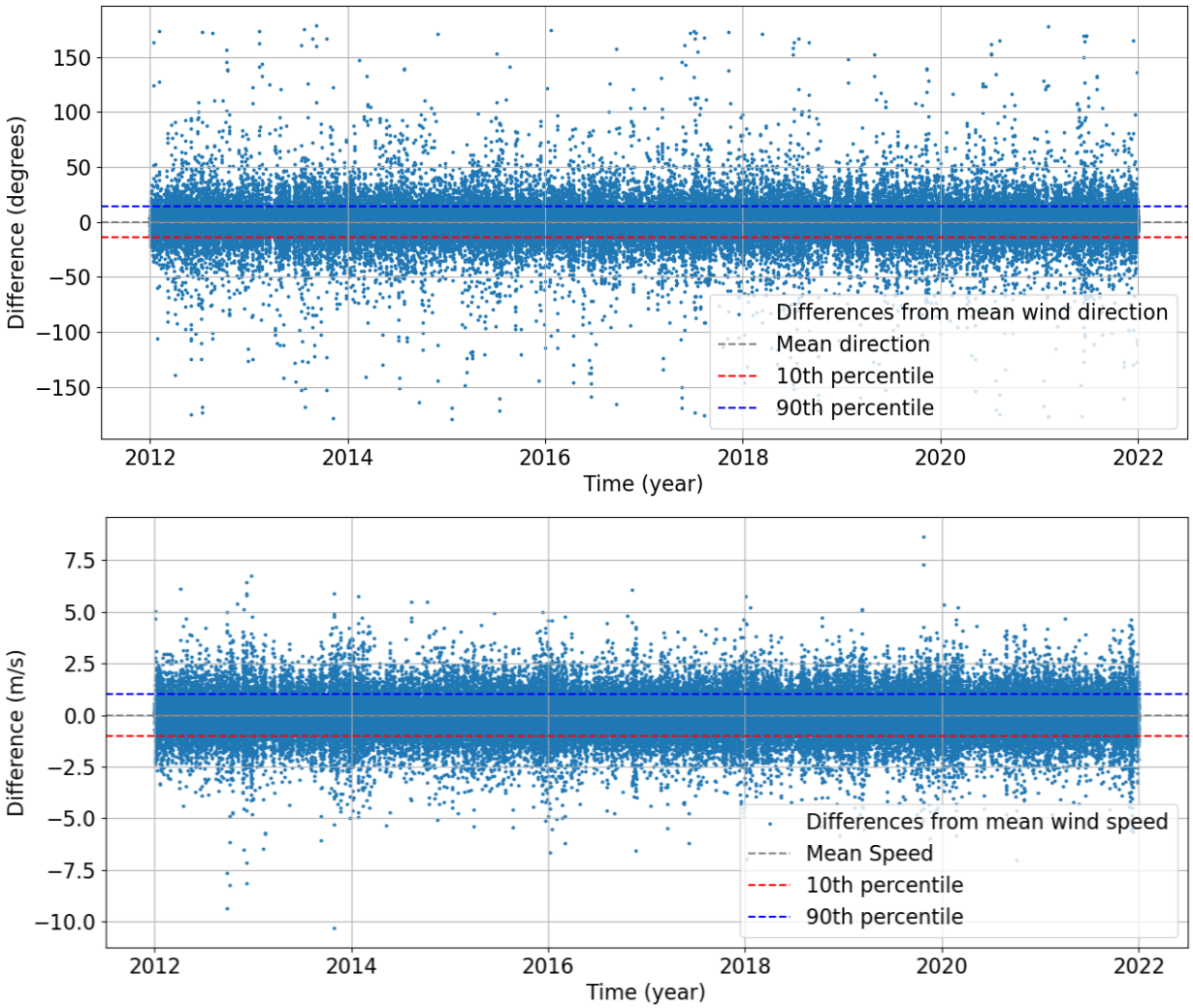

Figure 3.17: Difference of observations with 8-hour mean segments for wind direction (upper) and wind speed (lower)

Figure 3.17 shows that 80% of the observations fall within a change of 1 m/s for wind speed and around 15 degrees for wind direction. An OpenDrift simulation already accounts for a range of possible trajectories in both direction and travelled distance, as observed in Section 3.2. Therefore, a variation of 15 degrees in wind direction or 1 m/s in wind speed is considered unlikely to lead to significantly different outcomes in terms of the number of trajectories crossing a wind farm boundary. Furthermore, accounting for a 1 m/s difference in defining scenarios would result in an extremely large number of scenarios to be analysed, even with the assumptions of constant wind and wave forcing. Given that this pattern holds for 80% of the observations, maintaining constant wind and wave forces proves to be a viable first step in determining the allision probability of a drifting ship.

Creating scenarios from wind and wave forces

The wind forcing is represented by two variables: wind speed and wind direction. The wave forcing is characterised by the sea surface's significant wave height, the mean period derived from the second spectral density moment, and the wave direction. It is proposed to use multi-dimensional data binning to reduce all possible variations of these forces occurring simultaneously to a limited number of combinations. Multi-dimensional binning is a technique used in data processing and analysis that involves dividing a dataset with multiple dimensions (or variables) into a grid of bins or cells. Each bin corresponds to a specific range of values for each dimension, effectively dividing the multi-dimensional space into smaller, more manageable segments.

Variable	Units
Wind speed	m/s
Wind direction	degrees
Significant wave height (Hs)	m
Mean period (Tm02)	s
Wave direction	degrees

Table 3.9: List of wind and wave forcing variables

As an example of this technique, we derive two wind and wave scenarios from a five-hour dataset that includes significant wave height, wind speed, and wind direction. The necessary input for multi-dimensional data binning includes a dataset with hourly observations of these variables:

1. Create wind and wave dataset			
Observation	Hs [m]	Wind speed [m/s]	Wind direction [degrees]
2021-01-01 00:00:00	0.76	5.49	149.50
2021-01-01 01:00:00	0.77	5.37	147.58
2021-01-01 02:00:00	0.80	5.50	141.40
2021-01-01 03:00:00	0.82	6.04	135.40
2021-01-01 04:00:00	0.86	6.37	132.94

Table 3.10: Hourly observations of wind and wave conditions for multi-dimensional data binning example

For each of the considered variables, a number of bins (a specific range of values) is defined, spanning from the lowest to the highest value that has occurred, according to the dataset in use:

2. Define number of bins and the edge values for each variable			
	Number of bins	Range bin 0	Range bin 1
Hs [m]	2	0.76 - 0.81	0.81 - 0.86
Wind speed [m/s]	2	5.37 - 5.87	5.87 - 6.37
Wind direction [degrees]	2	132.94 - 141.22	141.22 - 149.50

Table 3.11: Defined value ranges for multi-dimensional data binning example

The totality of scenarios is formed by every possible combination of these bins across all variables. In this example, where each variable has two bins, there are 2^3, or 8 possible scenarios. The probability of any given scenario occurring is calculated based on the frequency of that specific combination of bins in the dataset:

3. For each combination of bins, count observations and calculate probability of occurrence		
Combination of bins (scenario)	Observation	Probability
(0, 0, 0)	-	0
(1, 0, 0)	-	0
(0, 1, 0)	-	0
(0, 0, 1)	1, 2, 3	75%
(1, 1, 0)	4, 5	25%
(1, 0, 1)	-	0
(0, 1, 1)	-	0
(1, 1, 1)	-	0

Table 3.12: All possible wind and wave combinations along with their probability of occurrence

For each scenario, the wind and wave parameters are set to the average values observed for each variable's bin. Thus, each combination of bins forms a scenario characterised by these averages, with its probability of occurrence determined by its frequency in the dataset. For example, consider the combination (0, 0, 1):

Scenario (0, 0, 1)		
	Calculation [m]	Representative value
Hs [m]	(0.76 + 0.77 + 0.80) / 3	0.78
Wind speed [m/s]	(5.49 + 5.37 + 5.50) / 3	5.45
Wind direction [degrees]	(149.50 + 147.58 + 141.40) / 3	146.16

Table 3.13: Calculating the representative value of each variable for a specific scenario

This approach simplifies the representation of environmental conditions for a specific starting location. By calculating the probability of crossing any wind farm boundary for each possible combination of wind and wave conditions, we can establish a probability that is independent of the specific wind and wave environment.

This simplification raises important questions about the accuracy and validity of using a bin configuration to represent all possible wind and wave conditions when at the moment a ship becomes adrift. It is necessary to determine whether the value ranges defined in the bins accurately reflect all potential trajectories of a drifting ship. For example, we can analyse whether it is adequate to assume that the significant wave height corresponds to the average of observations for a given wind speed and wind direction combination, assuming a direct correlation. If this assumption holds, we can reduce the number of scenarios to four in our detailed example.

Integrating current forcing into wind and wave scenarios

The current forcing is assumed to be independent of the wind and wave forcing, and can therefore be simply added to each combination of wind and wave forces.

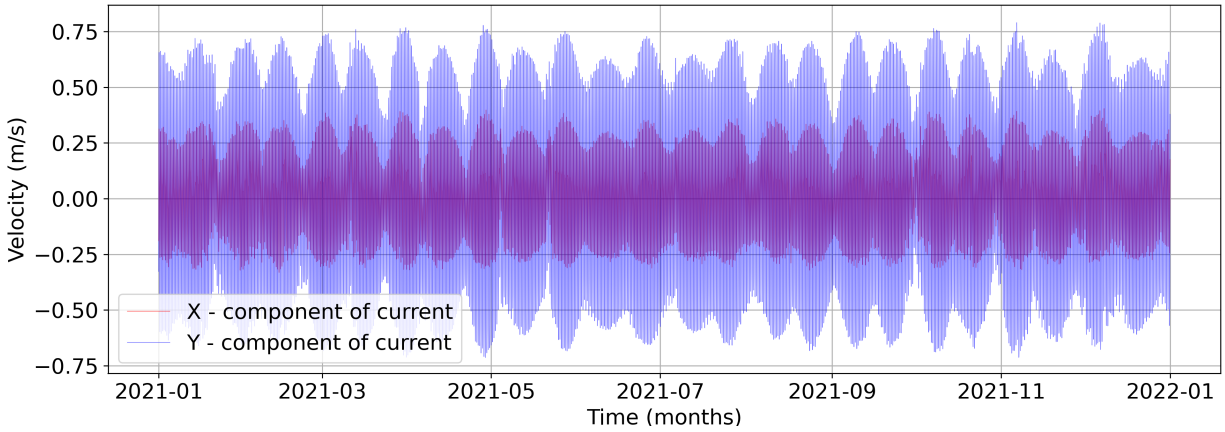

Figure 3.18: Continuous change in the current's maximum velocity throughout a year

The velocity of a current varies in magnitude throughout the year, as illustrated in Figure 3.18. Therefore, for simplicity, the current is represented by a single cycle with an average maximum velocity. It is assumed that the varying effects of currents with lower or higher maximum velocities on allision probability will average out over time. For example, the current as used in the scenario-based approach can be illustrated by Figure 3.19. This figure shows the current cycle which continuously changes in both magnitude and direction.

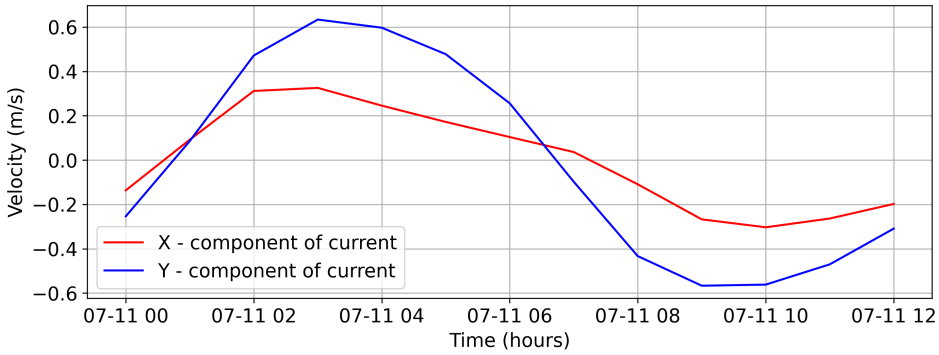

Figure 3.19: Continuous change in the current's magnitude and velocity throughout a single cycle

Referring back to Section 3.2.2, a ship's drift trajectory is influenced by the specific current segment it encounters. For the purpose of calculating the overall probability, from each combination of wind and wave forces, we can generate n combinations by combining it with n different current segments. Each of these n combinations has a resulting occurrence rate of $\frac{1}{n}$ multiplied by the occurrence rate of the respective wind and wave force combination. This approach is based on the assumption that the start of a ship's drift can occur at any moment along the current cycle, with each moment having an equal probability.

3.4.2. Drift probability calculation through scenario-based simulated trajectories

At the beginning of this chapter, Equation 3.4 was presented for calculating the allision probability in a single OpenDrift simulation. This equation forms the basis for explaining how P_{sim} is calculated through an analysis of trajectories simulated using OpenDrift:

- considering all possible wind and wave conditions,
- considering all possible current influences throughout a ship's trajectory,
- considering all possible ship types.

The resulting probability formula accounts for all three aspects and defines the probability that an arbitrary drifting ship allides with a wind farm from a certain starting location, considering all possible environmental conditions. This probability will be denoted as P_{drift}.

Drift probability for wind and wave scenarios

Having obtained a set of wind and wave combinations characterised by an average value for each variable and a probability of occurrence, we can conduct an OpenDrift simulation for each combination. This approach still assumes a specific ship geometry and excludes the influence of the current.

Next, Equation 3.4 can be used to calculate P_{sim} for each simulation. By multiplying P_{sim} with the probability of occurrence of the wind and wave combination for which the simulation was run, we obtain the probability that those environmental conditions are present and the ship drifts into the wind farm. By summing all these products, we obtain the probability of the ship drifting into the wind farm, considering all possible wind and wave conditions.

This procedure can be summarised with the following formula:

$$P_{drift} = \sum_{i=0}^{m} \left(\frac{N_{cross}(i)}{N_{sim}} \times P_{env}(i) \right) \tag{3.5}$$

Where:

P_{drift}	is the probability of a specific drifting ship crossing any wind farm boundary, considering all possible wind and wave force combinations
$N_{cross}(i)$	is the number of calculated trajectories that crossed any wind farm boundary under the influence of wind-wave forcing scenario i
N_{sim}	is the total number of calculated trajectories per simulation
$P_{env}(i)$	is the probability of occurrence of wind-wave forcing scenario i

Drift probability for wind, wave and current scenarios

In Section 3.4.1, we assumed the current to be represented by a single cycle with an average maximum velocity. The drift of a ship can now start at any point within the 12-hour cycle, with each instant having an equal probability of occurrence, as the current is assumed to be independent of wind and wave forcing.

We can conduct simulations for each wind-wave forcing scenario at multiple starting times along the current cycle. This approach still assumes a specific ship geometry.

Next, Equation 3.4 can again be used to calculate P_{sim} for each simulation. The probability of occurrence for each combination of environmental forces is now calculated as the probability of the wind-wave forcing scenario multiplied by the reciprocal of the number of current segments. This calculation ensures that each current segment contributes equally to the overall allision probability. By multiplying P_{sim}, just as before, with the probability of occurrence of the wind, wave, and current condition combination for which the simulation was run, we obtain the probability that those environmental conditions are present and the ship drifts into the wind farm. By summing all these products, we obtain the probability of the ship drifting into the wind farm, considering all environmental conditions.

This procedure can be summarised with the following formula:

$$P_{drift} = \sum_{i=0}^{m} \sum_{j=0}^{n} \left(\frac{N_{cross}(i,j)}{N_{sim}} \times P_{env}(i) \times \frac{1}{n} \right) \tag{3.6}$$

P_{drift}	is the probability of a specific drifting ship crossing any wind farm boundary, considering all possible environmental conditions
$N_{cross}(i,j)$	is the number of trajectories that crossed any wind farm boundary under the influence of wind-wave forcing scenario i and current segment j
N_{sim}	is the total number of calculated trajectories per simulation
$P_{env}(i)$	is the probability of occurrence of wind-wave forcing scenario i
n	is the number of current segments

Drift probability for multiple ship types

In the above formula, trajectories are simulated for a specific ship geometry, meaning the derived P_{drift} is specific to the geometry specified in the simulations. As observed in Section 3.2.2, there are differences in travelled distance and direction for different ship types. To obtain a P_{drift} value that accounts for all possible ship types, all simulations used to calculate P_{drift} in Equation 3.6 should be repeated for each ship type. Subsequently, these results should be averaged or normalised to ensure that the calculated P_{drift} reflects the distribution of ship types at a specific location.

Example calculation of drift probability

Now that we have outlined how to calculate the drift probability for a single location, let's examine a small example.

Two assumptions are made for the wind and wave conditions:

- The significant wave height and mean period are assumed to directly correlate with a combination of wind speed and wind direction, meaning that they are derived by averaging its observed values for each corresponding combination of wind speed and wind direction.
- The wave direction is assumed to always align with the wind direction.

These assumptions imply that we only need to specify value ranges for two variables: wind speed and wind direction.

Wind speed is divided into four equal value ranges from its lowest to its highest recorded value. Wind direction is segmented into four quadrants: northeast, southeast, southwest, and northwest. Given these categorisations, there are sixteen possible scenarios for the combined conditions of wind speed and direction, calculated as 4 (speed ranges) × 4 (direction quadrants) = 16 scenarios. Based on a dataset of ten years of wind and wave observations, the probability of occurrence is determined for each scenario. These scenarios are illustrated in Figure 3.20. For illustration, a wind rose has been created using the same data, as shown in Figure 3.21. Here, you can observe that the largest contribution comes from the southwestern quadrant, with wind speeds ranging from 5.5 m/s to 11 m/s, similar to what is indicated by the yellow square in Figure 3.20.

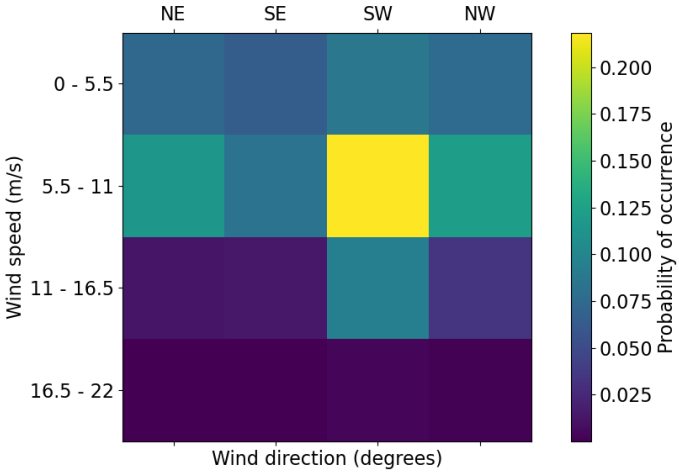

Figure 3.20: A 4 by 4 matrix of wind speed and direction combinations and their corresponding probability of occurrence

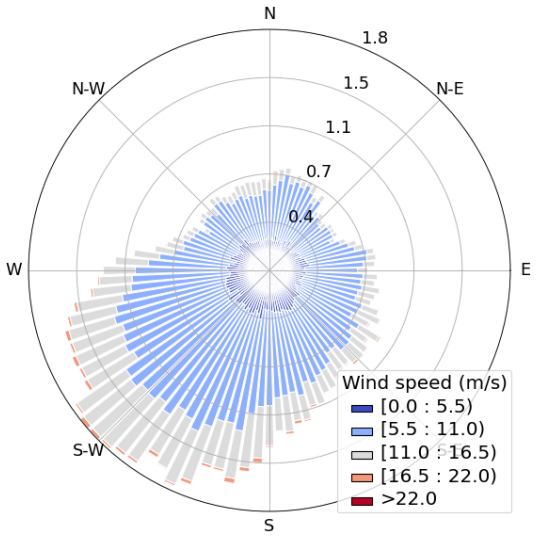

Figure 3.21: Wind rose for the same wind data

Each of these scenarios is subsequently combined with one of two current segments, illustrated by the blue and red areas in Figure 3.22. Together, this results in 32 combinations of wind, wave, and current scenarios. The probability of occurrence for these combinations is calculated by multiplying the occurrence rate of the wind and wave scenario, indicated by the colour of each square in Figure 3.20, by $\frac{1}{2}$, accounting for the two current segments.

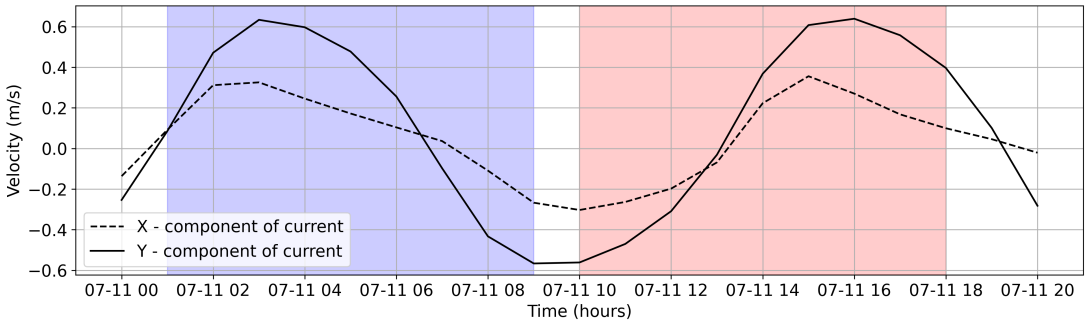

Figure 3.22: Current segment starting at 01:00 (blue) and 10:00 (red)

Next, these scenarios are implemented in the OpenDrift model to run the simulations. The simulated trajectories for each wind and wave condition combination with the red current segment are illustrated in Figure 3.23. The thick lines represents the average trajectory of all trajectories for each simulation.

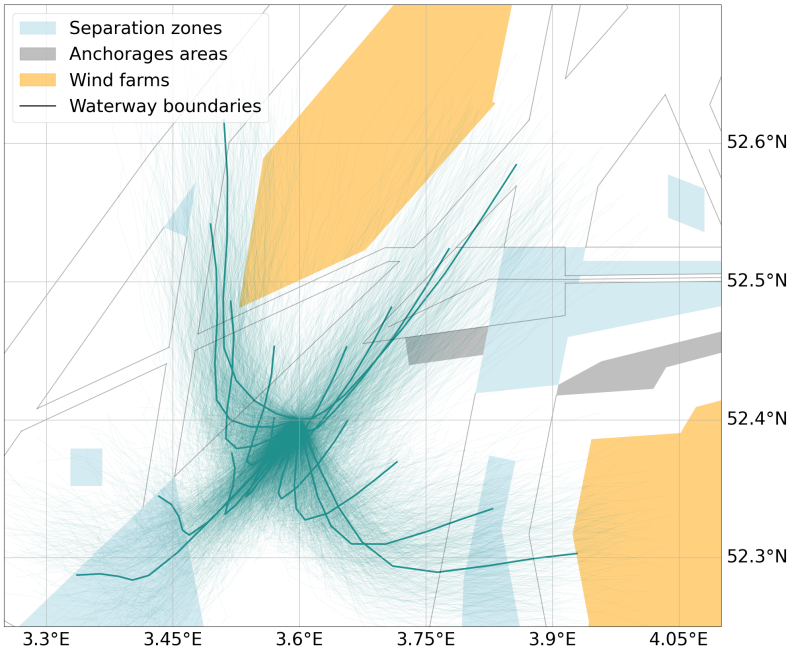

Figure 3.23: Trajectories for current segment starting at 10:00

The simulated trajectories are analysed to determine if they intersect any wind farm areas (represented by orange squares) during a specified period. By multiplying the proportion of trajectories that intersect the wind farm, denoted as P_{sim}, by the probability of occurrence of each wind, wave, and current combination for which the simulation was run, we obtain the probability that those environmental conditions are present and the ship drifts into the wind farm. By summing all these products, we can calculate P_{drift}, the probability of the ship drifting into the wind farm, considering all possible environmental conditions. This calculation procedure is outlined in Equation 3.7.

$$P_{drift} = \sum_{i=1}^{16} \sum_{j=1}^{2} \left(\frac{N_{cross}(i,j)}{N_{sim}} \times P_{env}(i) \times \frac{1}{2} \right) \tag{3.7}$$

This P_{drift} value accounts for just one specific ship type, for which the simulations were run. The account for multiple ship types, this procedure must be repeated for each ship type considered.

This procedure can now be applied to multiple locations around a wind farm area, which will result in a distribution of P_{drift} around these locations. This distribution will highlight which starting locations have the highest probability of a ship drifting into the wind farm, taking into account all possible environmental conditions.

3.4.3. Validity, reliability, and efficiency challenges of drift probability calculation

The established method of calculating the drift probability (P_{drift}) through OpenDrift simulations conducted for a set of environmental scenarios raises two concerns. Firstly, for more extreme conditions, the changes in wind speed and direction within 8-hour periods are likely to be greater, suggesting that keeping the wind and wave conditions constant may lead to an underestimation or overestimation of P_{sim}. Therefore, it is necessary to examine to what degree the greater variability in environmental forcing throughout a ship's drift affects the resulting drift probability (P_{drift}). This involves confirming that our assumptions are valid for the calculation of P_{drift} by comparing P_{drift} obtained through our scenario-based approach with those through the hindcast-data approac, which was discussed at the beginning of this chapter.

Secondly, the scenario-based representation of wind, wave, and current forces raises the question of how many combinations of these forces and how many current segments are needed for a valid and reliable representation of a ship's drift trajectory to calculate P_{drift}. The objective is to identify a minimal number of combinations that are both sufficiently valid for calculating P_{drift} and computationally feasible. In the next section, we will analyse P_{drift} values obtained through a scenario-based approach compared to those obtained through a hindcast-data approach, to determine a valid, reliable, and computationally feasible set of scenarios used to simulate trajectories and calculate the drift probability for a single starting location.

3.5. Determining the level of detail of scenarios through drift probability analysis

The wind, wave and current scenarios should be a valid representation of the forcing environment for calculating P_{drift} as defined in this study. This requires us to verify whether the assumptions made for creating the wind, wave, and current scenarios result in drift trajectory simulations that yield P_{drift} values similar to those obtained from simulations using time-varying hindcast data, which do not rely on these assumptions. The specific assumptions to be verified are:

1. the wind and wave forces remain constant throughout a ship's drift trajectory, and
2. the current forces are independent of the wind and wave forces.

Simultaneously, we need to define the OpenDrift settings and the set of wind, wave, and current scenarios that will be used to simulate drift trajectories for the P_{drift} calculations in this study. The settings and scenarios should be defined such that:

- the simulations are based on a valid representation of the environmental forces for our definition of P_{drift},
- the results are reliable (i.e., consistently reproducible),
- computation time is minimised.

Thus, we are looking for a minimally detailed OpenDrift setting configuration and set of scenarios that yield reliable and valid P_{drift} results. To achieve this, we will first examine and decide on the OpenDrift settings to be used. Next, through analysis of P_{drift} values, we will decide on the set of wind and wave force combinations and the number of current segments. The result is an implementation of our established method to calculate P_{drift} efficiently for a single starting location with the intention of expanding to multiple locations, covering multiple wind farm areas.

3.5.1. Selecting locations and OpenDrift settings for comparative drift probability analysis

The OpenDrift settings and forcing environment are evaluated for the same ship type and starting locations. The analyses are conducted at locations east of, and at increasing distances from, the Hollandse Kust West wind farm, indicated by the red points in Figure 3.24. These specific locations were selected for analysis because they are positioned at increasing distances and oriented differently relative to the wind farm. Additional analyses are performed at the locations marked by the blue points in Figure 3.24, each differently positioned relative to the Hollandse Kust West wind farm but at a comparable distance of 5 kilometres. The details of these locations are provided in Table 3.14.

The simulations are consistently carried out for a single ship type that has a geometry similar to that of the Julietta D. The details of this ship type, as required by OpenDrift, are documented in Table 3.15.

	red locations		blue locations	
	Longitude	**Latitude**	**Longitude**	**Latitude**
1	3.644°	52.459°	3.490°	52.550°
2	3.600°	52.434°	3.760°	52.790°
3	3.557°	52.408°	3.940°	52.770°
4	3.513°	52.383°	-	-

Table 3.14: Locations Hollandse Kust Zuid

Ship geometry	
Length	200 m
Beam	30 m
Draught	10 m
Height	25 m

Table 3.15: Ship geometry parameters

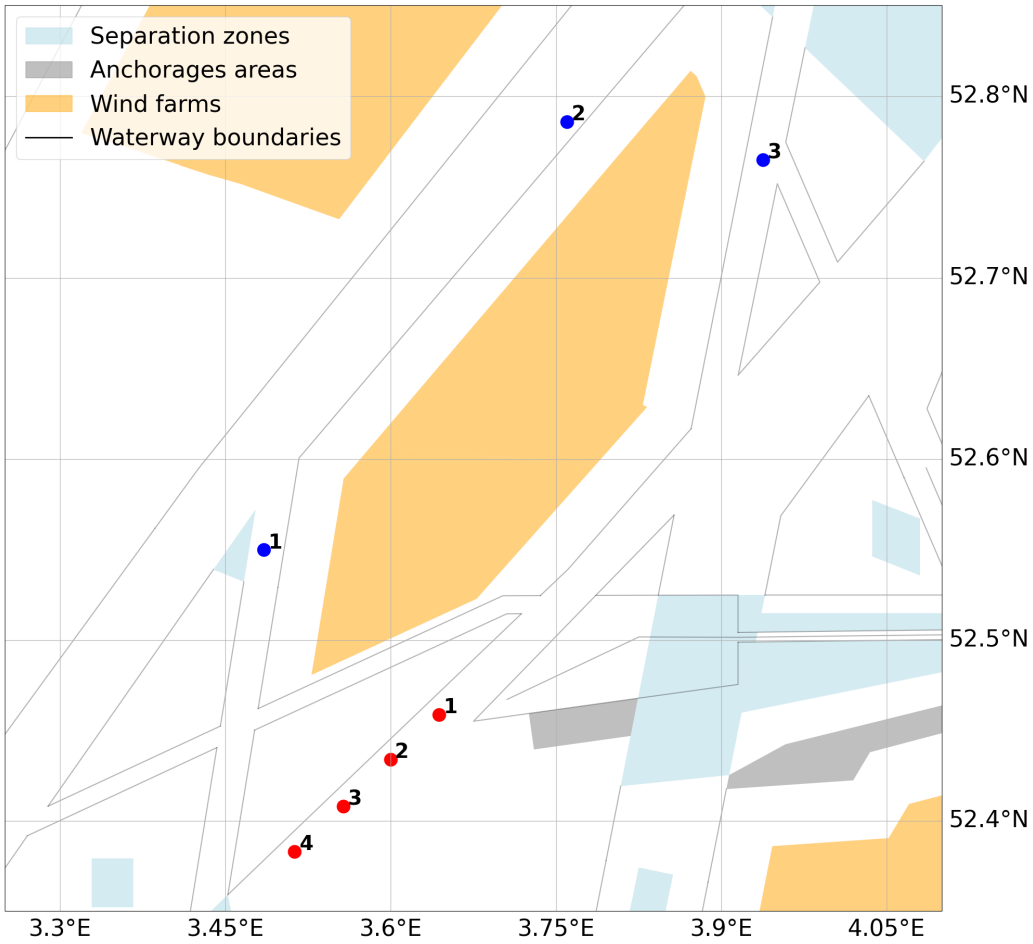

Figure 3.24: Locations for comparative analysis

The OpenDrift settings consist of starting locations, starting time, duration, time step, and number of trajectories, as previously discussed in Section 3.1.3. Regarding the number of trajectories, the larger the number, the greater the computation time required for each simulation. Therefore, our aim is to identify the minimal representative number of trajectories for each simulation that consistently leads to the same results upon repetition and matches the outcomes of simulations with a larger number of trajectories, thereby ensuring reliable probability calculations.

To reiterate, a simulation corresponds to a simulation of a specific ship's drift from a specific starting point under the influence of a specific combination of wind, wave, and current forces. Based on this, the probability P_{sim} can be determined. Reflecting on the sensitivity analysis in Section 3.2, where medium and large-sized ships were analysed over 8 hours with a total of 1,000 trajectories per simulation, we observe a pattern. By plotting the average location in terms of longitude and latitude against an increasing number of trajectories, we observe convergence at approximately 300 trajectories (Figure 3.25). This indicates that beyond 300 trajectories, the average location where the ship may end up does not significantly change. Similarly, convergence is noted when plotting the number of trajectories against the maximum distance between endpoints after 8 hours (Figure 3.26). This indicates that beyond 300 trajectories, the potential area where the ship may end up after 8 hours does not significantly increase. As the area where a ship is likely to end up converges at this point, it defines the number of trajectories required to achieve a reliable outcome.

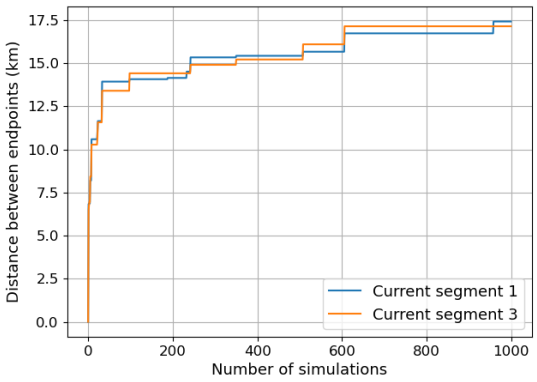

Figure 3.25: Dispersion of endpoints for increasing number of trajectories

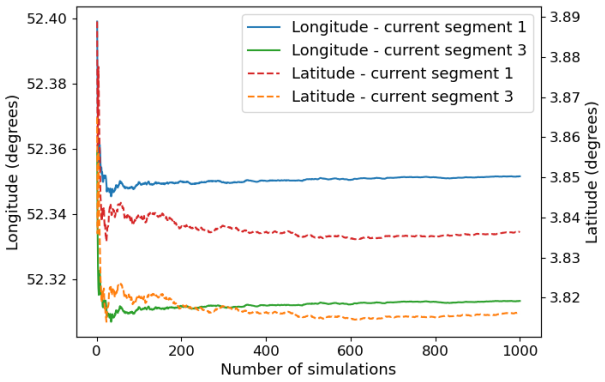

Figure 3.26: Average location for increasing number of trajectories

Given that more trajectories significantly increase computation time — each trajectory must be calculated and analysed to determine if it indicates an allision — it has been decided to perform calculations with 300 trajectories per simulation.

Regarding the duration, it has been decided to calculate the trajectories for a duration of 8 hours. The Julietta D case, where the ERTV reached the adrift ship very late, suggests that 8 hours is a sufficient timeframe. As for the time step, the available model data is on an hourly basis. Therefore, it has been decided to use a time step of 1 hour. Interpolating the model data for finer resolution is unnecessary, as OpenDrift already interpolates the data when calculating a ship's position change at each time step.

3.5.2. Deciding on a set of wind and wave force scenarios

OpenDrift simulations have been conducted at the four predefined locations east of the Hollandse Kust Zuid wind farm to decide on the level of detail required for wind and wave scenarios. These simulations used both the hindcast data-based approach and an increasing number of scenarios in the scenario-based approach. Through an analysis of the drift probability (P_{drift}) resulting from these simulations, a set of wind and wave scenarios will be selected. Each combination of wind and wave forces is initially combined with a set of six current segments. After establishing a set of wind and wave conditions, we will analyse the impact of the number of current segments on P_{drift} to determine the minimal number needed to achieve results comparable to those obtained through the hindcast data-based approach.

For the hindcast data-based simulations, we performed runs for the previously defined ship every three hours over a two-month period, from January 1, 2021, to March 1, 2021. In these simulations, the ship was subjected to hourly varying but spatially constant environmental forces. In the scenario-based approach, simulations were conducted for the same ship under the influence of six different sets of wind and wave conditions. These conditions were derived through multi-dimensional data binning of hindcast data observations over the same period the hindcast data-based simulation were run. This structure allows us to compare P_{drift} and validate the assumptions of the scenario-based approach. These sets of wind and wave conditions progressively increase in complexity, starting with the fewest wind and wave combinations in the first set and adding more in each subsequent set:

- Initially, only wind speed and wind direction are categorised, progressing through 4 by 4, 8 by 8, and 16 by 16 value ranges. The significant wave height and mean period are assumed to directly correlate with wind speed and direction combinations. The wave direction is aligned with the wind direction and is therefore excluded from the multi-dimensional data binning process.
- Subsequently, while maintaining the wind categorisation as 8 by 8 value ranges, the categorisation of significant wave height is adjusted first to 4 and then to 8 ranges. This adjustment allows for combinations of high wind speeds with low wave heights, and vice versa.
- Finally, while maintaining the wind categorisations as 8 by 8 and the wave height as 4 value ranges, the directional aspect of the waves is analysed for 8 directional intervals. This adjustment accounts for misalignment's between the wind and wave directions.

It's important to note that the categorisation of wind and wave direction always starts from the south. For a 4 by 4 categorisation, this results in ranges from south to west, west to north, and so forth. For an 8 by 8 categorisation, the divisions are finer, ranging from south to southwest, southwest to west, and so on. Additionally, any potential misalignment between wind and wave directions is represented as a combination of these orientation segments. To reiterate, its representative value is the average of the observed values within the specific orientation, based on the observations that correspond to a particular combination of wind and wave variables. Furthermore, it has been decided that the mean period is always assumed to be adequately represented by the average of observed values, again based on observations that correspond to a specific combination of wind and wave variables.

Each of the listed environments is simulated for each of a set of six current segments, starting at 01:00, 03:00, 05:00, 07:00, 09:00, and 11:00. These times correspond to the period of the selected current cycle. This is illustrated in Figure 3.27. By averaging the probability outcomes P_{drift} for these six current segments, we obtain the final P_{drift} results. As mentioned in Section 3.4, the current used should represent a cycle average in terms of maximum velocity and be independent of the wind and wave forces. For the latter to be true, the current should only represent the astronomical tide and not wind- and wave-driven currents. The data source used, as specified in Appendix E, does not solely model the astronomical tide. To comply with both requirements, a current cycle is selected that is both average in terms of maximum velocity and corresponds to a period of low wind speeds, to closely represent the astronomical tide. This selection process is outlined in the Appendix E.5.

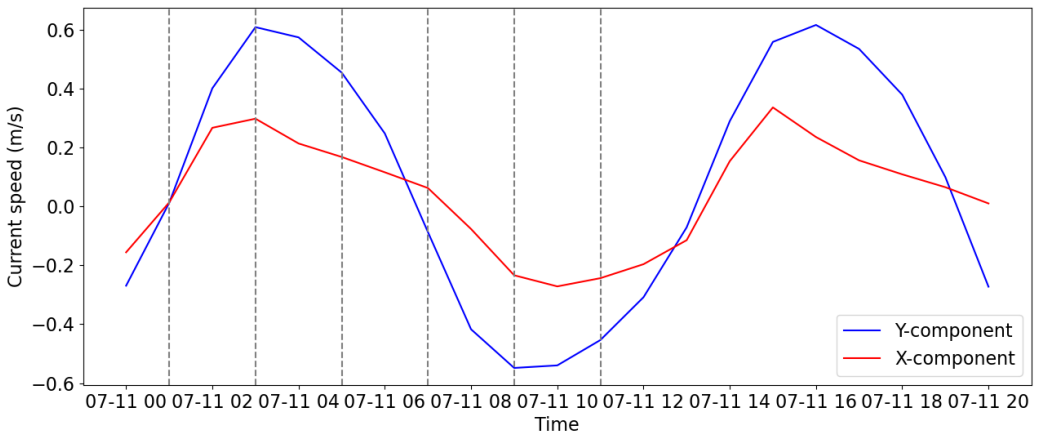

Figure 3.27: The selected current cycle for this study and simulated starting times, corresponding to 3.5° longitude, 52.6° latitude

The results are displayed in Table 3.16. On the left, the P_{drift} results for the hindcast data-based simulations are presented, while all other columns on the right show the P_{drift} results for simulations based on each of the listed scenario-based environments.

	Model data	Scenario-based approach					
Drift duration (hours)		**4x4**	**8x8**	**16x16**	**4x1, 8x8**	**8x1, 8x8**	**4x8, 8x8**
Longitude: 3.64 Latitude: 52.46							
2	3,08%	2,57%	2,92%	3,02%	2,91%	2,92%	2,95%
4	15,15%	13,02%	14,71%	14,75%	14,61%	14,58%	14,58%
6	22,82%	19,33%	22,22%	21,97%	22,10%	21,94%	21,91%
8	28,04%	23,18%	27,62%	27,25%	27,43%	27,21%	27,15%
Longitude: 3.60 Latitude: 52.43							
2	0,83%	0,64%	0,78%	0,82%	0,78%	0,78%	0,81%
4	11,44%	10,31%	11,32%	11,27%	11,31%	11,23%	11,29%
6	18,37%	15,73%	17,34%	17,35%	17,29%	17,18%	17,26%
8	23,18%	19,09%	21,93%	21,78%	21,83%	21,63%	21,71%
Longitude: 3.56 Latitude: 52.41							
2	0,09%	0,08%	0,11%	0,11%	0,10%	0,10%	0,11%
4	6,50%	6,07%	6,72%	6,69%	6,71%	6,68%	6,69%
6	12,70%	10,90%	12,20%	12,00%	12,14%	12,01%	12,05%
8	17,20%	14,02%	15,79%	15,51%	15,71%	15,52%	15,57%
Longitude: 3.51 Latitude: 52.38							
2	0,00%	0,00%	0,00%	0,00%	0,00%	0,00%	0,00%
4	2,60%	1,23%	2,87%	2,84%	2,87%	2,84%	2,86%
6	7,36%	4,43%	6,97%	6,83%	6,98%	6,86%	6,86%
8	11,57%	6,97%	10,00%	9,60%	9,95%	9,73%	9,78%

Table 3.16: P_{drift} values for simulations based on model data vs. a scenario-based approach for value ranges: wind speed x direction, wave height x direction

Validity of the scenario-based approach

The results indicate that P_{drift} derived from simulations based on an 8 by 8 categorisation of wind speed and direction are already quite similar to those obtained from the hindcast data-based simulations. These findings are promising as they validate the two assumptions used in this method for calculating P_{drift}.

It should be noted that since this method counts the number of trajectories crossing any wind farm boundary, analyses focusing on individual wind turbines may require a more refined resolution of the wind and wave variables to obtain results comparable to those based on the hindcast data-based approach. Moreover, the dataset used to analyse these assumptions is relatively small: it only covers January and February of 2021. This limitation is due to the computation time for simulating ship trajectories for time-varying conditions, which is about one minute per simulation. Running these simulations every three hours for two months of hourly data results in 473 simulations, representing a total of 8 hours of computing time for just one location.

For estimating P_{drift} the scenario-based method is considered a valid approach. It avoids the need for simulating each ship under the influence of time-varying conditions. Therefore, the method of simulating for constant wind and wave scenarios and a decoupled current is considered a reliable and efficient approach to extend allision probability calculations to multiple locations covering entire wind farms.

Resolution of wind and wave environment

The P_{drift} results from the scenario-based environment sets show convergence from an 8 by 8 categorisation of wind speed and direction. This categorisation corresponds to 64 potential combinations of wind speed and direction, combined with a corresponding average observed wave height, mean period, and wave direction. This means that the taking into account additional value ranges for any of the forcing variables does not have a significant effect on the resulting P_{drift} values.

To improve the robustness of the scenario-based approach, a slightly more detailed categorisation is selected. The selected categorisation includes four intervals for wave height and eight intervals for wind speed and direction. As a result, the mean period is aligned with observations specific to each combination of wave height, wind speed, and wind direction range. Taking into account four ranges for wave height ensures that scenarios with small wave heights and high wind speeds, or vice versa, are accounted for. Such conditions, although possible, may not have been observed during the two months of our analysis. Additionally, it is assumed that the wave direction is always aligned with the wind direction. All details of this configuration can be found in Table 3.17.

The scenarios will be created using ten years of hindcast data to accurately capture all possible environmental force combinations and their corresponding occurrence rate. The data sources for wind and wave observations are detailed in Appendix E. Additionally, an illustration of the 64 wind speed and direction combinations, along with their occurrence rates, can be found in Appendix E.4.

Variable	Value Ranges	Description
Wind speed	8	Evenly distributed from lowest to highest observation
Wind direction	8	(S-SW, SW-W, etc.)
Significant wave height	4	Evenly distributed from lowest to highest observation
Mean period	-	Assumed correlation
Wave direction	-	Aligned with wind direction

Table 3.17: Value ranges selected for creating wind and wave force combinations

3.5.3. Deciding on the set of current segments

The previous P_{drift} results were obtained by averaging the P_{drift} result for each of the six current segments, which start every two hours along the selected current cycle. This means that each wind and wave force combination is simulated six times, once for each segment. For an 8 by 8 categorisation for wind speed and direction, combined with four intervals for wave height, this amounts to 8 × 8 × 4 × 6 = 1536 simulations for just one location, assuming all combinations are present in the dataset.

To analyse the minimum number of segments required to achieve a similar result, the probability outcomes are averaged for:

- 4 segments, starting at the maxima and zero-crossings.
- 4 segments, starting one hour after the maxima and zero-crossings.
- 2 segments, starting at the two maxima.
- 2 segments, starting at the two zero-crossings.

The P_{drift} for each hour are detailed in Table 3.18.

	Drift duration (hours)							
Current segments	**1**	**2**	**3**	**4**	**5**	**6**	**7**	**8**
Longitude: 3.64 Latitude: 52.46								
6	0,00%	2,91%	9,48%	14,61%	18,74%	22,10%	24,92%	27,43%
4 (maxima and zero-crossings)	0,00%	2,81%	9,84%	15,08%	19,11%	22,19%	24,91%	27,44%
4 (off maxima and zero-crossings)	0,00%	2,73%	9,37%	14,10%	18,17%	21,60%	24,61%	27,16%
2 (starting at maxima)	0,00%	4,90%	11,84%	13,79%	15,88%	19,58%	23,90%	27,49%
2 (starting at zero-crossings)	0,00%	0,72%	7,84%	16,38%	22,34%	24,80%	25,91%	27,39%
Longitude: 3.60 Latitude: 52.43								
6	0,00%	0,78%	6,09%	11,31%	14,57%	17,29%	19,69%	21,83%
4 (maxima and zero-crossings)	0,00%	0,67%	6,04%	11,80%	14,92%	17,63%	20,04%	21,92%
4 (off maxima and zero-crossings)	0,00%	0,59%	6,10%	10,70%	14,01%	16,87%	19,25%	21,34%
2 (starting at maxima)	0,00%	1,29%	7,27%	9,60%	10,59%	13,58%	17,67%	20,69%
2 (starting at zero-crossings)	0,00%	0,05%	4,81%	14,00%	19,25%	21,68%	22,40%	23,14%

Table 3.18: P_{drift} for averaging for a different number of current segments

The results indicate that averaging across four segments is sufficient to achieve similar outcomes. This is especially true when the segments start at the maxima and zero-crossings of the current cycle, as these points most closely align with the results from averaging for six current segments. Conversely, averaging for only two segments, whether starting at the maxima or the zero-crossings, results in considerable differences at each time step.

Based on these findings, it has been decided to simulate each wind and wave scenario for four current segments, starting at the maxima and zero-crossings of the selected current cycle.

Neglecting the influence of current

Referring back to Section 3.2, where we analysed how wind, wave, and current forces influence a drifting ship's trajectory, one might assume that the cyclical influence of the current on the resulting P_{drift} averages out. In simpler terms, this would suggest that at locations near a wind farm, all possible trajectories formed through any of the segments for specific wind and wave conditions would intersect the wind farm. However, this assumption does not hold for specific orientations and distances from the wind farms, where certain trajectories for certain current segments might not intersect with the wind farm at all.

To further investigate this issue, P_{drift} is recalculated for the red points shown in Figure 3.24 based on simulations that only consider wind and wave forcing. This analysis uses data from January 1, 2021, to March 1, 2021, categorised into scenarios based on the selected configuration of wind and wave combinations, as detailed in Table 3.17. The resulting P_{drift} values are then compared with those obtained earlier when averaged for the four current segments, selected to be starting at the maxima and zero-crossings of the selected current cycle. The comparison is detailed in Table 3.19.

	Hour 1	**Hour 2**	**Hour 3**	**Hour 4**	**Hour 5**	**Hour 6**	**Hour 7**	**Hour 8**
Longitude: 3.64 Latitude: 52.46								
Including current	0,00%	2,81%	9,84%	15,08%	19,11%	22,19%	24,91%	27,44%
Excluding current	0,00%	0,26%	1,76%	4,41%	7,82%	10,70%	13,59%	16,09%
Longitude: 3.60 Latitude: 52.43								
Including current	0,00%	0,67%	6,04%	11,80%	14,92%	17,63%	20,04%	21,92%
Excluding current	0,00%	0,01%	0,35%	1,75%	4,29%	6,83%	9,55%	12,11%
Longitude: 3.56 Latitude: 52.41								
Including current	0,00%	0,06%	2,31%	6,59%	9,67%	11,68%	13,90%	15,68%
Excluding current	0,00%	0,00%	0,03%	0,35%	1,20%	2,56%	4,18%	5,92%
Longitude: 3.51 Latitude: 52.38								
Including current	0,00%	0,00%	0,22%	2,47%	5,09%	6,61%	8,02%	9,76%
Excluding current	0,00%	0,00%	0,00%	0,03%	0,19%	0,63%	1,42%	2,56%

Table 3.19: P_{drift} for in- and excluding current at increasing distance

The results indicate that P_{drift} differs significantly, by approximately 10 percent point at each location, when the influence of the current is excluded in the simulations.

P_{drift} is also calculated for the blue locations shown in Figure 3.24, for the same environmental conditions, both including and excluding the current. These locations are differently oriented and positioned at an equal distance of 5 kilometres from the wind farm. For these locations, one might expect that all trajectories influenced by the current would intersect the wind farm, given their close proximity to a large wind farm area. The results are presented in Table 3.20.

	Hour 1	Hour 2	Hour 3	Hour 4	Hour 5	Hour 6	Hour 7	Hour 8
Longitude: 3.49 Latitude: 52.55								
Including current	0,10%	5,31%	12,05%	17,96%	23,35%	27,54%	30,91%	34,00%
Excluding current	0,06%	4,48%	11,96%	19,83%	26,12%	30,16%	33,36%	35,84%
Longitude: 3.76 Latitude: 52.79								
Including current	0,22%	6,27%	14,38%	19,93%	23,44%	26,52%	28,69%	30,43%
Excluding current	0,09%	3,56%	9,93%	16,39%	20,61%	24,28%	27,18%	29,32%
Longitude: 3.94 Latitude: 52.77								
Including current	0,00%	0,74%	3,68%	7,33%	10,24%	12,35%	14,71%	16,50%
Excluding current	0,00%	0,64%	3,66%	7,14%	10,37%	12,65%	14,64%	16,52%

Table 3.20: P_{drift} for in- and excluding current at different orientations

The results continue to show variation in P_{drift}. For locations to the southwest (the first) and northwest (the second), P_{drift} differs for certain hours of drift duration but ultimately converges to the same value at 8 hours. This suggests that, despite differences for shorter drift durations, all possible trajectories for specific wind and wave conditions from these locations eventually cross the wind farm. For the last location to the northeast, P_{drift} remains approximately equal for each hour of drift duration.

The variability in hourly P_{drift} values obtained through simulations that include and exclude the current highlights the importance of including the current in the scenario-based approach. Additionally, insights into how specific current segments affect P_{drift} for different drift durations or the time until these probabilities converge can be valuable for strategic purposes. Therefore, the current will be incorporated into the scenario-based approach.

3.6. Summary of outcomes and decisions

For this study, OpenDrift is selected as the trajectory prediction model to be integrated into a method for estimating allision probabilities. This decision is based on the high accessibility of OpenDrift as an open-source tool and its relatively simple approach to simulating trajectories. By using OpenDrift's trajectory predictions to represent a ship's unfavourable drift direction—a direction indicating an allision—the opportunity arises to move beyond the need for the assumptions that state-of-the-art methods rely on:

1. the ship moves in a purely lateral direction (one degree of freedom),
2. the wind and waves act in the same direction,
3. the wind direction and wind speed are kept constant, and
4. the current is accounted for as an estimated speed in the already established drift direction (wind direction).

The analysis of OpenDrift simulations, involving different combinations of forces, showed to what extent a ship's trajectory depends on wind, wave, and current forcing. The analysis can be summarised in a number of key findings:

- wind forcing is dominant over wave forcing in terms of travelled distance,
- a ship's initial orientation is a crucial parameter in determining how it displaces with the waves,
- for small waves, their influence is negligible,
- for more extreme wave conditions, the influence of waves is greater for larger ships in terms of wet area, leading to larger travelled distances and greater deviations when wind and waves are not aligned,
- the ratio between area exposed to the wind and wetted area of a ship is an important parameter in terms of travelled distance and deviation from the wind direction,
- The influence of the current is time-dependent, leading to various possible travelled distances and deviations from the wind direction.

The influence of wind, wave, and current forces on a drifting ship's trajectory is clearly observed in the trajectory of the Julietta D. Therefore, it can be stated that OpenDrift is somewhat capable of predicting a ship's trajectory. However, accurately predicting its entire path is challenging due to the need for precise geometry information, reliance on modelled environmental data and the assumption of a 'clean' drift.

In conclusion, to reconstruct a drifting ship's trajectory accurately, knowledge of all three types of forces is essential. Excluding any of these forces can lead to predictions that significantly deviate from a ship's actual trajectory.

An initial option for simulating the potential trajectories that a drifting ship might take based on all possible environmental conditions is to conduct OpenDrift simulations using spatially and temporally varying hindcast data. However, considering the variability of forcing in both time and space results in extensive computation time. To account for all possible environmental conditions while limiting computation time, two assumptions have been made:

- the wind and wave forces remain constant throughout a ship's drift trajectory, and
- the current forces are independent of the wind and wave forces.

We can now account for wind and wave conditions by creating scenarios for the wind and wave force variables—significant wave height, mean direction, wave direction, wind speed, and wind direction—using multi-dimensional data binning. The current is divided into a number of segments representing its cyclic influence and thus the variety throughout a ship's drift trajectory. These segments can simply be added to each scenario, resulting in a total of wind, wave, and current combinations equal to the product of the number of wind and wave combinations and the number of current segments. We have now accounted for the variability in wind, wave, and current forcing at the moment the ship becomes adrift and for the variability in current forcing throughout its drift trajectory, enabling the calculation of P_{drift} based on OpenDrift simulations, as detailed in Equation 3.6.

Next it should confirmed be that the wind, wave and current scenarios are a valid representation of the environmental conditions for calculating P_{drift}. Simultaneously, the OpenDrift settings and the set of wind, wave and current scenarios that will be used to simulate drift trajectories for the P_{drift} calculations in this study need to be defined.

The OpenDrift settings have been selected to be:

- 300 trajectories per simulation,
- with a time step of 1 hour,
- for a duration of 8 hours.

These settings have been confirmed to produce reliable outcomes. Furthermore, a duration of 8 hours is considered sufficient for potential interventions with external measures, thereby providing relevant allision probabilities.

For a single location, simulations will be conducted for the following scenario-based environment:

- The environment is categorised into eight value ranges for wind speed and direction, and four value ranges for significant wave height, with each range evenly distributed from the lowest to the highest recorded value.We assume that the mean wave period correlates directly with any of these combinations, and the wave direction is always aligned with the wind direction (Table 3.17). This scenario-based environment is created based on 10 years of hindcast data. The data source is detailed in Appendix E, and an illustration of the probability of occurrence for combinations of wind speed and direction can be found in Section E.4.
- Each wind and wave combination is paired with one of a set of 4 current segments, which start at both the maximum points and zero-crossings of a typical current cycle, as illustrated in Figure 3.27. The current is implemented in OpenDrift as a current field, accurately representing the current for each location. It has an average maximum velocity, and its period corresponds to a period of low wind speeds, thereby approximating an astronomical tide. The selection process can be found in Section E.5.

This scenario-based approach has been validated as an effective method for calculating P_{drift}. The selected combination balances computational efficiency with robustness and allows for various wind and wave conditions. Furthermore, incorporating the current is essential, as neglecting it leads to inaccurate P_{drift} values around a wind farm.

Referring back to the assumptions made in state-of-the-art methods, for our study, assumptions 2 and 3 are reiterated. Comparing P_{drift} from the established methodology with P_{drift} obtained through temporally varying model data revealed that for our definition of allision—crossing any wind farm boundary—it is sufficient to assume that wind and waves are constant throughout a ship's trajectory and act in the same direction. Conversely, assumptions 1 and 4 are not incorporated into the established methodology. If wind and current are not aligned, the influence of the current causes a ship to deviate from the wind direction, resulting in trajectories under certain current segments not crossing the wind farm area. Therefore, the influence of the current on P_{drift} does not average out, and excluding the current would lead to considerable differences in P_{drift} values.

4

Implementation of method

In the previous chapter, a method was established to simulate trajectories using OpenDrift for a set of wind, wave, and current combinations that cover the possible environmental conditions at a single location. These trajectories are then used to calculate P_{drift} for that location: the sum of all products of P_{sim}, the probability of allision in a single OpenDrift simulation, and P_{env}, the probability of occurrence of the wind, wave, and current combinations used in the simulation. Through analysis of P_{drift} values, a set of wind and wave force combinations and a number of current segments were determined that proved to provide a valid representation of the environment for calculating P_{drift}. This approach resulted in reliable outcomes and minimised computation time.

Chapters 4, 5 and 6 address the second research objective: **Evaluate the practical implications of a trajectory prediction-based approach to estimating the probability of drifting ship allisions for optimising risk-reducing strategies**. We will implement the established method to obtain a P_{drift} distribution around multiple wind farms. Subsequently, the P_{drift} are combined with corresponding shipping density values ($P_{allision}$), which result in the $P_{allision}$ distribution for this study.

In this chapter we will elaborate on the simplifications made to scale the method for calculating P_{drift} to multiple locations, covering multiple wind farms. This discussion will address the selection of starting locations, the spatial resolution of the environment, and the classification of ship types used in our analysis. Once the method for scaling the P_{drift} calculations is established, we will discuss how we will determine the shipping density values across our area of interest. Both aspects will result in the calculation of allision probability levels around multiple wind farms, which will be presented in Chapter 5.

4.1. Scaling drift probability calculations to multiple wind farms

All previous analyses focused on a single or a few locations to determine P_{drift} and were based on a single ship geometry. To determine the drift probability for multiple locations, covering multiple wind farms, several decisions need to be made regarding:

- the specific locations for analysis,
- the spatial resolution of the environmental scenarios for which the simulations will be performed,
- the types of ships considered.

4.1.1. Considered locations

To determine the probability of a ship drifting into a wind farm, irrespective of its starting location, we need to know the distribution of:

- the drift probability (P_{drift}) around the wind farm, and
- the probability of presence of a drifting ship ($P_{activity}$), around the wind farm.

As discussed at the beginning of Chapter 3, the probability of engine failure is assumed to be uniform across the North Sea. Consequently, areas with high shipping activity have an increased probability

of a ship becoming adrift. Therefore, conducting simulations in areas with minimal shipping activity is unnecessary. Because of this, we confine our area of interest to the North Sea fairways, defined using data from Rijkswaterstaat (Dutch Government, 2024). Within Figure 4.1, these fairways are illustrated in red for a section of the North Sea that includes the wind farms Hollandse Kust West, Hollandse Kust Zuid, and Hollandse Kust Noord. Within these fairways, a grid with cells measuring 3 by 3 kilometres is established, marked by thick red lines. The simulations points are situated at the intersections of each grid cell, presented as blue points. This arrangement ensures that we capture the highest and lowest P_{drift} values at the boundaries of the fairways. Due to the irregular shapes of the fairways, clusters of intersection points have formed. If intersections are less than 1.5 kilometres apart, they are consolidated into one point, represented by the central point of the respective cluster.

To limit the number of simulations, we only run simulations for points within 25 kilometre of the border of each wind farm, amounting to about 200 locations per wind farm area, as shown by the green points for the Hollandse Kust Zuid wind farm in Figure 4.1. Beyond a 25 kilometre range, the probability of a ship drifting into the wind farm is zero for a drift duration of up to 8 hours.

4.1.2. Spatial resolution of the environment

OpenDrift can run simulations for the same wind and wave force combination simultaneously at multiple locations, thereby reducing the amount of computation time. Therefore, it would be too time-consuming to create a unique scenario-based environment for each considered location. Moreover, creating this scenario-based environment for each location requires extracting this data and converting it into a constant wind-wave environment for each location. On the other hand, the ERA5 dataset, which is used to extract the U10 and V10 components of the wind forcing, is based on a relatively coarse grid. The ERA5 dataset consists of data points every 0.25 degrees in longitude and latitude. It was therefore decided to base the environment grid on this grid size and create a constant wind-wave environment at each grid point in the ERA5 dataset for our area of interest. For all locations considered, simulations will be performed based on the constant wind-wave environment created for the nearest environment grid point.

The current will be implemented within OpenDrift as a current field, corresponding to the period of the selected current shown in Figure 3.27, with further details provided in Section E.5. This approach, using a continuous field rather than a spatially constant cycle, ensures accurate representation of current variations across different locations and captures the average magnitude of the current for each specific location.

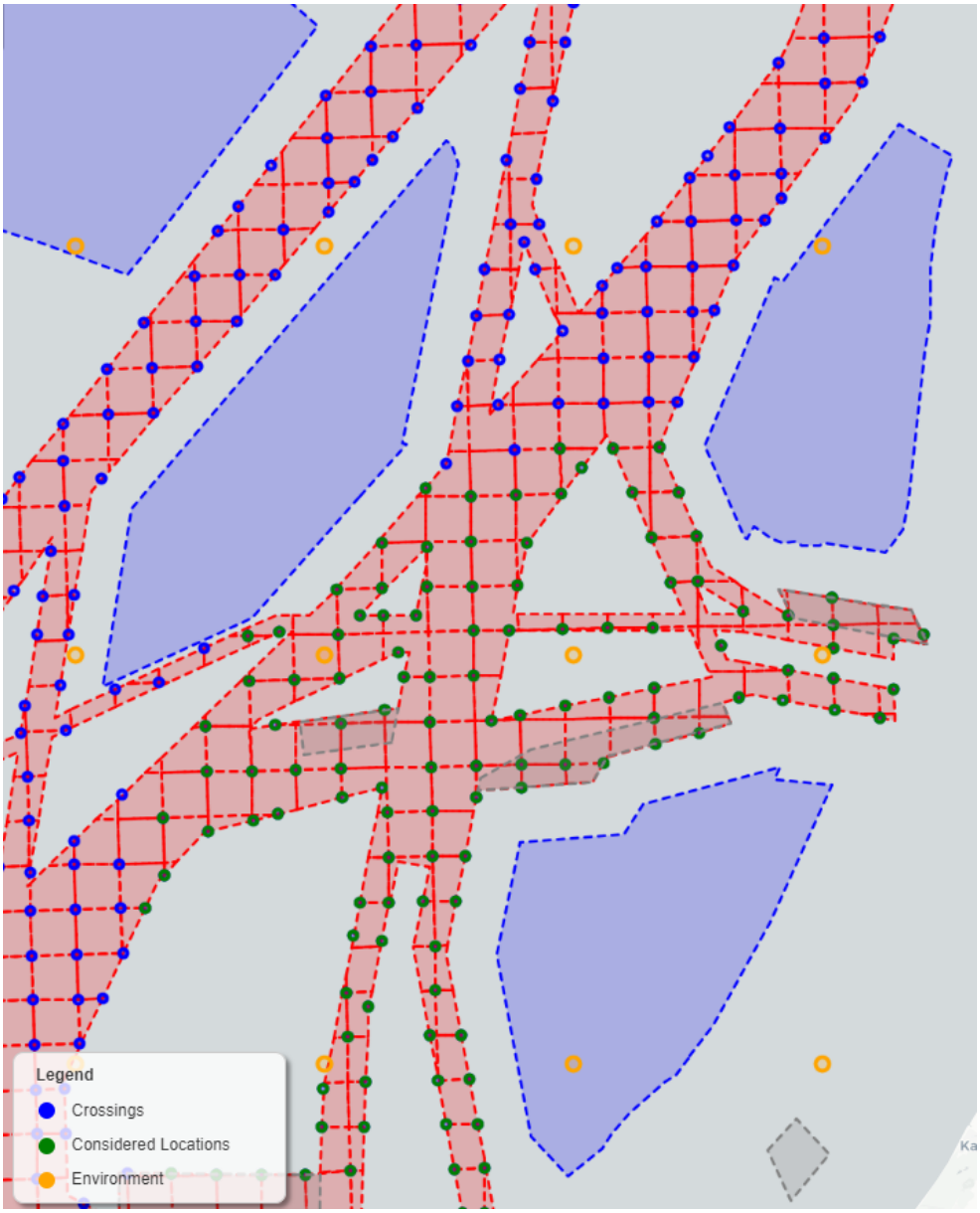

Figure 4.1: Visualisation of the considered locations of Hollandse Kust Zuid

4.1.3. Considered ship types

In Chapter 3, the predictive capability of OpenDrift is analysed using just one real-world case: the Julietta D incident. Therefore, it is not possible to definitively state that OpenDrift accurately predicts outcomes for other ship geometries. Furthermore, OpenDrift models a ship's wind-exposed surface as a square determined by the ship's height from the waterline, length, and orientation. More importantly, considering multiple ship types requires us to repeat the simulation and P_{drift} calculation procedure for each type. So, based on the limited knowledge of OpenDrift's predictive accuracy, and to limit the amount of computation time needed, it has been decided to apply the established method to only one ship geometry. Although P_{drift} is based solely on a single ship geometry, we can still approach the final research objective by interpreting the outcomes. It is important to keep in mind that the probabilities might differ if all ship types were accounted for.

Length	200 m
Beam	30 m
Draught	10 m
Height	25 m

Table 4.1: Ship geometry parameters

The geometry used in applying the established method will be similar to that of the Julietta D but will represent a container ship type, with details provided in Table 4.1. The chosen container type is consistent with the geometry of a fully cellular container ship, as described in Rodrigue (2024). Assuming that the height from the waterline to the main deck is one-third of its draught, the overall height was calculated by averaging the height of four TEU-size containers stacked above the main deck.

4.2. Probability of presence of a drifting ship

In the previous section, the procedure for simulating trajectories to determine the distribution of P_{drift} around multiple wind farms was established. What remains to obtain an allision probability level is to multiply the P_{drift} values by the probability of the presence of a drifting ship at each location, denoted as $P_{activity}$ as illustrated in Figure 3.1.

4.2.1. Definition of drifting ship presence probability

The calculated P_{drift} values can be scaled by the shipping density value of a specific area to obtain an allision probability level for that area. This probability represents the chance that (i) a ship becomes adrift in the considered area and (ii) subsequently allides with a wind farm. Since we neglected the probability of engine failure, this level does not represent an occurrence rate but serves as a comparative value against other areas.

Referring back to the formula in Section 3.4.2, which calculates P_{drift} by averaging the P_{drift} results for different ship types, the final probability formula for a single starting location is obtained by incorporating $P_{activity}$ values for each specific ship type as follows:

$$P_{allision} = \sum_{k=0}^{p} \left(\sum_{i=0}^{m} \sum_{j=0}^{n} \left(\frac{N_{cross}(i,j,k)}{N_{sim}} \times P_{env}(i) \times \frac{1}{n} \right) \times P_{activity}(k) \right) \tag{4.1}$$

$$P_{allision} = \sum_{k=0}^{p} \left(P_{drift}(k) \times P_{activity}(k) \right) \tag{4.2}$$

where:

$N_{cross}(i,j,k)$	is the number of trajectories that crossed any wind farm boundary under the influence of wind-wave forcing scenario i and current segment j for ship type k
N_{sim}	is the total number of calculated trajectories per simulation
$P_{env}(i)$	is the probability of occurrence of wind-wave forcing scenario i
n	is the number of current segments
$P_{activity}(k)$	the probability of presence of ship type k
$P_{drift}(k)$	is the probability of a drifting ship of type k crossing any wind farm boundary, considering all possible environmental conditions

As decided in the previous section, the OpenDrift simulations will only be conducted for one ship type. Therefore, the formula used is for this study simplified to:

$$P_{allision} = P_{drift}(k) \times P_{activity} \tag{4.3}$$

The formula calculates $P_{allision}$ for a single starting location by multiplying a ship-specific (k) drift probability by the overall shipping density value of that location.

4.2.2. Determining shipping density values through AIS data

What remains is to quantify the probability of the presence of a drifting ship using a shipping density value. To establish this value, AIS data is used. AIS, an automated tracking system, uses transceivers on ships and is used by Vessel Traffic Services (VTS). The system enables ships to view marine traffic in their area and to be seen by that traffic. It transmits information such as a unique identification, position, navigational status, speed, etc., at specific frequencies. These frequencies vary depending on the ship's speed and its navigational status. To determine the relative activity in a specific area, the number of AIS transmissions over the course of a year is counted for each considered area. This figure is then divided by the total counts from all areas to derive a normalised probability value.

As mentioned, P_{drift} is calculated based on simulated trajectories at each crossing of the 3 by 3 kilometre fairway grid. One approach is to assume that this drift value remains constant for a 3 by 3 kilometre area around each considered crossing and to determine the shipping density for that area. However, this method is too coarse for some fairways, failing to adequately capture the variability in shipping density across the width of the fairway. Consequently, we chose to calculate shipping densities for a finer grid of 1 by 1 kilometre, which provides the necessary detail to reflect density variations between the boundaries and the centre of each fairway. Subsequently, P_{drift} values are linearly interpolated to obtain a value for each cell in the more refined $P_{activity}$ grid.

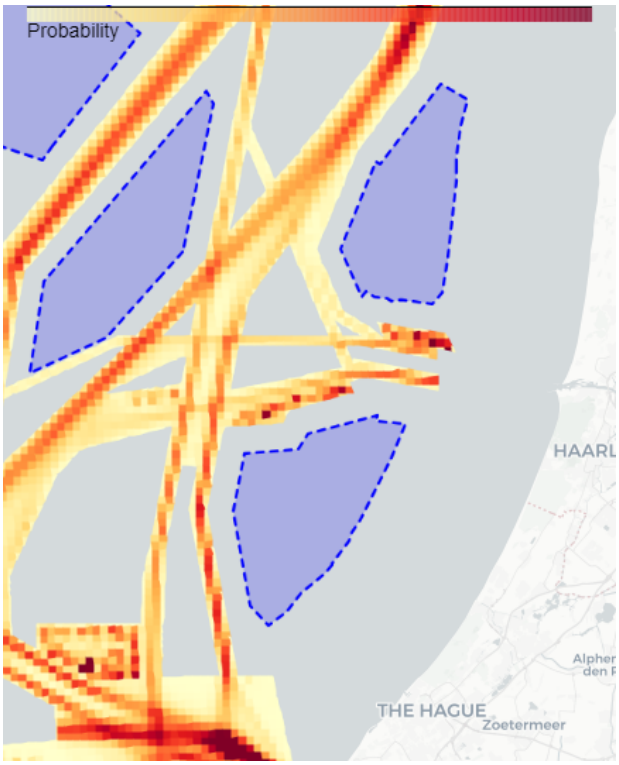

Figure 4.2: Activity probability

The transmission count is sourced from an AIS dataset provided by Rijkswaterstaat (Dutch Government, 2024). The counted transmissions per cell refer to ships that are:

- larger than 75 meters in length,
- classified as ship types between 70 and 90, corresponding to cargo and tanker ships.

These selection criteria were chosen because our study focuses on relatively large ships, which are prohibited from navigating through wind farms and are assumed to pose a greater risk of potential damage. The signal count resulted in the shipping density map presented in Figure 4.2.

Because of a limited AIS dataset the allision probability analyses will only be conducted for the wind farms:

- Hollandse Kust West
- Hollandse Kust Zuid
- Hollandse Kust Noord

By multiplying the P_{drift} value of each grid cell by its corresponding shipping density value, the allision probability level for each cell is calculated, as described in Equation 4.3.

4.3. Summary of outcomes and decisions

In this chapter, various decisions and simplifications have been made to simulate trajectories efficiently while determining the distribution of P_{drift} around multiple wind farms. These simplifications include:

- Conducting simulations for locations within a 25-kilometre radius outside the boundary of a wind farm, at intersections of a 3 by 3 kilometre grid overlaid on the fairways.
- Basing each simulation on the scenario-based environment determined for the closest grid point in the ERA5 dataset.
- Performing simulations for only one ship type, similar to the geometry of the Julietta D.

Although P_{drift} can easily be determined for a smaller fairway grid, for areas outside the fairway boundaries, and for multiple ship types, simulations in this study are limited.

To determine the allision probability level, each P_{drift} value is multiplied by the corresponding shipping density value for each considered location. The shipping density is calculated by counting the AIS transmissions over a year within a smaller grid measuring 1 by 1 kilometre. The AIS dataset is filtered to include:"

- ships larger than 75 meters in length,
- ships classified as types between 70 and 90, corresponding to cargo and tanker ships.

This count is then divided by the total count from all cells within the considered area to obtain a normalised probability value. To calculate the allision probability level for each 1 by 1 kilometre grid cell, the P_{drift} values are matched with the smaller grid through linear interpolation.

Due to a limited AIS datasets, the method is only implemented to cells around the wind farms Hollandse Kust West, Noord, and Zuid. The results of the allision probability for these wind farm areas will be presented in Chapter 5.

5

Allision probability results

In this chapter, the results of the allision probability calculations are presented for the Hollandse Kust West, Zuid, and Noord wind farms. First, the distributions of the drift probability (P_{drift}) and activity probability ($P_{activity}$) are shown to illustrate how they contributed to the final allision probability distribution for Hollandse Kust West. We then analyse the overall probability level of Hollandse Kust West both individually and relative to Zuid and Noord. Next, we will explore how the overall allision probability level varies between wind farms and how the allision probability distribution varies around a single wind farm due for different more specific environmental conditions

5.1. Allision probability results

The OpenDrift simulations for the calculation of P_{drift} have been performed for the Hollandse Kust West, Zuid and Noord areas. The obtained P_{drift} value of each cell is multiplied with the shipping density of that cell ($P_{activity}$), according to Equation 4.3. To illustrate this procedure both the probability distribution of P_{drift} for a drift duration of 8 hours and $P_{acitivty}$ are presented for Hollandse Kust West in Figure 5.1 and Figure 5.2, respectively.

As mentioned in the beginning of Chapter 3, the $P_{allision}$ value of each cell represents a probability level rather than an occurrence rate. Despite this simplification, these values still allow us to compare the relative probabilities across different locations. Therefore, for this and all subsequent results, it has been decided to present the outcomes as heat maps without absolute numbers. Each figure or set of figures is accompanied by an explanation of how it should be interpreted. In the Figures 5.1, 5.2 and 5.3, the value of each cell can be interpreted on a scale from low to high, illustrating the distribution of the probability level, whether P_{drift}, $P_{activity}$, or $P_{allision}$, of Hollandse Kust West.

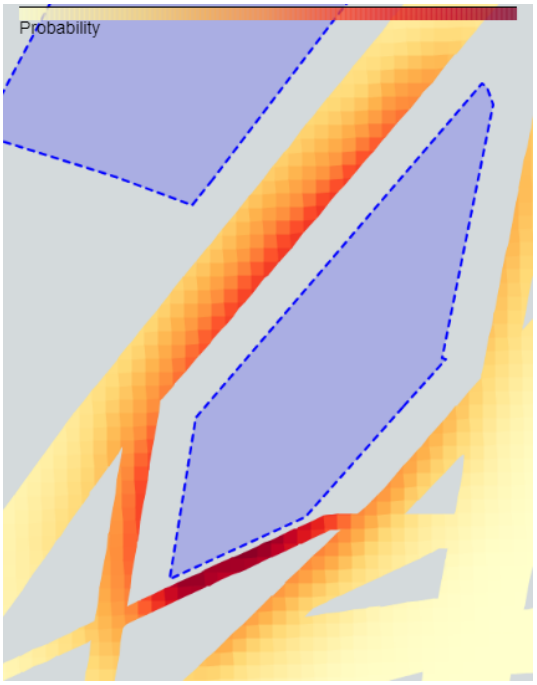

Figure 5.1: Drift probability

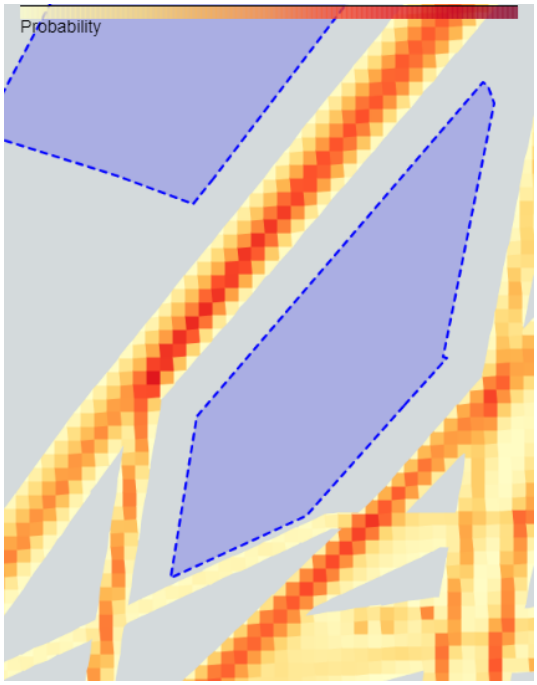

Figure 5.2: Activity probability

The drift probability distribution in Figure 5.1 shows that the closer a ship is to the wind farm, the higher the probability it will drift into the wind farm. This effect is particularly noticeable in the small fairway southeast of the wind farm. Furthermore, the area west of the wind farm shows higher probability values and extends further than the area to the east.

The activity probability distribution in Figure 5.2 shows that the probability of a ship being present is highest in the large fairways, particularly in their middle sections. In the smaller fairways, such as the one southeast of the wind farm, the probability is notably lower.

By multiplying these two probability maps, we can determine the overall allision probability distribution for a drift duration of 8 hours. This distribution is presented for Hollandse Kust West in Figure 5.3.

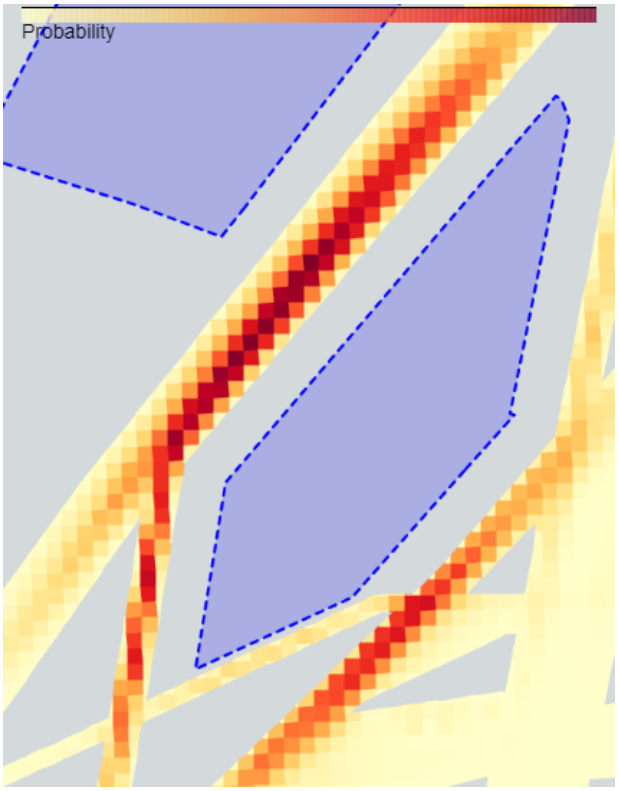

Figure 5.3: Allision probability level

The distribution of $P_{allision}$ shown in Figure 5.3 indicates that the highest allision probability levels are located to the west and south of each boundary segment of Hollandse Kust West. To the north and east, it is particularly lower. Moreover, in the fairways oriented in these directions, the highest probability is found in the middle of the fairways and is greater for the wider fairways. For comparison, the drift, activity and allision probability distribution around Hollandse Kust Zuid are presented in Appendix C.

The wind farm Hollandse Kust West is presented as an example of this method, while Hollandse Kust Zuid is detailed in the appendix. However, simulating trajectories and subsequently calculating P_{drift} can easily be extended to multiple wind farms. An illustration of the distribution of P_{drift} across the entire Dutch North Sea region is presented in Figure 5.4.

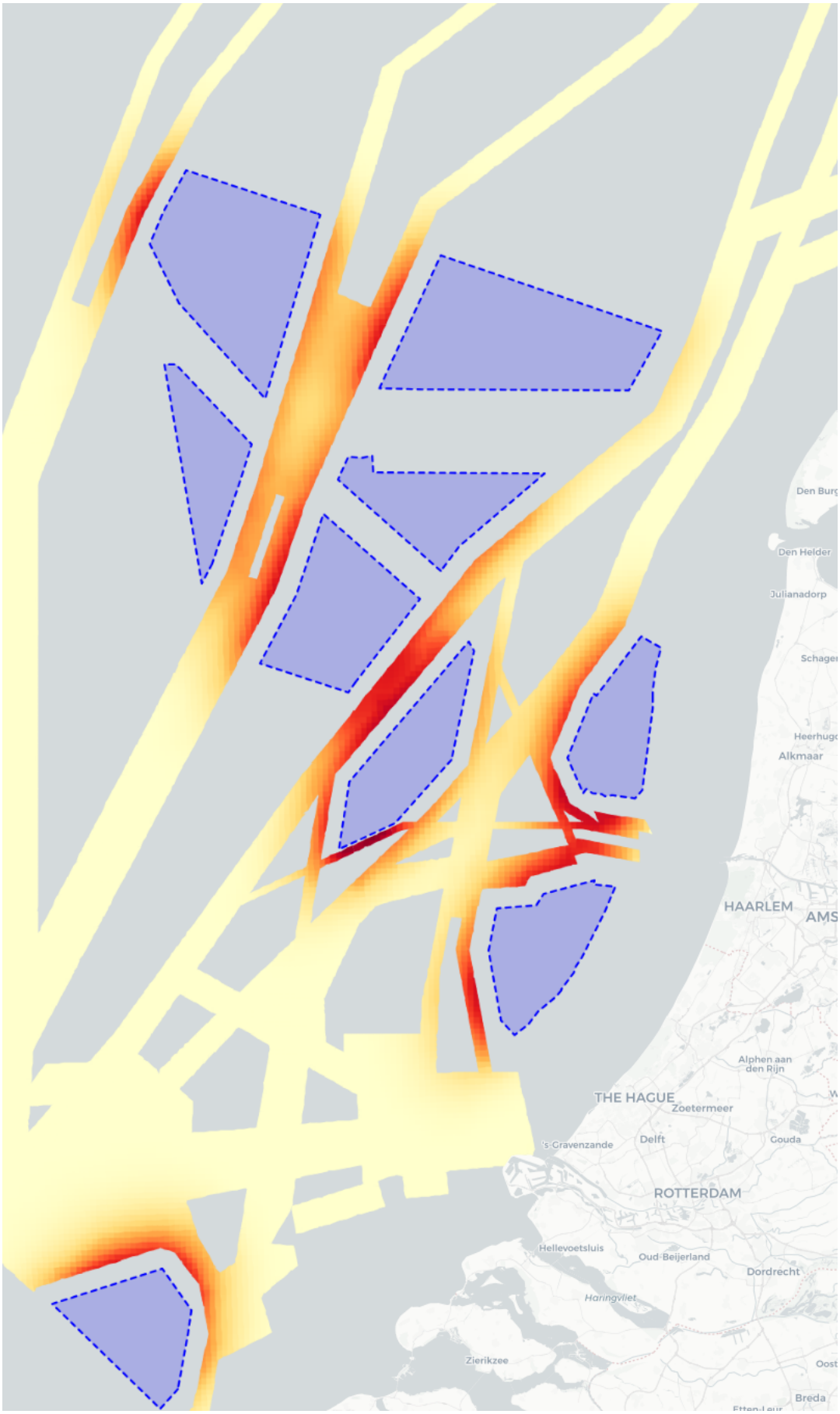

Figure 5.4: P_{drift} heat map across the Dutch North Sea region

5.1.1. Single wind farm analysis

The height of $P_{allision}$ within an area, corresponding to a specific orientation relative to a wind farm such as the southeastern quadrant relative to its centre, depends on the aggregation of the product of P_{drift} and $P_{activity}$.

Therefore, an orientation relative to a wind farm that:

- is aligned such that the environmental conditions significantly influence P_{drift}, and
- includes a substantial fairway area close to the wind farm with high shipping activity,

would exhibit a $P_{allision}$.

To make this more insightful, the allision probability levels have been aggregated across larger areas to provide a clearer overall picture. The area around the wind farm is divided into five rings, each with a width of 5 kilometres, extending outwards from the boundary of the wind farm. The inner ring covers the area from 0 to 5 kilometres from the boundary, while the outer ring covers the area from 20 to 25 kilometres. Furthermore, each ring is segmented into eight orientations relative to the wind farm.

Aggregation is achieve by first multiplying P_{drift} of each cell by the corresponding $P_{activity}$, and then dividing the product by the area of the respective cell. This adjustment is necessary because the grid of cells is irregular in terms of cell size, meaning that each cell does not uniformly contribute to the overall allision probability.

$$P_{allision}(cell) = P_{drift}(cell) \times \frac{P_{activity}(cell)}{area(cell)} \tag{5.1}$$

Next, these products are summed for all cells within each one-eighth of a ring. This aggregated probability for each one-eighth ring segment is illustrated for Hollandse Kust West for a drift duration of 8 hours in Figure 5.5.

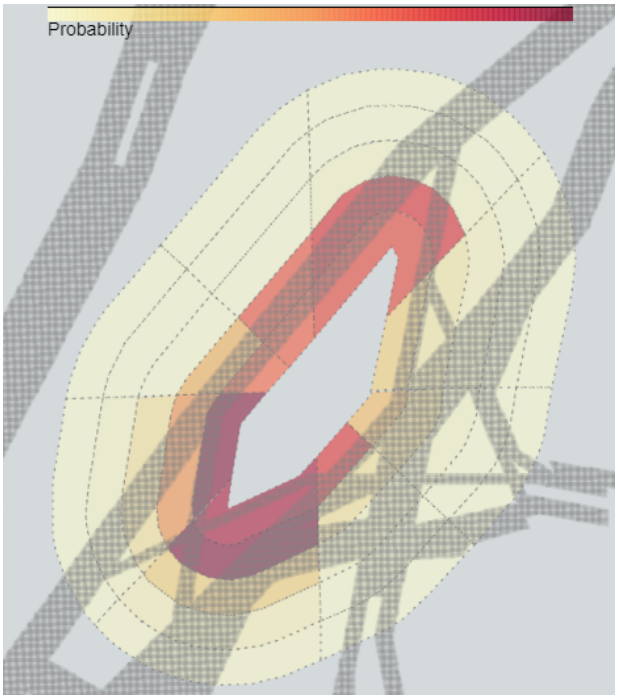

Figure 5.5: Probability of allision for ring segments

It is important to note that since a wind farm area is not always perfectly symmetrical, the area of each one-eighth ring is not equal. Each segment represents the allision probability level within a specific kilometre range from the wind farm boundary, corresponding to a particular directional range relative to the centre of the wind farm.

Figure 5.5 illustrates that the highest aggregated allision probability is found in the southwestern quadrant. More specifically, it occurs in the 0-5 kilometre range from orientations south-southwest and southwest to west, and in the 5-10 kilometre range from a south-southwest orientation.

Each of the previous figures represents allision probability levels based on a drift duration of 8 hours. However, the $P_{allision}$ varies for each hour of drift duration and may also exhibit different distributions across various drift durations. The corresponding probabilities for drift durations of 2, 4, and 6 hours are presented in Figures 5.6, 5.7 and 5.8, respectively.

Figure 5.6: Distribution at 2 hours

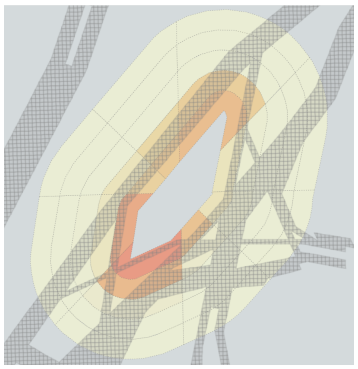

Figure 5.7: Distribution at 4 hours

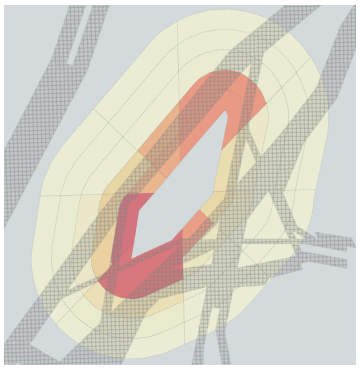

Figure 5.8: Distribution at 6 hours

The figures indicate that the highest probability of allision for each hour of drift duration is consistently found in the southwestern quadrant. Additionally, the distribution at 6 hours is practically identical to that at 8 hours.

The locations for which simulations are performed extend up to 25 kilometres from the wind farm boundary segments, beyond which the allision probability is zero. By summing the aggregated $P_{allision}$ values of each ring in each quadrant, we can illustrate the hourly contribution of each quadrant to the hourly overall allision probability level. This method is demonstrated in Figure 5.9, where the overall allision probability level (the sum of all rings) for an 8-hour drift duration is normalised to 100%.

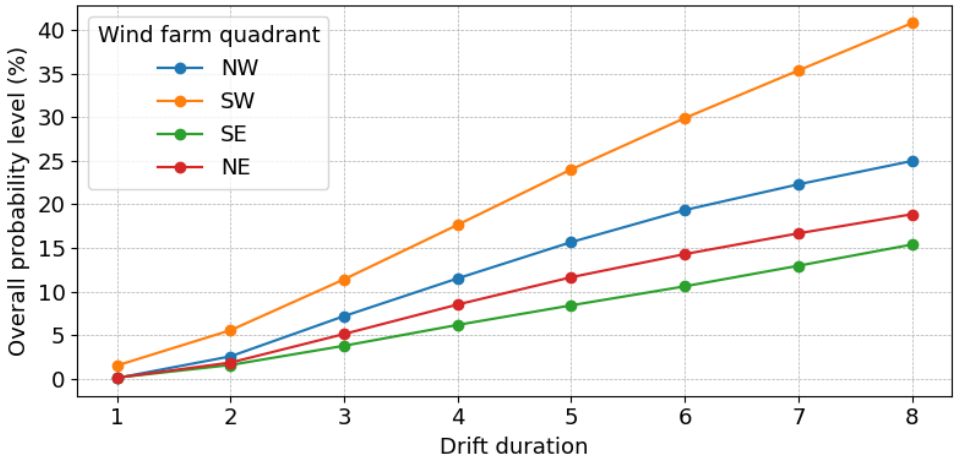

Figure 5.9: Contribution per quadrant to hourly overall allision probability level

This graph indicates that the probability of allision in the southwestern quadrant is the largest contributor to the overall allision probability every hour, being more than twice as high as that in any other quadrant. At an 8-hour drift duration, 40 percent of the overall allision probability level for Hollandse Kust West originates from the southwestern quadrant.

5.1.2. Comparative analysis of multiple wind farms

As we have conducted simulations for three wind farms, we can also create an aggregated allision probability level for each wind farm and compare them to one another. By comparing these allision probability levels, we can identify which wind farm has the highest $P_{allision}$ level, or in other words, the greatest contribution to the combined overall allision probability level of the three wind farms. This comparison is visualised in the bar graph in Figure 5.10, where the combined overall allision probability level (the sum of the overall allision probability of all three wind farms) for an 8-hour drift duration is normalised to 100%.

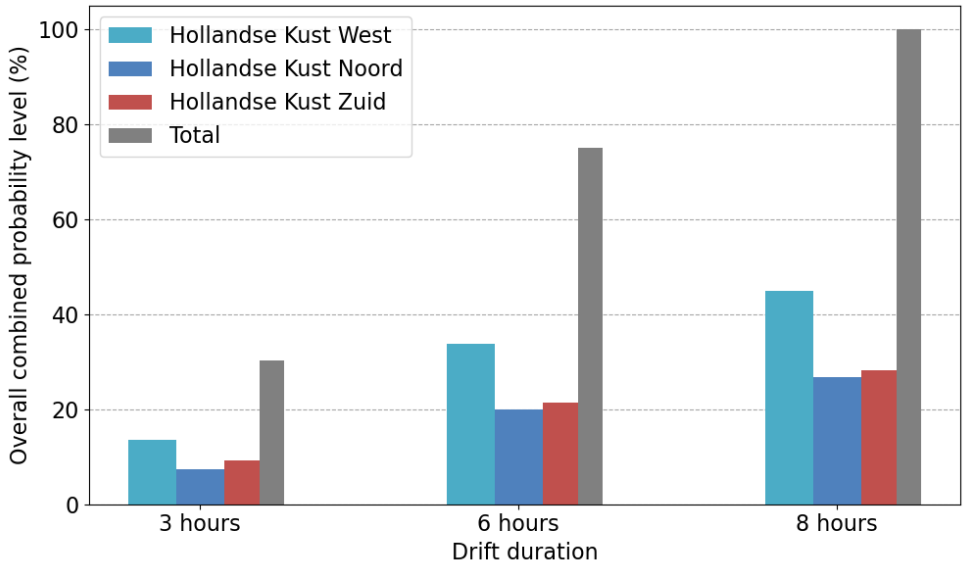

Figure 5.10: Contribution to the combined overall allision probability level

Based on this bar chart, we can conclude that Hollandse Kust West has the highest $P_{allision}$ level, indicating that a drifting ship allision is more likely to occur there compared to Hollandse Kust Zuid and Noord. The allision probability is lowest for wind farm Hollandse Kust Noord.

This classification is based on the overall allision probability, encompassing all possible combinations of wind, wave, and current forces. However, the classification between wind farms may differ when examining specific wind directions.

5.2. Allision probability results for specific environmental conditions

The methodology enables us to show how the overall $P_{allision}$ value varies between different wind farm areas and how the distribution of $P_{allision}$ changes around an individual wind farm under the influence of specific environmental force combinations.

5.2.1. Allison probability distribution for specific wind directions

The same aggregation of probabilities is performed, but separately for the $P_{allision}$ contributions of wind directions from each quadrant. This means that for each wind farm, the $P_{allision}$ results corresponding to the range of wind directions from each quadrant are aggregated. This aggregated allision probability level, specific to each wind farm and wind direction range, is then translated into its contribution to the overall allision probability level, encompassing all three wind farms, over an 8-hour drift duration. This is illustrated as 100% in Figure 5.10. The contributions for each wind direction range are shown in Figures 5.11, 5.12, 5.13, and 5.14.

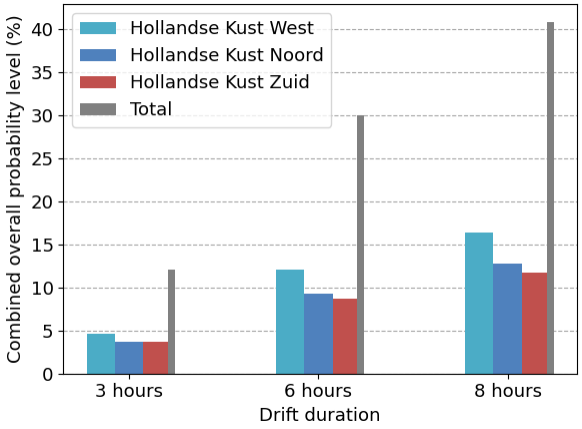

Figure 5.11: Southern to western winds

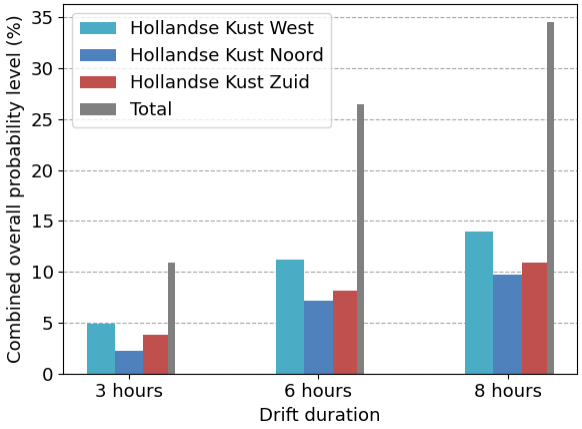

Figure 5.12: Western to northern winds

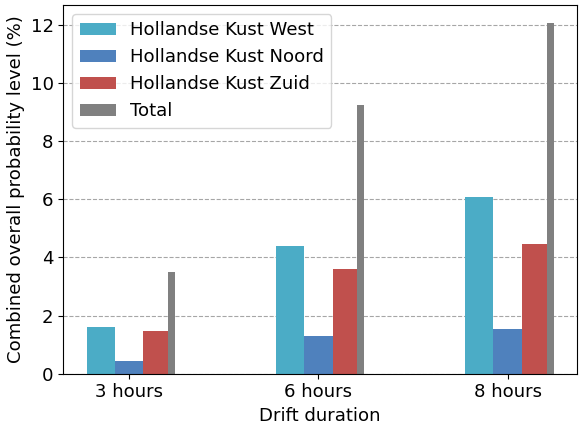

Figure 5.13: Northern to eastern winds

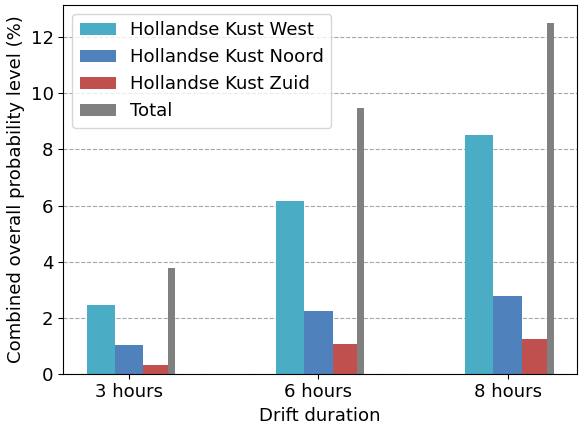

Figure 5.14: Eastern to southern winds

Figure 5.15: Insert caption

To clarify, summing the 8-hour drift duration $P_{allision}$ results for each wind direction range across all wind farms will total 100%, similar to how summing the 8-hour drift duration $P_{allision}$ results for each wind farm equals 100%, as illustrated in 5.10. The figures indicate that for each wind direction, Hollandse Kust West has the highest overall allision probability level compared to Zuid and Noord. For winds from the southwestern quadrant, the contributions are almost equal. However, for southeastern winds, the

contributions from Hollandse Kust Zuid and Noord are negligible compared to those from Hollandse Kust West.

5.2.2. Probability distribution for specific current and wind direction combinations

When considering the drift of ships, knowing the wind direction provides a good indication of which part of a wind farm is at risk. However, as discussed in Chapter 3, the influence of the current changes continuously in magnitude and direction. To visually demonstrate the impact of the current, the allision probability level of each of the four simulated segments for winds from the southwestern quadrant is determined for Hollandse Kust Zuid. Figures 5.16, 5.17, 5.18, and 5.19 show the $P_{allision}$ distribution for each of the four current segments for a drift duration of 8 hours, exclusively for winds from the southwestern quadrant. To clarify, if all the probability levels from the four figures were aggregated, we would obtain the overall allision probability level of Hollandse Kust Zuid for winds from the southwestern quadrant.

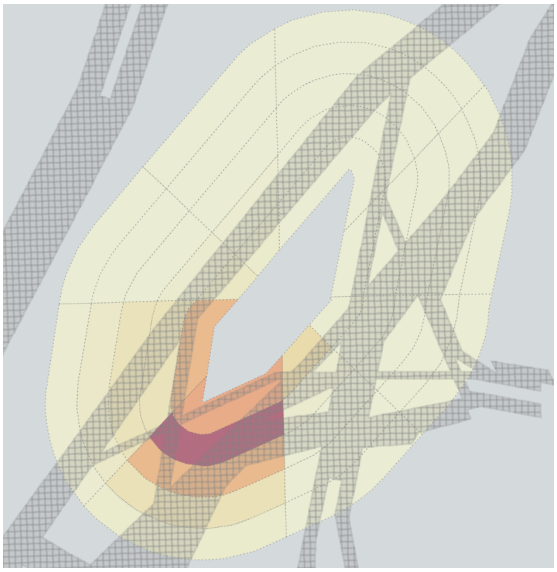

Figure 5.16: 01:00

Figure 5.17: 04:00

Figure 5.18: 07:00

Figure 5.19: 10:00

Figure 5.20: Probability distribution for the range of southwestern winds and varying starting times of the current

These figures show that for certain segments, the allision probability level is significantly higher than for others. For instance, the current segment starting at 01:00 results in the highest allision probability level and even includes a probability of allision in the 15 to 20-kilometre range. Moreover, despite exclusively considering winds from the southwestern quadrant, the probability of allision is higher for the northwestern and northeastern quadrants considering the current segment starting at 07:00.

Previous results only considered the $P_{allision}$ results for an 8-hour drift duration. In Figure 5.21, the hourly contribution of a current segment to the wind direction range-specific probability of allision is illustrated. In this figure the wind direction range-specific allision probability level for an 8-hour drift duration is normalised to 100%.

Previous results focused exclusively on the $P_{allision}$ values for an 8-hour drift duration. In Figure 5.21, the hourly contributions of a current segment to the allision probability for winds from the southwestern quadrant are illustrated. For this figure, the wind direction range-specific allision probability level for an 8-hour drift duration is normalised to 100

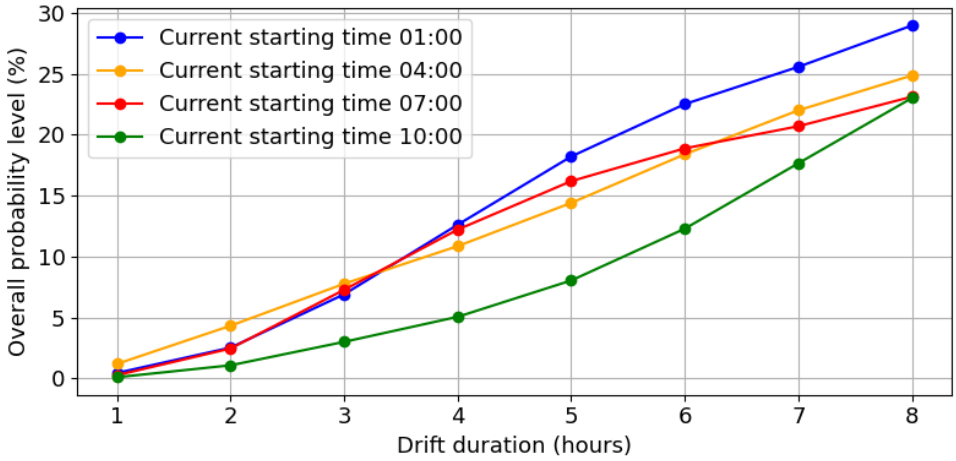

Figure 5.21: Contribution per current segment to the allision probability level for southwestern winds

The results indicate that the current segment starting at 10:00 contributes significantly less to the allision probability level for winds from the southwestern quadrant for short drift durations. However, as the duration reaches 8 hours, the influence of this segment increases substantially, ultimately contributing nearly 25%, which is almost equal to the other segments. The contributions from segments starting at 04:00 and 07:00 increase linearly over time. In contrast, the segment starting at 01:00 provides the largest contribution from a drift duration of 4 hours onwards. All previous analyses for Hollandse Kust Zuid show similar results and are presented in Appendix C.

6

Interpretation & discussion

In this chapter the results of the implemented method are interpreted and their practical implications are explored. Next, the validity and limitations of the implemented method are discussed.

6.1. Interpretation of results

The overall $P_{allision}$ results from Section 5.1 showed that:

- Hollandse Kust West has the highest allision probability level both overall and, as discussed in Section 5.2, for wind direction range-specific results.
- The largest contribution to the overall allision probability level for Hollandse Kust West is found in the southwestern quadrant relative to its centre.
- The most significant contribution to the overall allision probability level for all wind farms is due to winds from the southwestern quadrant.

These findings are explained by the geographical location of Hollandse Kust West, which is surrounded on all sides by fairways, unlike Hollandse Kust Noord and Zuid. While the latter two are not completely surrounded by fairways, they still show high probability values, though not as high as Hollandse Kust West. The dominance of southwest winds in the Dutch North Sea region explains the higher $P_{allision}$ results in the southwest regions of each wind farm. Southwestern winds occur more frequently and are on average stronger than winds from any other direction. This is made visual in Appendix E.4.

Further analysis of specific current segments revealed:

- Although $P_{allision}$ results correspond to a southwest wind direction, the highest $P_{allision}$ results are not necessarily found southwest of Hollandse Kust West.
- The contribution to the overall wind direction range-specific allision probability level varies between the different simulated current segments.
- The time required to reach a wind direction range-specific allision probability level differs for each of the current segments.

The different allision probability distributions can be explained by the current segments used in the simulations, as shown in Appendix E.5. Figure 5.16 and Figure 5.18 illustrate how exposure to different directional currents—northern in the first and southern in the second—affects the allision probability distribution. Figure 5.16 shows almost no contribution from any area other than the southwestern quadrant, whereas Figure 5.18 shows a relatively low contribution from the southwestern quadrant, despite the wind direction range being from that specific quadrant.

The contribution to the overall wind direction range-specific probability of allision is influenced by the cyclical behaviour of the current. In some segments, the current is directed towards the wind farm for longer periods, thereby increasing the probability of crossings. Conversely, in other segments, the current is for longer periods directed away from the wind farm, which reduces the probability of crossings. Variations in the time taken to reach a certain wind direction range-specific allision probability level are due to differences in initial current velocities. In some segments, currents have a higher velocity at the start of the drift simulation, leading to more simulations crossing the wind farm during shorter drift durations.

6.2. Implications for risk-reducing strategies

The results in Chapter 4 and their interpretation in the previous section first presented the distribution of the allision probability and then showed how this distribution varies for more specific environmental conditions. For the latter, we chose to demonstrate how the wind farm with highest probability varied with different wind directions, and how, when the wind direction is known, the $P_{allision}$ distribution changes for a specific current segment. However, the model offers many more advantages beyond just these results.

6.2.1. Implications for monitoring and resource deployment

This model is built on predictions of a ship's drift trajectory, providing insights into:

- the origins of allision threats, rather than determining which turbine is most likely to be hit, and
- the average available response time for each location in the fairways, based on a predefined drift duration.

For monitoring, it is easier to target areas if you know the locations where the allision probability is highest. Moreover, if a ship behaves unpredictably in an area with a high P_{drift}, the decision to send out an ERTV can be made more quickly.

Regarding resource deployment, understanding the origins of threats can be used to strategically position ERTVs. By ensuring their reach covers areas with the highest probability of allisions ($P_{allision}$), such positioning could minimise the overall allision risk. For instance, positioning ERTVs between wind farms may reduce the overall allision probability more effectively than just positioning them at the wind farm with the highest probability of allision.

Concerning the average available response time, these insights can help identify areas where:

- it is almost impossible to recover a ship adrift within the time available, and
- timely recovery is always feasible because the threats are at a considerable distance.

This information is invaluable for optimally positioning ERTVs and determining the necessary number to ensure timely interventions in areas with the highest probability of allision in the Dutch North Sea region.

The results also indicated that:

- For different wind direction ranges, Hollandse Kust West consistently exhibits the highest allision probability level.
- The probability distribution and the time until a certain probability level is reached vary across different current segments for a specific wind direction range.

With knowledge of the allision probability level distribution under the influence of specific environmental conditions, this could form a basis for dynamic strategies in monitoring, ERTV positioning, and rerouting of large ships.

For example, conducting analyses for specific wind direction ranges across all wind farms could reveal that areas other than Hollandse Kust West, which the results initially indicated, are at the highest risk for a given wind direction. This finding would necessitate a change in the targeted monitoring area, and ERTVs should be repositioned accordingly. The $P_{allision}$ distribution for specific current segments could also form a basis for dynamic strategies. However, given that currents vary hourly, implementing mitigation measures that must be adjusted hourly presents a significant challenge.

6.2.2. Future developments

The insights discussed above can be useful for future planning and spatial development of fairways and wind farm areas. Knowing which locations are considered low or high threat sites can help in determining new locations for wind farms.

It's also worth mentioning a study conducted by MARIN, which presents the concept of placing barriers at certain wind farms to protect them from drifting ships (MARIN, 2022). By using these conceptual barriers at specific locations, along with the strategic placement of ERTVs, this trajectory prediction-based approach can help determine an optimal layout to minimise risk.

6.2.3. Operational use

This study focused on the probability of a drifting ship crossing a wind farm. Given the predictive performance of OpenDrift, as demonstrated in Chapter 4, OpenDrift could also be used as an operational tool. This tool could provide insights from the moment a ship starts to drift. It could assist the Dutch Coast Guard in preventing any unwanted situations.

In the case of a ship adrift, an operational drift model can be used to:

- Determine the probability of the ship entering a wind farm or even alliding with a wind turbine.
- Determine the available time for response.

Using this information, the Dutch Coast Guard can make decisions on whether the ship should use its anchor or if it can wait for external assistance. In the best case, the operational model would show a zero allision probability, indicating no urgency in recovering the ship.

6.3. Research validity and limitations

The established model is based on multiple assumptions, which raise concerns about its validity. Moreover, the model is limited to a allision probability level, which is only one part of what needs to be considered to obtain a meaningful value for a cell or an entire wind farm.

6.3.1. Research validity

The established methodology is based on the open-source Python package OpenDrift. From there, multiple assumptions are made to determine the drift probability (P_{drift}) and the activity probability $P_{activity}$, which in turn determine the allision probability ($P_{allision}$) for each cell upon which the results are based. Consequently, the validity of the methodology depends on the following aspects:

- The OpenDrift package
- The environment and ship geometry used to run the simulations
- The shipping activity

The validity of OpenDrift, or its ability to accurately predict the drift motion of a ship, has been analysed for only a single case: the Julietta D incident. It remains uncertain whether it can accurately predict drift motions for other ship types. Smaller ships, for instance, would likely deviate more from the wind direction (drifting to leeward) as discussed in Section 2.4.2. Moreover, for more extreme wave conditions, the influence of waves is more significant for larger ships, as discussed in Section 3.2. However, for a medium-sized ship like the Julietta D, this effect is less pronounced. Moreover, the observed spread in trajectories from a single simulation varies only for a specific ship type. This spread is not determined using a true Monte Carlo technique, where simulations would be conducted across an uncertainty range for variables that are uncertain or stochastic by nature. Instead, the spread is based on a horizontal diffusivity component that is specific to a ship's geometry.

The level of detail in this study, with eight intervals each for wind speed and direction and four for wave height, is relatively low. However, given that the current also needed to be simulated, this results in around 1,000 simulations per location. This level of detail has proven valid for our probability definition: the probability of crossing a wind farm. However, if we were to determine the probability of an allision with a specific wind turbine, this might not suffice. Additionally, the P_{drift} results are based on a single ship type. The allision probability might vary for different ship types, as each type's travelled distance and deviation from the wind direction can differ under identical forcing conditions. This variability was observed in Section 3.2.

$P_{activity}$ is defined to represent the shipping density at a specific location. In this study, the number of AIS signals is used to estimate the average time a ship spends in a cell. However, this method may not be accurate enough because the frequency of AIS signals depends on the ship's speed. Consequently, a faster-moving ship emits more signals than a slower-moving one over the same distance, even though the slower ship spends more time in the area. To obtain valid results, the number of signals must be adjusted to account for a ship's speed. For this study, however, it is assumed that simply counting AIS signals is sufficient to capture the distribution of shipping activity across the Dutch North Sea region.

6.3.2. Research limitations

In this study, the allision probability P_{drift} is calculated assuming a 'clean drift,' without considering any avoidance measures. Therefore, the determined probability level only reflects the situation in which the crew on a ship cannot avoid the allision by their own means or through external assistance.

In terms of allision avoidance through the crew's own measures, possibilities include repairing the engine or using the anchor. To what extent these measures reduce the probability is not considered in this study. Allision avoidance by external assistance is also not considered. For example, a ship may be intercepted by an ERTV. How much this would reduce the probability is also not accounted for. Finally, assuming a clean drift means that we do not consider any alterations in a ship's drift due to anchor use, its initial speed, or any other intervening events. The initial speed is excluded in this study, as literature suggests, and as discussed in Section 2.4.2, that a drifting ship typically reaches a stable state in less than half an hour. Given that we are considering drift periods of up to eight hours, it was decided to neglect this effect.

7

Conclusion & recommendations

This chapter summarises the findings related to the research objectives and questions. Additionally, several steps for further research are highlighted as recommendations.

7.1. Conclusions to the research questions

The expansion of offshore wind farms in the Dutch North Sea region significantly impacts maritime safety. Coupled with the already high shipping activity in the North Sea, this expansion leads to more ships being present near marine infrastructure, thereby increasing the risk of collisions. In cases where ships become adrift or experience a blackout, they are at an increased risk of allision. The Dutch Coast Guard is responsible for preventing such accidents. However, monitoring poses a challenge given the high level of activity in the North Sea and the limited number of operators. Furthermore, assistance from an ERTV is the only measure in place to prevent such accidents. To effectively manage the expansion of offshore wind farms in terms of maritime safety, Rijkswaterstaat must minimise the risk of allisions. For risk-reducing purposes, this includes gaining a comprehensive understanding of the integral image of drifting ship allision risks across the Dutch North Sea region. This understanding must be valid, reliable, and provide the necessary insights, such as how dynamic factors like weather conditions and shipping activity affect these risks. However, the work of Ellis et al. (2008) highlights significant transparency issues and a heavy reliance on assumptions in state-of-the-art risk assessment methods, which result in variations in the estimated return periods between different models by up to a factor of seven. Consequently, to meet the first research objective, state-of-the-art methods for determining the probability of drifting ship allisions were explored, and potential areas for improvement in these techniques were identified.

7.1.1. Sub-question 1

The first research objective has been addressed through sub-question 1: *How do state-of-the-art methods determine the probability of drifting ship allisions, and what potential areas for improvement can be identified in these techniques?* A literature review of the state-of-the-art methods for estimating the probability of allision revealed two key research gaps:

- Validity of state-of-the-art probability estimation: The numerous assumptions, simplifications, and lack of transparency in existing models make it difficult to confirm their accuracy in reflecting actual allision probabilities.
- Limited insights of probability estimations for risk-reducing purposes: The probability estimations result in an occurrence rate for a specific wind turbine, which provides limited insights for risk-reducing strategies.

To achieve a valid, reliable, and insightful integral image of drifting ship allision risks across the Dutch North Sea region, risk assessment methods must be grounded in the core of the incident: a ship's drift trajectory. The knowledge gaps and the need for effective risk management have led to the exploration of a trajectory prediction-based approach for estimating allision probabilities. This approach is summarised in the main research question: **How does a trajectory prediction-based estimation method improve our**

understanding of the integral image of drifting ship allision probabilities in the Dutch North Sea region to provide well-substantiated insights for risk-reducing measures?

To answer the main research question, two further research objectives have been defined:

2. Explore the advancements and substantiation offered by a trajectory prediction-based approach to estimating the probability of drifting ship allisions.
3. Evaluate the practical implications of a trajectory prediction-based approach to estimating the probability of drifting ship allisions for optimising risk-reducing strategies.

Each of these objectives is translated into a sub-question, which will be addressed in the following paragraphs.

7.1.2. Sub-question 2

Through the development of a trajectory prediction-based method for estimating the probability of drifting ship allisions, its potential improvements for probability estimation are explored: *How does a trajectory prediction-based method advance and substantiate drifting ship allision probability estimations in the North Sea?*. The established trajectory prediction-based method for estimating the probability of allision is structured as shown in Figure 7.1:

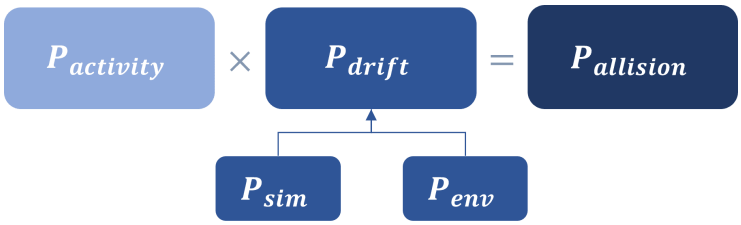

Figure 7.1: Trajectory prediction-based method structure

To define P_{drift}—the probability that an arbitrary drifting ship allides with a wind farm, considering all possible environmental conditions—it was decided to use the open-source Python package OpenDrift as ship drift trajectory prediction model. Next to it being easily accessible, it provides a limited complexity in calculating a ship's drift trajectory.

A sensitivity analysis of this model yielded many observations. The main findings include that wind forcing generally dominates over wave forcing, although extreme wave conditions can significantly affect a ship's travelled distance and result in deviations from the wind direction. In addition, the magnitude and direction of the current are crucial, as they can cause significant deviations from the wind direction and result in various travelled distances specific to the current segment to which the ship is subjected. This analysis concluded that all three forces—wind, wave, and current—need to be known to accurately predict a ship's drift trajectory. This conclusion is substantiated by the analysis of the trajectory of the Julietta D, which could only be replicated by the exact combination of forces present at the time of the incident. Excluding any of these forces resulted in predictions that were significantly off from its actual trajectory. In addition, the use of the Julietta D's specific geometry in the reconstruction, and the analyses of the medium and both large ships in the sensitivity analyses, highlighted the importance of knowing a ship's geometry, albeit less significant than the influence of the environmental forces on a ship's drift trajectory.

P_{drift} is determined by conducting multiple OpenDrift simulations, and subsequently calculating P_{sim}—the probability of an allision in a single OpenDrift simulation—numerous times for all possible combinations of wind, wave, and current forces with occurrence rate (P_{env}). Since each OpenDrift simulation is specific to a ship type, the procedure must be repeated across different classifications of ships. The resulting allision probability for a specific starting location of a ship's drift is then calculated by multiplying P_{drift} by a shipping density value of the considered location, representing the probability of presence of an adrift ship.

Through an analysis of the resulting P_{drift} values at different locations around the Hollandse Kust West wind farm, it was concluded that maintaining constant wind and wave forces throughout a ship's drift is a valid assumption for calculating P_{drift}, as evidenced by comparisons with P_{drift} results from simulations using

time-varying hindcast data. Additionally, including the current proved crucial for accurately calculating P_{drift}. For specific orientations and distances relative to the Hollandse Kust West wind farm, the P_{drift} results that exclude the current significantly differ from those obtained when including the current. Specifically in the southeastern area, excluding the current results in a P_{drift} value that is about 10 percentage points lower, significantly underestimating the present risk. This highlights two major improvements brought by the trajectory prediction model over state-of-the-art methods: (1) it avoids the assumption that the ship moves in a purely lateral direction, and (2) it avoids estimating the current as a uniform speed in the wind direction.

7.1.3. Sub-question 3

The last research objective explores the practical implications of using a trajectory prediction-based method for risk-reduction purposes, as addressed through sub-question 3: *What are the practical implications of a trajectory prediction-based method for estimating the probability of drifting ship allisions to improve risk-reducing strategies for maritime safety in the North Sea?*

First the method was implemented to calculate the distribution of $P_{allision}$ around the wind farms Hollandse Kust West, Hollandse Kust Zuid, and Hollandse Kust Noord. The results indicated that Hollandse Kust West has the highest allision probability value, both overall and for wind directions from each of the four quadrants (northeast, southeast, southwest, and northwest). Furthermore, for all wind farms, the largest contribution to their overall probability level is from the southwestern quadrant, as southwestern winds occur more frequently and are stronger than winds from any other direction. Further analysis of different current segments for winds from the southwestern quadrant revealed that the highest probabilities are not necessarily found in that quadrant. Different current segments lead to varied distributions of the allision probability level around a wind farm. Moreover, these segments significantly influence the time required to reach a particular probability level, with some segments achieving it faster than others.

The trajectory prediction-based method provides detailed insights into the origins of potential threats and the time available to respond at a given probability of allision, and can be easily extended to multiple wind farms. These insights are valuable for optimising the positioning of ERTVs. Additionally, the model offers specific insights for various environmental conditions, such as wind direction ranges and current segments. Environmental specific insights can be valuable for implementing dynamic measures, such as repositioning ERTVs or rerouting large ships.

7.1.4. Main research question

In this study, we introduce a first approach to a trajectory prediction-based method for estimating the probability of drifting ship allisions. This approach was employed to investigate how a more detailed method of determining probabilities enhances the state-of-the-art way of estimating this probability across the Dutch North Sea region, directly addressing the main research question: **How does a trajectory prediction-based estimation method improve our understanding of the integral image of drifting ship allision probabilities in the Dutch North Sea region to provide well-substantiated insights for risk-reducing measures?** The main research question can best be answered by addressing the two knowledge gaps identified in the literature: the validity of state-of-the-art probability estimations and the limited insights of probability estimations for risk-reducing purposes.

Regarding the validity of state-of-the-art methods, except for neglecting a ship's mass, integrating a trajectory prediction model into a method for estimating the probability of drifting ship allisions offers a way to challenge the assumptions made in such methods:

1. the ship moves in a purely lateral direction defined by the wind direction,
2. the wind and waves act in the same direction,
3. the wind direction and wind speed are kept constant, and
4. the current is accounted for as en estimated speed in the already established drift direction (wind direction).

For our study, assumptions 2 and 3 are reiterated. Comparing P_{drift} from the established methodology with P_{drift} obtained through time-varying hindcast data revealed that for our definition of allision—crossing any wind farm boundary—it is sufficient to assume that wind and waves are constant throughout a ship's drift trajectory and act in the same direction.

Conversely, assumptions 1 and 4 are not incorporated into the established method. If wind and current are not aligned, the influence of the current causes a ship to deviate from the wind direction, resulting in trajectories under certain current segments not crossing the wind farm area. Therefore, the influence of the current on P_{drift} does not average out, and excluding the current would lead to considerable differences in P_{drift} values. If the method were refined to specifically consider individual turbines rather than the entire wind farm area, the influence of the current could have even greater effects, potentially invalidating assumptions 2 and 3.

Compared to the insights generated from state-of-the-art probability estimations, a trajectory prediction-based approach offers several advantages. If the method in the present study were expanded to a model capable of estimating the actual risk level, which involves determining both occurrence rates and potential consequences, it would provide a robust framework for making strategic decisions. Moreover, it would offer a way for more precise monitoring under specific environmental conditions, optimise the positioning of ERTVs, and serve as a basis for more dynamic, environment-specific, risk-reducing strategies. Expanding the model developed in this study could improve the validity and efficiency of decision-making. Consequently, a robust risk-reducing strategy would enable Rijkswaterstaat to responsibly exploit the abundant potential the North Sea has to offer.

7.2. Further research recommendations

This chapter provides several recommendations for further research, addressing the validity and limitations of the current study. These suggestions aim to generate valuable information that can actually be used by Rijkswaterstaat to implement or improve risk-reducing measures, as discussed in Section 6.2.

1. Research should focus on validating any ship drift prediction model. Specifically for OpenDrift, it requires validation across more real-world cases and a broader range of ship types. This validation should determine whether the analytical methodology used to calculate trajectories is sufficiently predictive. Regarding allision probability calculations, rather than validating an existing model, research could explore alternative methods for calculating the potential drift trajectory of a large ship. As discussed in Section 3.1.3, the analytical methodology embedded in OpenDrift is deterministic in terms of ship size and generates horizontal variation through a diffusion coefficient and a jibing probability. This approach does not accurately reflect the stochastic nature of each forcing variable or parameter. It is recommended that research should focus on conducting simulations that account for the uncertainty of variables by simulating them within a predefined range. Ensuring that each variable falls within this specified range during simulations could provide a more accurate reflection than methods that rely solely on a diffusion coefficient and jibing probability. This approach aligns with a typical Monte Carlo method, commonly used in other applications of trajectory prediction for probability analysis, as discussed in Section 3.1.1.
2. Either OpenDrift or any other model should be expanded to include a probability of engine failure per ship per hour and a more precise representation of the number of ships present per hour at a particular location. This improvement would allow the methodology to produce values corresponding to an occurrence rate, excluding any risk-reducing measures. Furthermore, the probability of allision avoidance by own measures, such as engine repair and anchor use, should be incorporated.
3. Using this expanded methodology, we can generate large probability datasets that might include multiple ship types, a more detailed environmental context, or even specific wind turbines instead of entire wind farms. These large datasets would enable us to examine the efficiency and optimal implementation of various external risk-reducing measures.
4. Finally, this methodology can be expanded to incorporate the potential consequences of an allision. By understanding not only the probability of an allision but also potential consequences such as value loss, damage, and loss of life, cost-benefit analyses can be conducted. This allows for a comparative evaluation of the outcomes or investments in risk-reducing measures against other threats, like powered collisions.

References

Bahlke, C. (2017). Harbours and shipping [Last updated on 21.12.2017]. In S. Kloepper et al. (Eds.), *Wadden sea quality status report 2017*. Common Wadden Sea Secretariat. http://qsr.waddensea-worldheritage.org/reports/harbours-and-shipping

Chai, T., Weng, J., & De-qi, X. (2017). Development of a quantitative risk assessment model for ship collisions in fairways. *Safety Science*, *91*, 71–83. https://doi.org/10.1016/j.ssci.2016.07.018

Chen, P., Huang, Y., Mou, J., & van Gelder, P. H. (2019). Probabilistic risk analysis for ship-ship collision: state-of-the-art. *Safety Science*, *117*, 108–122. https://doi.org/10.1016/j.ssci.2019.04.014

Chen, Y., Zhu, S., Zhang, W., Zhu, Z., & Bao, M. (2022). The model of tracing drift targets and its application in the South China Sea. *Acta Oceanol. Sin.*, *41*, 109–118.

Crisostomi, E., Maciejowski, J., & Lecchini-Visintini, A. (2008). *Combining monte carlo and worst-case methods for trajectory prediction in air traffic control: A case study* (tech. rep.). https://www.researchgate.net/publication/228682652

Dagestad, K. F., Röhrs, J., Breivik, O., & Ådlandsvik, B. (2018). OpenDrift v1.0: A generic framework for trajectory modelling. *Geoscientific Model Development*, *11*(4), 1405–1420. https://doi.org/10.5194/gmd-11-1405-2018

Dutch Government. (2024). *Data register of the dutch government*. https://data.overheid.nl

Duursma, A., van Doorn, J., Koldenhof, Y., & Valstar, J. (2019, May). *WIND OP ZEE 2030: Gevolgen voor scheepvaartveiligheid en mogelijk mitigerende maatregelen* (tech. rep.). Rijkswaterstaat.

Ellis, J., Forsman, B., Hüffmeier, J., & Johansson, J. (2008, June). *Methodology for Assessing Risks to Ship Traffic from Offshore Wind Farms* (tech. rep.). SSPA Sweden AB. Göteborg, Sweden.

Friis-Hansen, P., Frouws, K., & Dalhoff, P. (2004). Reduction of ship collision risks for offshore wind farms: SAFESHIP. https://www.researchgate.net/publication/367344627

Fujii, Y., & Shiobara, R. (1971). The analysis of traffic accidents. *Journal of Navigation*, *24*(4), 534–543. https://doi.org/10.1017/S0373463300022372

Goerlandt, F., & Kujala, P. (2014). On the reliability and validity of ship-ship collision risk analysis in light of different perspectives on risk. *Safety Science*, *62*, 348–365. https://doi.org/10.1016/j.ssci.2013.09.010

Goerlandt, F., & Montewka, J. (2015). Maritime transportation risk analysis: Review and analysis in light of some foundational issues. *Reliability Engineering and System Safety*, *138*, 115–134. https://doi.org/10.1016/j.ress.2015.01.025

Government of the Netherlands. (2024, May). *Offshore wind energy* [Information about future offshore wind energy plans and development up to 2050 in the Netherlands]. https://english.rvo.nl/topics/offshore-wind-energy/new-offshore-wind-farms

Hackett, B., Breivik, O., & Wettre, C. (2006, January). *Forecasting the drift of objects and substances in the ocean*. Norwegian Meteorological Institute. https://www.researchgate.net/publication/233918946

Harrison, R. L. (2009). Introduction to Monte Carlo simulation. *AIP Conference Proceedings*, *1204*, 17–21. https://doi.org/10.1063/1.3295638

Hermans, M., Kauffman, S., & Indah-Everts, S. (2020, October). *Netwerkevaluatie Noordzee 2018-2019* (tech. rep.). MARIN. Wageningen.

Hörteborn, A., & Ringsberg, J. W. (2021). A method for risk analysis of ship collisions with stationary infrastructure using AIS data and a ship manoeuvring simulator. *Ocean Engineering*, *235*. https://doi.org/10.1016/j.oceaneng.2021.109396

IMO. (2018). *Revised guidelines for Formal Safety Assessment (FSA) for use in the IMO rule-making process* (tech. rep.). London, England.

Kim, S. J., Seo, J. K., Ma, K. Y., & Park, J. S. (2021). Methodology for collision-frequency analysis of wind-turbine installation vessels. *Ships and Offshore Structures*, *16*(4), 423–439. https://doi.org/10.1080/17445302.2020.1735835

Koldenhof, Y. (2021). Samson: Ship-object model. *Maritime Research Institute Netherlands (MARIN)*.

Kujala, P., Hänninen, M., Arola, T., & Ylitalo, J. (2009). Analysis of the marine traffic safety in the Gulf of Finland. *Reliability Engineering and System Safety*, *94*(8), 1349–1357. https://doi.org/10.1016/j.ress.2009.02.028

Kustwacht. (2022, February). Botsing op zee zorgt voor stuurloos vrachtschip Julietta D. https://kustwacht.nl/incident/botsing-op-zee-zorgt-voor-stuurloos-vrachtschip-julietta-d/

Lušić, Z., & Čorić, M. (2015). Models for estimating the potential number of ship collisions. *Journal of Navigation*, *68*(4), 735–749. https://doi.org/10.1017/S0373463314000903

MacDonald, A., Cain, M., Aggarwal, R. K., Vivalda, C., & Lie, O. E. (1999). Collision risks associated with FPSOs in Deep Water Gulf of Mexico. *Offshore Technology Conference*.

MARIN. (2022, March). *Maritime 'crash barriers' to avert collisions with wind turbines*. https://www.marin.nl/en/news/crash-barriers

Martins, M. R., & Maturana, M. C. (2010). Human error contribution in collision and grounding of oil tankers. *Risk Analysis*, *30*(4), 674–698. https://doi.org/10.1111/j.1539-6924.2010.01392.x

Mehdi, R. A., Schröder-Hinrichs, J. U., van Overloop, J., Nilsson, H., & Pålsson, J. (2018). Improving the coexistence of offshore wind farms and shipping: an international comparison of navigational risk assessment processes. *WMU Journal of Maritime Affairs*, *17*(3), 397–434. https://doi.org/10.1007/s13437-018-0149-0

Montewka, J., Ehlers, S., Goerlandt, F., Hinz, T., Tabri, K., & Kujala, P. (2014). A framework for risk assessment for maritime transportation systems - A case study for open sea collisions involving RoPax vessels. *Reliability Engineering and System Safety*, *124*, 142–157. https://doi.org/10.1016/j.ress.2013.11.014

Montewka, J., Goerlandt, F., & Kujala, P. (2014). On a systematic perspective on risk for formal safety assessment (FSA). *Reliability Engineering and System Safety*, *127*, 77–85. https://doi.org/10.1016/j.ress.2014.03.009

Nap, A. (2022, April). *Risico-indicatoren scheepvaartveiligheid MOSWOZ* (tech. rep.). Rijkswaterstaat.

Noordzeeloket. (2023). Scheepvaartveiligheid rondom windparken op zee (MOSWOZ). https://www.noordzeeloket.nl/functies-gebruik/windenergie/scheepvaart-moswoz/

Povel, D. (2006). Collision risk analysis for offshore structures and offshore wind farms. *International Conference Offshore Mechanics and Arctic Engineering*.

Rodrigue, J.-P. (2024). *The geography of transport systems* (6th ed.). Routledge. https://doi.org/10.4324/9781003343196

Spouge, J. (1991). CRASH: computerised prediction of ship-platform collision risks. *Offshore Europe Conference*. http://onepetro.org/SPEOE/proceedings-pdf/91OE/All-91OE/SPE-23154-MS/3196274/spe-23154-ms.pdf/1

Transport Malta. (2023). *Marine safety investigation report: Safety investigation into the loss of control of the maltese registered bulk carrier julietta d* (Interim Safety Investigation Report No. 02/2023). Marine Safety Investigation Unit. Floriana, Malta.

van der Werff, S., van Koningsveld, M., & Baart, F. (2024). Vessel behaviour under varying environmental conditions in coastal areas. *Proceedings of the 35th PIANC World Congress*.

Yan, S., Zhang, J., Parvej, M. M., & Zhang, T. (2023). Sea drift trajectory prediction based on Quantum Convolutional Long Short-Term Memory Model. *Applied Sciences (Switzerland)*, *13*(17). https://doi.org/10.3390/app13179969

Zhang, X., Cheng, L., Zhang, F., Wu, J., Li, S., Liu, J., Chu, S., Xia, N., Min, K., Zuo, X., et al. (2020). Evaluation of multi-source forcing datasets for drift trajectory prediction using lagrangian models in the South China Sea. *Appl. Ocean. Res.*, *104*.

A

SAMSON

Within the SAMSON model the wind and wave forces are calculated, along with the wave resistance, in the following way (Koldenhof, 2021):

$$F_{wind} = \frac{1}{2}\rho_a A_{in} C_{dw} v_b^2 \tag{A.1}$$

$$F_{wave} = \frac{1}{16}\rho_w g \zeta_b^2 L_i R^2 \tag{A.2}$$

$$F_{resistance} = \frac{1}{2}\rho_w L_i T_{in} C_d v_{drift}^2 \tag{A.3}$$

The equilibrium between all forces is assumed and this results in a drift speed of:

$$v_{drift}(i,n,b) = \sqrt{\frac{\rho_a}{\rho_w}\frac{A_{in}C_{dw}}{L_i T_{in} C_d} v_b^2 + \frac{1}{8}\frac{\zeta_b^2 g R^2}{T_{in} C_d}} \tag{A.4}$$

Where:

- A_{in} is the lateral wind surface of ship i in loading condition n,
- C_d is the lateral resistance coefficient of the underwater body of the ship,
- C_{dw} is the lateral wind resistance coefficient,
- g is the gravity,
- L_i is the length of the ship i,
- ρ_a is the density of air (GL=1.3 kg/m^3),
- ρ_w is the density of water (GL=1024 kg/m^3),
- R is the wave drift coefficient,
- T_{in} is the draught of the ship i in loading condition n,
- v_{drift} is the drift condition of ship i in loading condition n by wind and waves for Beaufort class b,
- v_b is the wind velocity for Beaufort class b,
- ζ_b is the significant wave height for Beaufort class b.

B

OpenDrift

B.1. Wind Forcing

The wind force, F_{wind}, on a ship's surface is calculated by the formula:

$$F_{\text{wind}} = 0.5 \cdot \rho_{\text{air}} \cdot C_{\text{f}} \cdot A_{\text{dry}} \cdot V_{\text{wind}}^2 \tag{B.1}$$

where:

- F_{wind} is the force exerted by the wind on the object.
- ρ_{air} is the density of air.
- C_{f} is the wind drag coefficient,
- A_{dry} is the dry area of the object exposed to the wind. In the context of a ship, this would be the part of the ship's superstructure exposed to the air.
- V_{wind} is the wind speed (relative) to the object.

B.2. Wave Forcing

The calculation of the wave force, F_{wave}, involves several steps. OpenDrift uses the following equation for the wave spectrum:

$$S_\zeta(\omega) = \frac{124 \cdot H_s^2}{T_m^4} \cdot \omega_s^{-5} \cdot \exp\left(\frac{-496}{T_m^4} \cdot \omega_s^{-4}\right) \tag{B.2}$$

Where:

- H_s is the significant wave height,
- S_ζ is the spectral density,
- T_m is the mean wave period, and
- ω: is the wave frequency.

This is similar to the Brettschneider wave spectrum, assuming that T_m is equal to the the variance spectrum density's second frequency moment.

$$S_\zeta(\omega) = \frac{124 \cdot H_s^2}{T_1^4} \cdot \omega_s^{-5} \cdot \exp\left(\frac{-496}{T_1^4} \cdot \omega_s^{-4}\right) \tag{B.3}$$

Where:

$$T_1 = \frac{T_m}{0.921} \tag{B.4}$$

The total wave force and wave damping are then calculated by integrating over the entire spectrum, taking into account the ship's length and the wave energy distribution.

$$F_{\text{wave}} = \rho_{\text{water}} \cdot g \cdot L \cdot \sum_{i=0}^{N_{\text{SPEC}}-1} 0.5 \cdot (f_1 + f_2) \cdot \Delta\omega \cdot \sigma_1 \cdot S_\zeta(\omega_i)^2 \tag{B.5}$$

$$\beta_2 = \rho_{\text{water}} \cdot \sqrt{g \cdot L} \cdot \sum_{i=0}^{N_{\text{SPEC}}-1} 0.5 \cdot (d_1 + d_2) \cdot \Delta\omega \cdot \sigma_1 \cdot S_\zeta(\omega_i)^2 \tag{B.6}$$

where:

- ρ_{water} is the density of water ($1025\,\text{kg/m}^3$).
- g is the acceleration due to gravity (approximately $9.81\,\text{m/s}^2$).
- L represents the length of the ship or object.
- N_{SPEC} is the number of spectral points used in the calculation, determining the resolution of the wave spectrum.
- $\Delta\omega$ is the difference in angular frequency between successive spectral points.
- ω_i is the angular frequency at the ith spectral point.
- f_1, f_2 and d_1, d_2 are coefficients that account for the interaction between the waves and the ship's structure.

σ represents a scaling factor that limits the wave energy considered, by focusing only on the portion of the wave energy spectrum that exerts force on a ship in relation to the ship's length.

$$\sigma = \sqrt{\frac{g}{L_s}} \cdot \omega \tag{B.7}$$

B.3. Diffusion of simulations

The way OpenDrift models horizontal diffusivity is examined through an analysis of the spread of endpoints in simulations under the influence of different environmental conditions and for various ship types. The random displacement remains consistent over time but predominantly varies between ship types and depending on whether the influence of wave and current forcing is accounted for, as illustrated in Figure B.1.

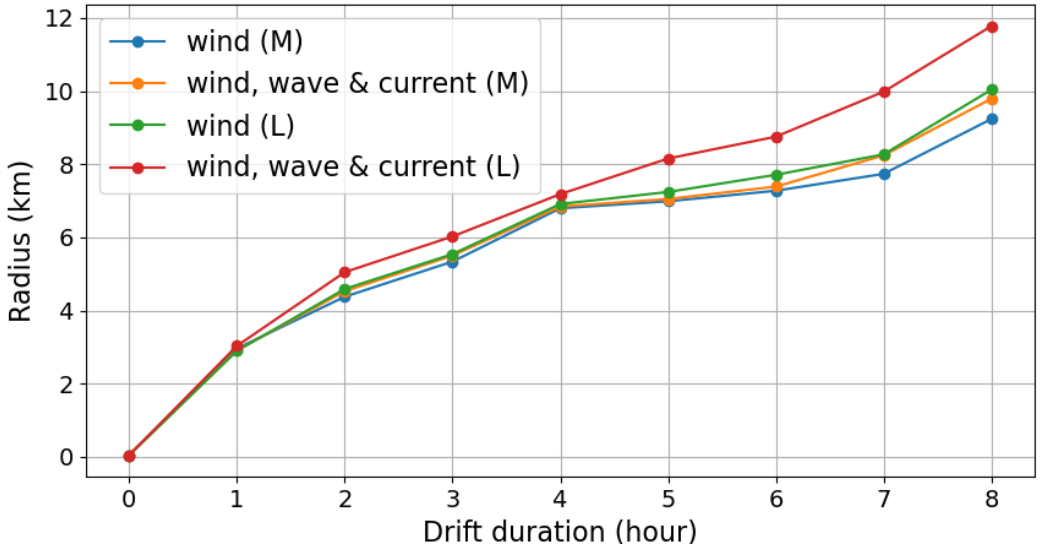

Figure B.1: Horizontal diffusion of simulations per hour drift duration for different environmental conditions and ship types

C

Additional results

C.1. Overall allision probability results Hollandse Kust Zuid

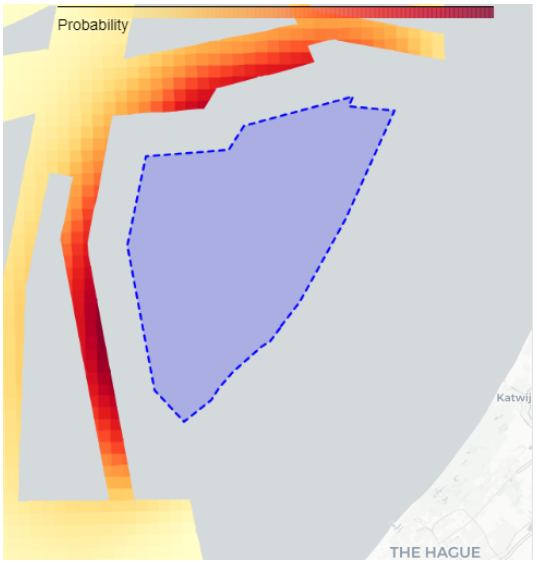

Figure C.1: Drift probability

Figure C.2: Activity probability

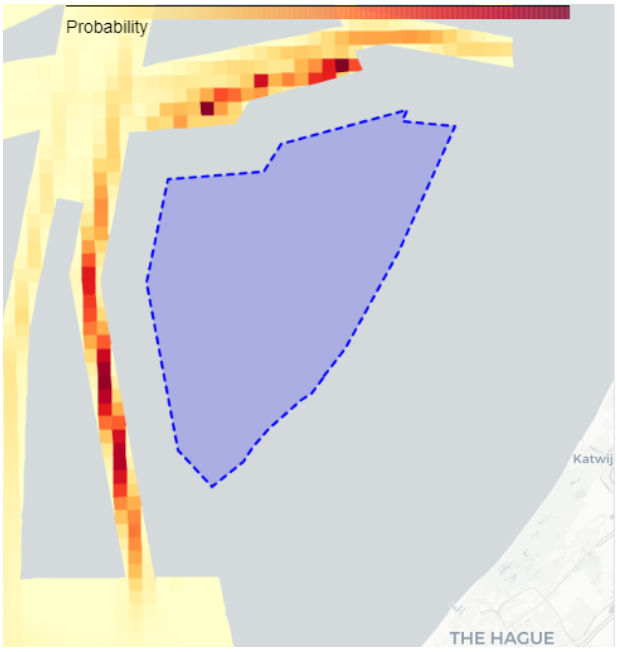

Figure C.3: Allision probability level

C.2. Hourly allision probability results Hollandse Kust Zuid

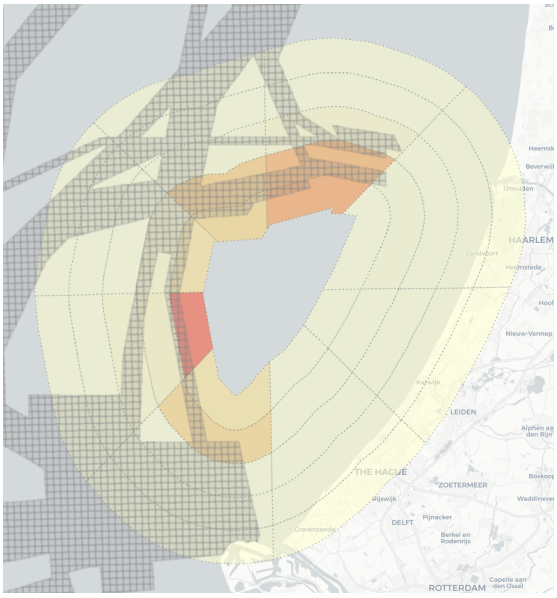

Figure C.4: 2 hours

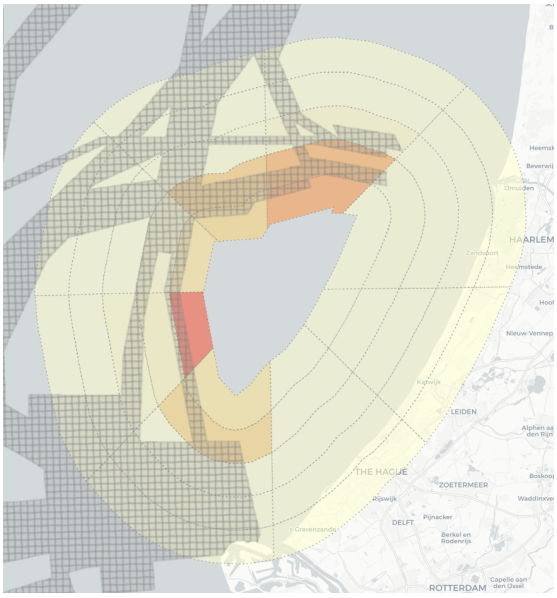

Figure C.5: 4 hours

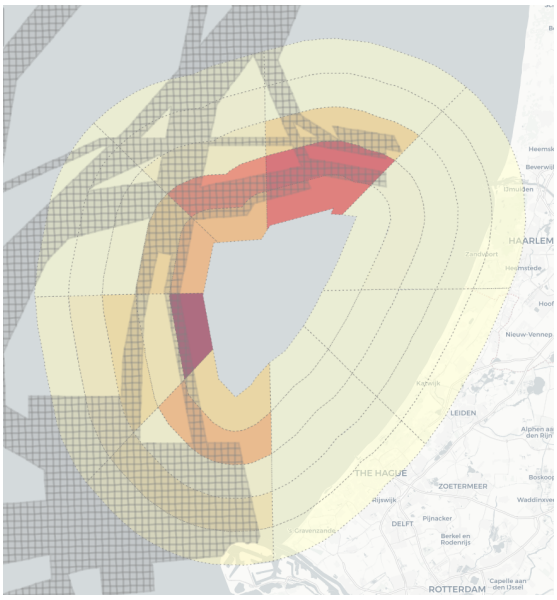

Figure C.6: 6 hours

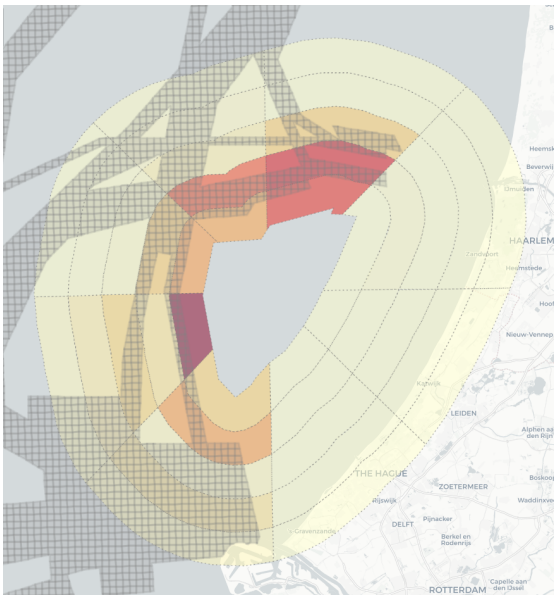

Figure C.7: 8 hours

Figure C.8: Overall allision probability distribution for increasing drift duration

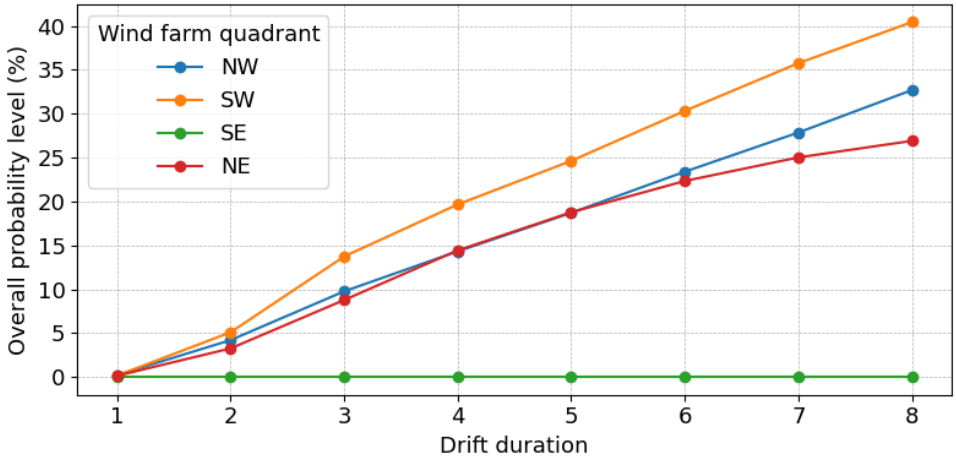

Figure C.9: Contribution per quadrant to hourly overall allision probability level of Hollandse Kust Zuid

C.3. Influence of different current segments for a specific wind direction range

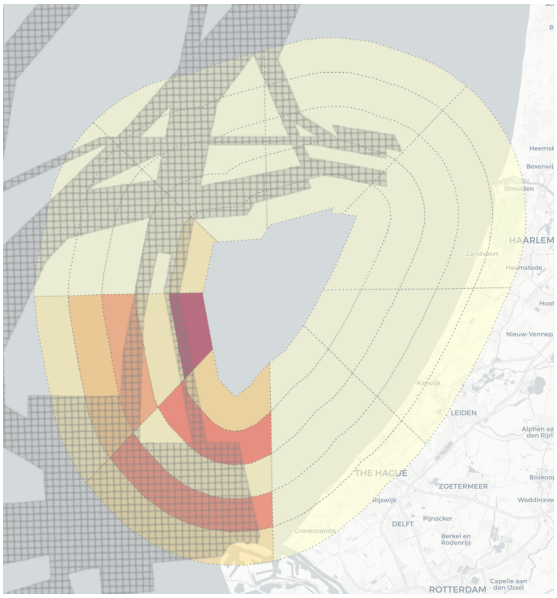

Figure C.10: 01:00

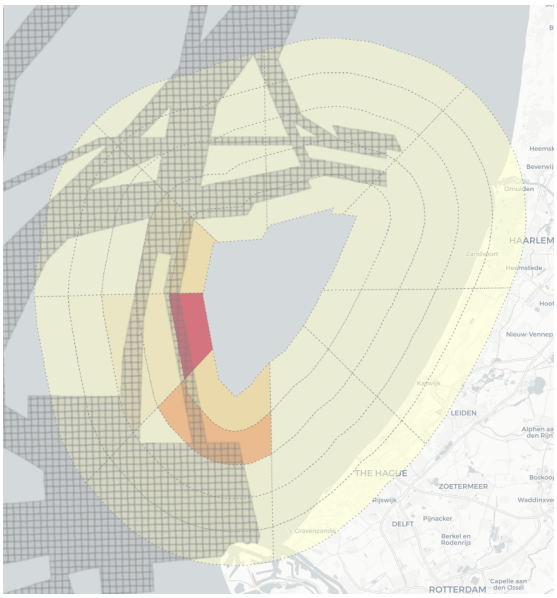

Figure C.11: 04:00

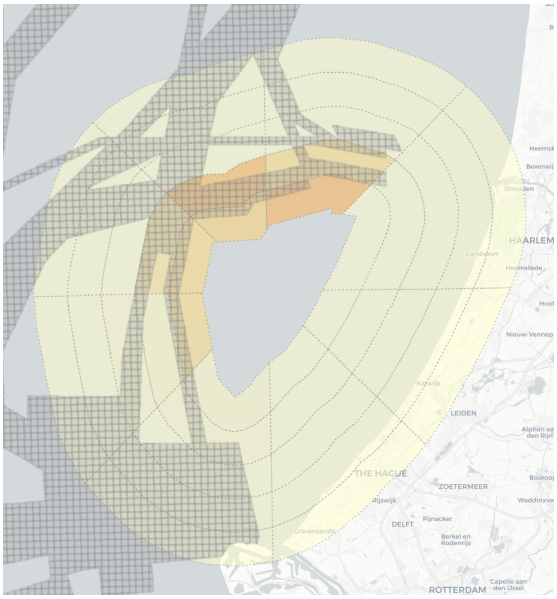

Figure C.12: 07:00

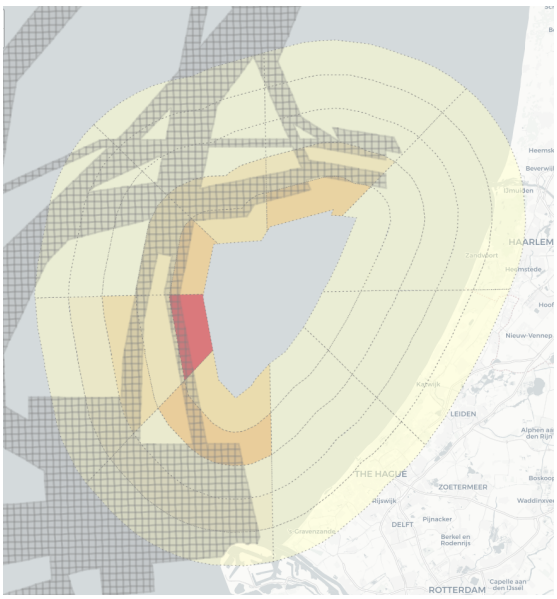

Figure C.13: 10:00

Figure C.14: Allision probability distribution of Hollandse Kust Zuid for the range of southwestern winds and varying starting times of the current

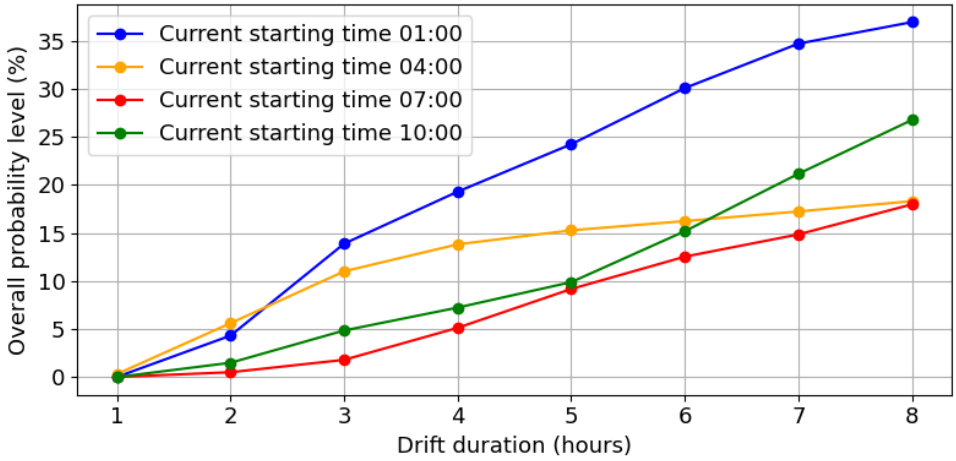

Figure C.15: Contribution per current segment to the southwestern wind range-specific allision probability level

D

Python modules

The Python modules can be found on the NauticalSafety GitHub page, under the branch name 'SietseEppenga'.

D.1. Environment

- The Python script for creating the wind and wave forcing set through multi-dimensional data binning is called 'multi_dimensional_data_binning.ipynb'.
- The Python script for creating a current field to use in OpenDrift is called 'current_dcsm_OpenDrift.ipynb'.

D.2. Geography

- The Python script for creating the fairway polygon and grid are called 'create_grid_svdw.ipynb' (van der Werff et al., 2024) and 'create_fairway_grid.ipynb'
- The Python script for defining the wind farm areas and the considered locations is called 'wind_farms.ipynb'
- The Python script for calculating $P_{activity}$ is called 'fairway_density.ipynb'.

D.3. Methodology

- The Python script for calculating the trajectories for each environmental forcing combination is called 'sd_simulation_tool.ipynb'.
- The Python script for calculating P_{drift} is called 'probability_calculation.ipynb'.

D.4. Visualisation

- The Python script for generating heat maps are called 'visualisation_allision.ipynb' and 'visualisation_drift.ipynb'
- The Python script for creating the rings and generating the ring heat maps is called 'ring_probability.ipynb'. Ring heat maps for a specific wind direction range and current segment can be generated with 'ring_probability_current.ipynb'

E

Data sources

E.1. ERA5

- Provider: European Centre for Medium-Range Weather Forecasts (ECMWF)
- Description: fifth generation of ECMWF atmospheric reanalyses of the global climate, providing hourly updates on atmospheric, land, and oceanic conditions.
- Access: data obtained via Deltares
- Parameters: wind data for U10 and V10 from 2012 to 2021.

E.2. DCSM

- Provider: Deltares
- Description: an in-house developed database and modelling system used for high-resolution simulation and analysis of hydrodynamics and meteorology in coastal and marine environments.
- Access: accessed internally at Deltares.
- Parameters: wave data for significant wave height, mean period and direction from 2012 to 2021

E.3. DCSM-FM

- Provider: Deltares
- Description: an extension of the DCSM database that utilises a flexible mesh grid system to provide high-resolution data on water currents and other hydrodynamic variables in coastal and open sea regions.
- Access: accessed internally at Deltares.
- Parameters: current data for x,y-components of current speed from 2021

E.4. Wind-wave scenarios used in OpenDrift

The figure below displays matrices representing combinations of wind speed and wind direction, along with their corresponding probability values, at 3.75m 52.5 (longitude, latitude). In the simulations, these values are divided among four wave height ranges, resulting in four distinct matrices for each range:

Significant wave height (m)			
0.12 - 1.51	1.51 - 2.90	2.90 - 4.28	4.28 - 5.67

Table E.1: Significant wave height ranges in simulations

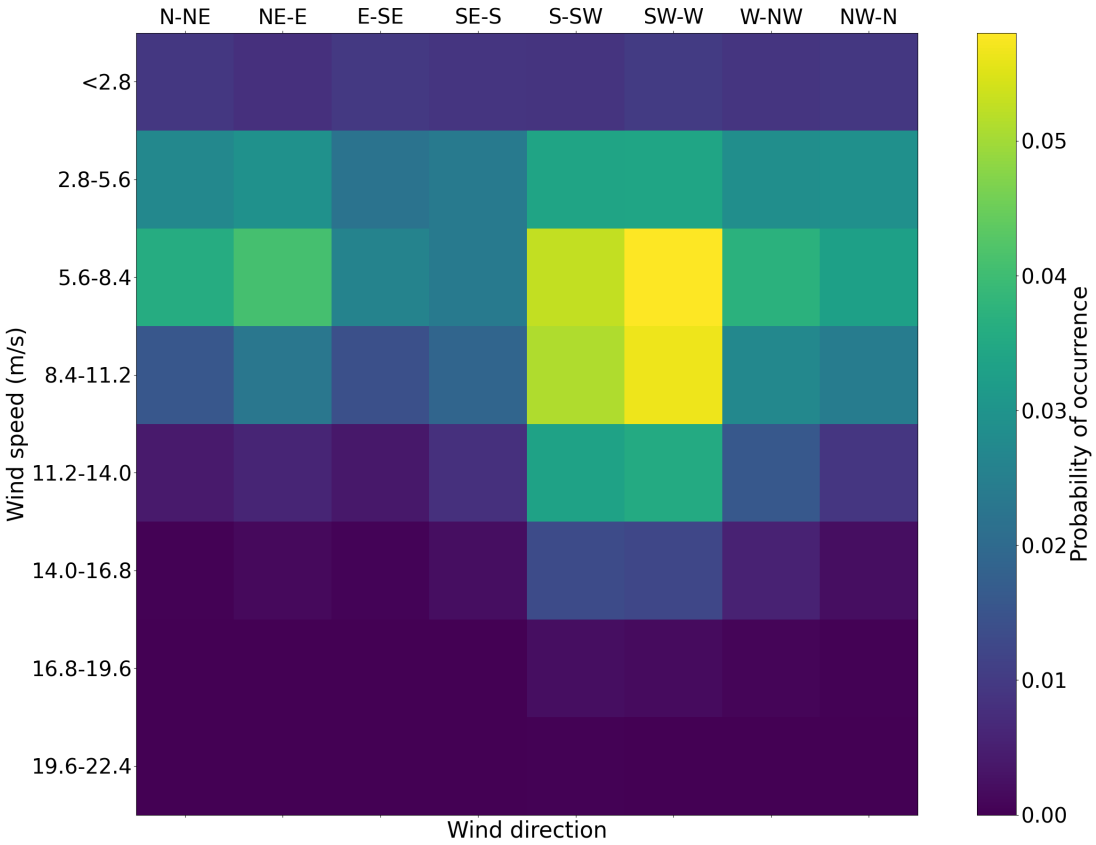

Figure E.1: 8 by 8 matrix of wind speed and direction combinations used in simulations

E.5. Current field used in OpenDrift

Date: 2021-07-11

Time	U_{10} (m/s)	V_{10} (m/s)
00:00	-1.39	-0.22
01:00	0.08	-0.78
02:00	0.47	-1.03
03:00	-0.58	-1.94
04:00	-2.07	-2.89
05:00	-2.45	-1.68
06:00	-1.32	-0.14
07:00	0.16	0.56
08:00	-0.14	0.45
09:00	-0.43	0.35
10:00	-0.47	-0.48
11:00	-0.38	0.59
12:00	0.86	1.99
13:00	1.69	2.62
14:00	3.31	1.97
15:00	4.20	0.55
16:00	2.69	-0.78
17:00	2.32	-0.68
18:00	1.41	-0.66
19:00	-0.11	-0.57
20:00	-1.15	0.34

Table E.2: Wind speeds during the current cycle used in the methodology

The Python scripts for selecting a period with low wind speeds and analysing the corresponding current are called 'identifying_periods_with_low_wind_speeds.ipynb' and 'visualisation_of_current.ipynb'.

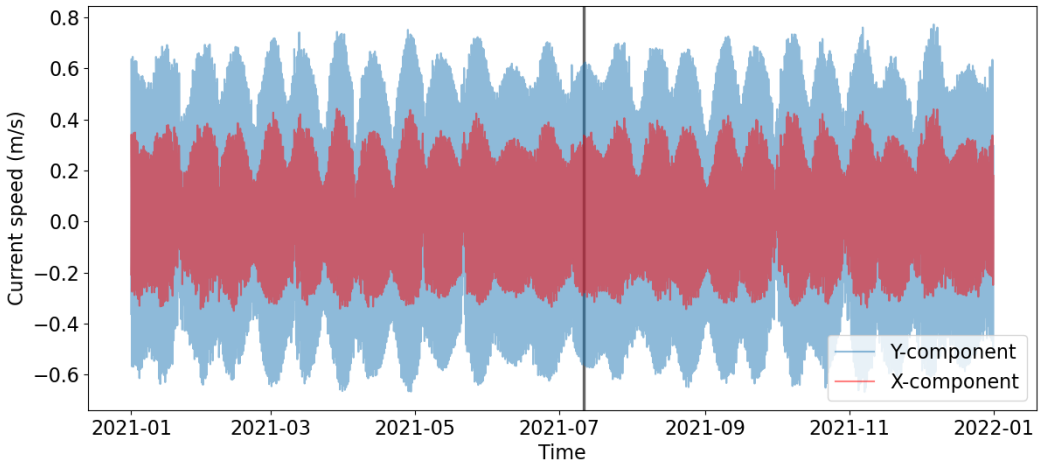

Figure E.2: Current at 3.75, 52.5 (longitude, latitude) with in grey the selected period

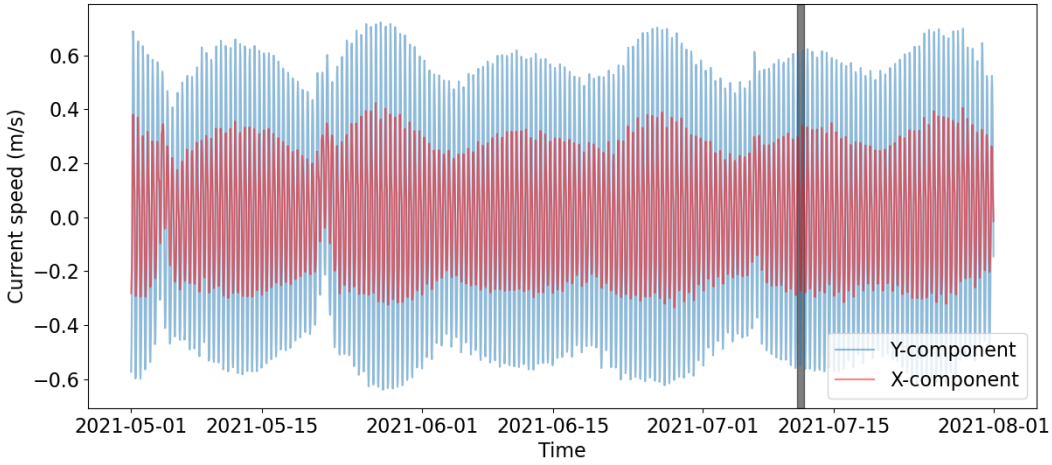

Figure E.3: Current at 3.75, 52.5 (longitude, latitude) with in grey the selected period

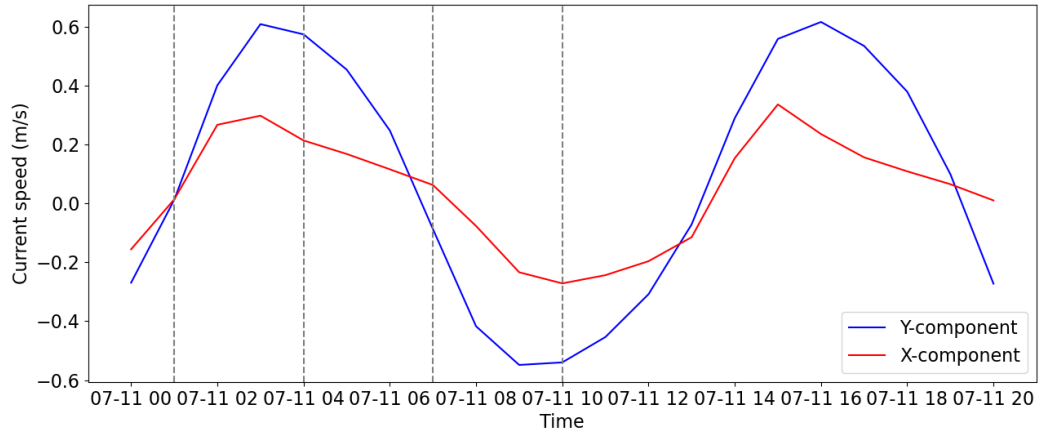

Figure E.4: Selected current cycle at 3.75, 52.5 (longitude, latitude) with in grey the selected starting times